SKB

TECHNICAL REPORT

89-16

Swedish Hard Rock Laboratory Evaluation of 1988 year pre-investigations and description of the target area, the island of Äspö

Gunnar Gustafson, Roy Stanfors, Peter Wikberg

June 1989

SWEDISH HARD ROCK LABORATORY
EVALUATION OF 1988 YEAR PRE-INVESTIGATIONS AND
DESCRIPTION OF THE TARGET AREA, THE ISLAND OF ÄSPÖ

Gunnar Gustafson, Roy Stanfors, Peter Wikberg

June 1989

SWEDISH HARD ROCK LABORATORY

Evaluation of 1988 Year Pre-investigations and
Description of the Target Area,
the Island of Äspö

Gunnar Gustafson
Roy Stanfors
Peter Wikberg

June 1989

CONTENTS

ABSTRACT

The site investigations for the Swedish Hard Rock Laboratory have been focussed on the southern part of the Äspö island. Geological, geohydrological and chemical investigations have been made in three deep boreholes on Äspö. The results are used to evaluate previous predictions of the properties of the rock mass and to set up new predictions, more detailed than the previous ones.

At the southern part of Äspö a basic rock type called the Äspö diorite dominates at the depths of 300 — 600 m. The hydraulic conductivity is lower here than in the surrounding Småland Granite. The groundwater chemistry in contact with the Äspö Diorite has a high iron content.

The methods and techniques used for the investigations have been optimized and integrated. During the drilling operation both hydraulic tests and groundwater sampling were performed.

SUMMARY

The second stage of the site investigations for the Hard Rock Laboratory has been concentrated to the island of Äspö.

In order to get more detailed information about the geological conditions on Äspö a number of geological and geophysical studies were performed.

Very detailed geological mapping along cleaned trenches across the island resulted in a map to the scale of 1:2000 and in order to detect possible low-dipping fracture zones in the Äspö area reflection seismics was used.

Complementary tectonic studies described — mostly steeply dipping — shear and fracture zones trending EW-ENE, NNE-NE, NW and N-S as well as a possible, gently dipping fracture zone trending ENE. Data concerning 4 500 mapped fractures are presented. A summarized rosette diagram shows predominant orientation sectors around WNW, N-S and ENE.

A detailed geophysical investigation — comprising geomagnetic and geoelectric mapping methods — was performed in order to indicate fracture zones on Äspö. Especially important was the interpretation of the dip of the fracture zones.

Three deep core boreholes, KAS 02, KAS 03 and KAS 04 have been drilled and investigated on Äspö. All geological data have been used to present models of the Äspö site in different scales.

The geohydrological investigations were concentrated to the deep core boreholes where packer tests of 3 and 30 m intervals were performed as well as short pumping tests of the entire boreholes. Interference tests were also performed in 9 selected conductive sections in the core boreholes.

All collected pertinent data have been subject to a thorough analysis where the statistical and spatial distributions of conductivity data are correlated to geological and geophysical parameters. Major hydraulic conductors were identified and correlated to zones identified by other methods.

Numerical modelling was made by a FEM-model (Finite Element Model) of the regional flow and a generic study of the position of the salt water zone in a heterogeneous rock by a FDM-model (Finite Difference Model).

Conceptual models of the geohydrological features of the Äspö area are presented in different scales.

The groundwater chemistry at the sampled sections of the boreholes KAS 02, KAS 03 and KLX 01 has been analyzed by chemometric analyses. The results are compared to the previous predictions and the data has been used to present models of the groundwater chemistry in different scales at Äspö.

ACKNOWLEDGEMENT

1 INTRODUCTION

PREVIOUS INVESTIGATIONS

The site investigations for the Hard Rock Laboratory were started in 1986 with a regional survey comprising many different methods (magnetic, coaxial EM, radiometric and two-station VLF).

A gravity measurement and some ground geophysical profiles (magnetic and VLF) complemented the aerogeophysical survey on the islands of Ävrö and Äspö and in the Laxemar area.

Lineaments in the Simpevarp area were interpreted from different digital terrain models and the solid rock was mapped to a scale of 1:10 000 in an area nearest to Simpevarp and to a scale of 1:50 000 in a larger outer area. Fracture mapping and special tectonic studies were carried out with the main goal of describing the geometry of the fractures and of characterizing the main sets of tectonic zones identified as lineaments in the area.

During the investigations in 1987 drilling was performed at different stages in the areas of Ävrö, Äspö and Laxemar.

A number of percussion boreholes were sited to obtain preliminary information on the bedrock composition and the hydraulic properties of the shallow portion of the bedrock.

Three core boreholes (KAS 02, KAS 03 and KAS 04) were sited in a preliminary geological and geohydrological model of Äspö and the core borehole KLX 01 in the central part of a major block at the Laxemar area.

A first attempt was also made to describe the rock mass in different scales.

The surface hydrology of the Simpevarp region was compiled to provide basic input.

In order to make use of existing geohydrological data an analysis was made of regional well data from the SGU Well Records and a compilation made of geohydrological data from the Simpevarp area, where results from the pre-investigations and construction works for the power plants and CLAB were also used.

Pumping tests were performed in the boreholes drilled in 1987 and evaluated.

In order to assess the influence of the Hard Rock Laboratory on the geohydrological conditions a generic model was made of two layout alternatives.

Chemical data was obtained from well records of the Kalmar County and from the shallow percussion drilled holes at Laxemar, Äspö and Ävrö. Additionally some surface waters sampled at Äspö and Laxemar were also analyzed. These data indicated that the groundwater of Äspö was different from the surface water. The differences were, however, plausible and in agreement with the data in the well records. A high salinity of the shallow groundwaters of Äspö indicated, however, that stagnant conditions prevail in the bedrock of Äspö.

The results of these investigations were summarized in a technical evaluation 1988. /SKB, TR 88-16 Gustafson-Stanfors-Wikberg/.

Since 1988 the island of Äspö has been the principal target area for the continued site investigations on the HRL.

An illustration of the investigation area is given in Figure 1-1.

The preinvestigations have been divided into different scales, regional, local and detailed, into different disciplines, geology, geohydrology and chemistry. The present report is a co-evaluation of the results obtained from the investiga-
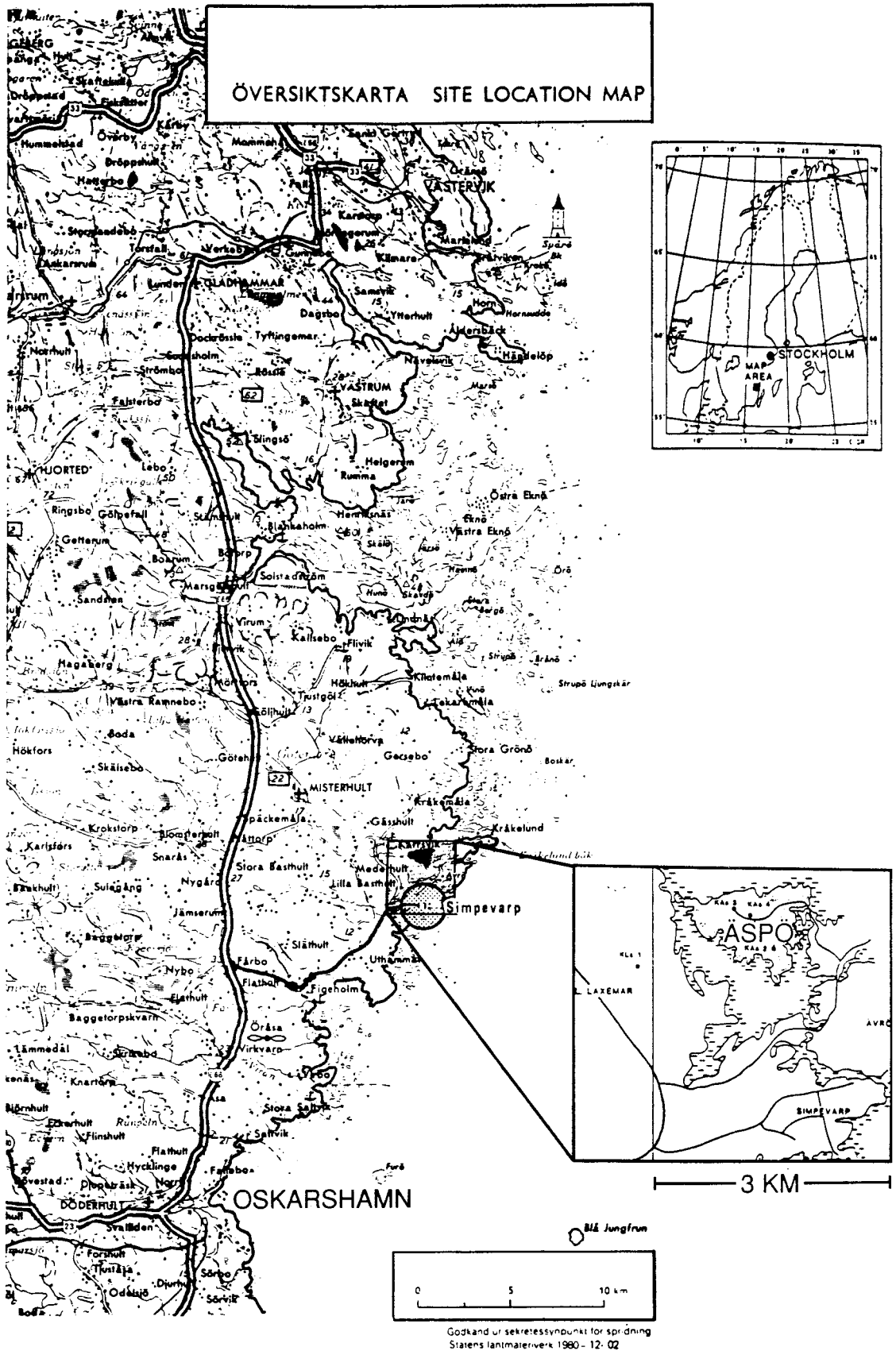
1

Figure 1-1. Key map of the location of the core-drillings.

tions on the Äspö island local scale. The vast majority of the data in this stage have been obtained from three deep boreholes; KAS 02, 03 and 04.

The data have been used to present models of the Äspö site in different scales with respect to the geological, geohydrological and chemical conditions. These models are compared to the predictions made in the previous report, Gustafson-Stanfors-Wikberg, 1988.

The conclusions with respect to the structural framework is illustrated in Figure 1-2.

GEOLOGY

The second phase of the site investigation programme has been concentrated to more detailed studies on the island of Äspö, see Figure 1-1.

The solid rock on Äspö has been mapped to the scale of 1:2 000.

A very detailed study of the bedrock has been performed along cleaned trenches across the island. The description of the rocks include chemical and modal analysis.

Detailed structural analysis of terrain features on Äspö has been performed based on the study of topographical maps, 1:4 000, contoured for 1.0 m. Maps showing lineaments and rock blocks of different orders are presented.

A fracture mapping programme has been carried out on outcrops following the cleaned trenches. The project report includes in different manners geographically integrated results regarding strikes, dips and fracture densities, lengths and spacing.

The geological deformation structure with concentration to Äspö and the adjoining area to the east of Äspö has been continued.

The main aims of the study were to understand the geological history of the rocks of the island of Äspö and to study examples of the main sets of tectonic zones with a view to relating how they developed in four dimensions (3rd space with time) to current experimental and theoretical understanding of brittle rock failure.

Two reflecting seismic profiles have been recorded on the island of Äspö. The scope was to identify possible larger subhorizontal fracture zones at depth down to approximately 1 000 m.

In order to investigate and delineate the local tectonical setting at the island of Äspö, detailed magnetic and electric mapping of the entire island was carried out during the autumn of 1988. A detailed analysis of the groundmagnetic total field measurements and resistivity profiling over Äspö puts the results in a regional to semi-regional perspective.

During the investigations 1987—88 four core boreholes were sited in preliminary geological and hydrogeological models of Äspö and Laxemar. The most important data concerning the geological and geophysical evaluation of these four boreholes were compiled in a report.

GEOHYDROLOGY

The geohydrological investigations in one second phase was concentrated on hydraulic tests in the core boreholes on Äspö and in Laxemar, a hydraulic parameter evaluation based on tests, borehole geophysics and core mapping, and models of the regional ground water flow and the saline water front.

An evaluation of packer tests and spinner surveys in the boreholes was presented. Field data from the tests were given.
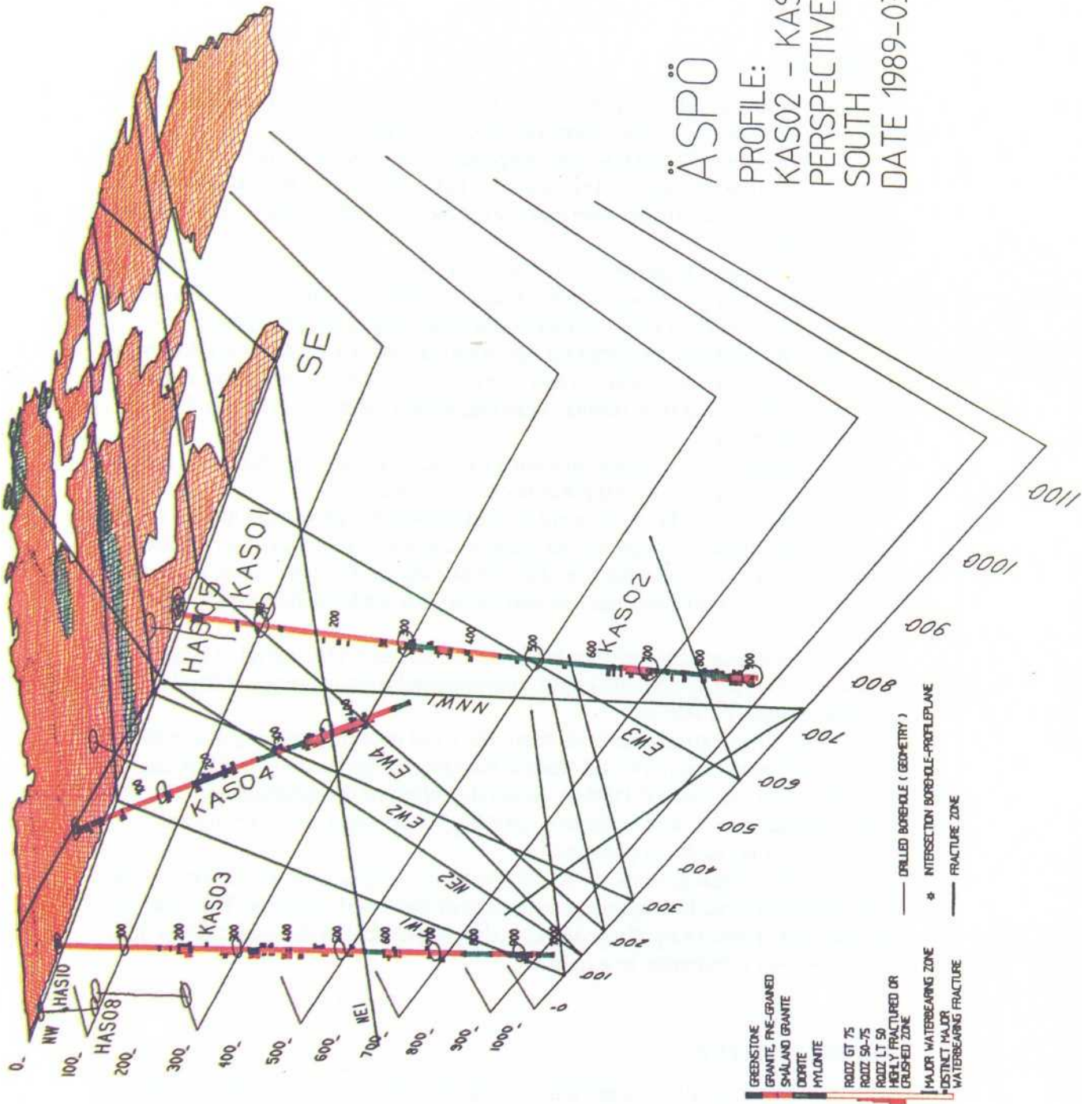
Figure 1-2. Tentative perspective of Äspö.

Transient interference pump tests were performed in the boreholes KAS 02 and KAS 03, and from these major hydraulic conductors were identified.

A thorough evaluation and correlation study of geohydrological, geophysical and geological data was performed in order to assess the hydraulic properties of structure and lithological units and to test the relevance of different investigation methods.

A model of the regional groundwater flow has been set up. This model has also been used to assess the area of influence from the laboratory.

A generic study of the behaviour of the saline water front in a fractured rock simulated by a stochastic continuance was also performed.

CHEMISTRY

The investigations in the second phase have been focused on the deep drillholes KAS 02 and KAS 03. Results of groundwater analyses are presented and fracture mineralogy has been studied.

2 GEOLOGY

In order to get more detailed information about the geological conditions on Äspö a number of geological and geophysical studies were performed during the second stage of the pre-investigation.

The aim of the first study (2.1.1) was to obtain information to make a description of the lithological distribution and petrological characteristics of the different rocks on Äspö. Very detailed mapping was performed along cleaned trenches across the island, and a geological map to a scale of 1:2000 was prepared. A classification of the rocks based on chemical and mineralogical analyses is presented.

The object of the second study (2.1.2) was to use the reflection seismic method to detect possible low-dipping fracture zones in the Äspö area. Two reflection seismic profiles were recorded across Äspö using a 2H-channel ABEM Terraloc with a record time of 500 msec. Two possible subhorizontal zones at depths of 300—500 and 950—1150 metres were identified.

The aim of the third investigation (2.1.3) was to perform complementary field analyses in the Äspö area to the study on the main tectonic zones in the Simpevarp region reported earlier.

Main — mostly steeply dipping — shear and fracture zones are described, trending EW-ENE, NNE-NE, NW and N-S. A possible, gently dipping fracture zone trending ENE is also indicated. A simplified working model of the anisotropy of apparent permeability is also presented.

The principal aim of the fracture mapping programme presented in 2.1.4 was to make complementary measurements along the cleaned trenches to obtain results for use in geohydrological and rock mechanics model studies.

Data concerning 4500 mapped fractures — such as orientation, length, aperture and fracture filling — are presented. A summarized rosette diagram shows predominant orientation sectors around WNW, N-S and ENE.

The main aim of the detailed geophysical investigation — reported in 2.1.5 — was to indicate fracture zones on Äspö using geomagnetic and geoelectric mapping methods. Especially important was the interpretation the dip of the fracture zones. Detailed bedrock and fracture interpretation based on ground-magnetic data is presented on very detailed maps. Fracture zones interpreted as open, but filled with water and/or clay, were delineated by combinating a geoelectric and geomagnetic data.

During the first phase of the drilling programme for the Hard Rock Laboratory four core boreholes, KAS 02, KAS 03, KAS 04 and KLX 01 were drilled. The most important data concerning the geological evaluation of the four core boreholes are summarized in 2.1.6.

Sections 2.1.1 — 2.1.6 contain an extract of the 6 reports mentioned above.

2.1 GEOLOGICAL STUDIES

2.1.1 Description to the Detailed Map of the Rocks of Äspö Island

This report is a description to the maps of solid rocks of Äspö island /Kornfält-Wikman, 1988/. It comprises petrological characteristics of the rocks which were also studied also in trenches where the rock surface had been uncovered (Figure 2-1).

GEOLOGICAL MAP OF THE ÄSPÖ ISLAND

SWEDISH HARD ROCK LABORATORY

Figure 2-1. Geological map of Äspö island.

LEGEND

Position of orientation point within a trench

Foliation, dip in degrees

Foliation, dip vertical

Foliation, dip unknown or vertical

Mylonitized fracture zone (<0.5 m)

Mylonite

Strongly foliated rocks

Diabase

Dikes of fine-grained, greyish red to red younger granite

Granite, fine-grained, greyish red to red

Granite, medium-grained, greyish red (Ävrö-granit)

Granite, granodiorite, quartz monzonite and quartz monzodiorite, medium-grained, porphyritic, augen 1-3 cm, reddish grey

Metavolcanite, (metaandesite, metadacite) fine-grained, grey

Xenoliths of greenstone

Greenstone (metabasalt), fine-grained, left Greenstone, (dike-formed), right

SGU

Karl-Axel Kornfält
Hugo Wikman
1988

Trenches

0   100   200   300   400 m

STOCKHOLM

MAP AREA

The rocks will be described in chronological order beginning with the oldest. The relative ages of the mafic rocks (greenstones and intermediate metavolcanics) are, however, unknown. There is also some uncertainty as to the age of the greenstones in relation to the porphyritic granitoids, as will be commented on in the following section.

GREENSTONE (METABASALT)

Across the island of Äspö, from SW to NE, there are a number of outcrops of greyish black, fine-grained, often rather homogeneous, basic rocks probably of volcanic origin. They are always strongly altered to greenstone.

The modal composition, with very little quartz and hardly any potash feldspar, indicates an originally basaltic composition. The chemical analysis does not contradict this assumption.

The rock has often been intruded by a fine-grained, greyish red granite. There are also a few intrusions of fine, medium-grained, porphyritic granite of the same type as in the country rock. Along the border between the medium-grained, porphyritic granitoid and the greenstone, there are sometimes accumulations of fine-grained, greyish red granite.

According to Kornfält and Wikman the greenstone is older than the granitoids in the area. They base their opinion on the fact that the greenstone occurs as xenoliths in the porphyritic granitoid. The greenstone is also intruded by fine medium-grained, porphyritic granitoids.

If the granite intrusions were a result of back-veining, the granite veins ought to be concentrated to the border zones of the greenstone massifs and not equally distributed, as they are.

Greenstone, Dyke-type

In borehole KAS 04 a variety of greenstone occurs which in some respects differs from the "common" type described in the preceding section. Firstly, this greenstone is shaped more like a dyke than the other. Secondly, compared with the "common" greenstone it has somewhat coarser grains, with approx. 2 mm long, lath-shaped, plagioclase crystals.

However, the chemical composition of the two greenstone varieties is very similar which is clear from the analyses.

The modal analyses show that the dyke-type greenstones contain more plagioclase and chlorite than the "common" greenstone.

The eastern dyke-type greenstone can be followed along a distance of about 200 m. It narrows like a wedge at both ends and no continuation was observed on either side, in spite of the unusually well exposed bedrock.

Owing to these observations it is unlikely that the dyke-type greenstone is younger than the bordering reddish grey, porphyritic granitoid.

Presumably the dyke-type greenstones represent a subvolcanic equivalent to the "common" greenstone.

GREY, FINE-GRAINED, INTERMEDIATE METAVOLCANICS

Intermediate metavolcanics constitute only minor parts of Äspö island. They are made up of grey to dark-grey, fine-grained rocks and are often penetrated by granites. The boundaries between the granite and the intermediate metavol-

canics are irregular and difficult to map in detail. It is also hard to separate mac-roscopically the intermediate metavolcanics from the greenstones. However, the former are slightly greyer on weathered surfaces.

The modal analyses of the intermediate metavolcanics show that they are mainly metadacites. One sample has a composition corresponding to ametaan-desite. This sample has black spots of hornblende. Another sample has red spots of potash feldspar.

The metadacite and metaandesite presumably represent an intermediate part of the volcanism which also gave rise to the basic extrusives, now forming the greenstones.

REDDISH GREY, FINE, MEDIUM-GRAINED TO MEDIUM-GRAINED, PORPHYRITIC GRANITE, GRANODIORITE, QUARTZ MONZONITE AND MONZODIORITE

The predominating rock on Äspö island is a reddish grey (occasionally greyish red), fine, medium-grained to medium-grained granitoid with megacrysts (1—3 cm) of red microcline.

In this group, usually called Småland granite (together with the granite in the following section), four different rocks can be distinguished using the IUGS clas-sification system (1973, 1980).

As is evident from Figure 2-2, the modal analyses plot in a rather restricted area around the borderlines between the fields of granite, quartz monzonite, quartz monsodiorite and granodiorite, the porphyritic granites are thus not as heterogeneous as the number of rock names would suggest.

As can be seen from the modal analyses, the contents of sphene are rather high. This has already been noticed by /Swedmark, 1904/ who, on his original map of the region, called this granite sphene-granite.

GREYISH RED, FINE, MEDIUM-GRAINED GRANITE (ÄVRÖ GRANITE)

During the mapping of the Simpevarp area /Kornfält & Wikman, 1988/ a greyish red variety of the Småland granites was observed on Ävrö island, which is situated just to the south-east of Äspö. Small areas of this granite have also been observed on south-eastern and south-western Äspö during the present mapping. It has been called Ävrö granite and differs somewhat from the porphyritic granitoid described in the previous section.

The Ävrö granite is thus greyish red instead of reddish grey, and its microcline megacrysts are rather small (about 1 cm) and sparsely scattered compared to the porphyritic granitoid. The Ävrö granite is a true granite which is evident Figure 2-2.
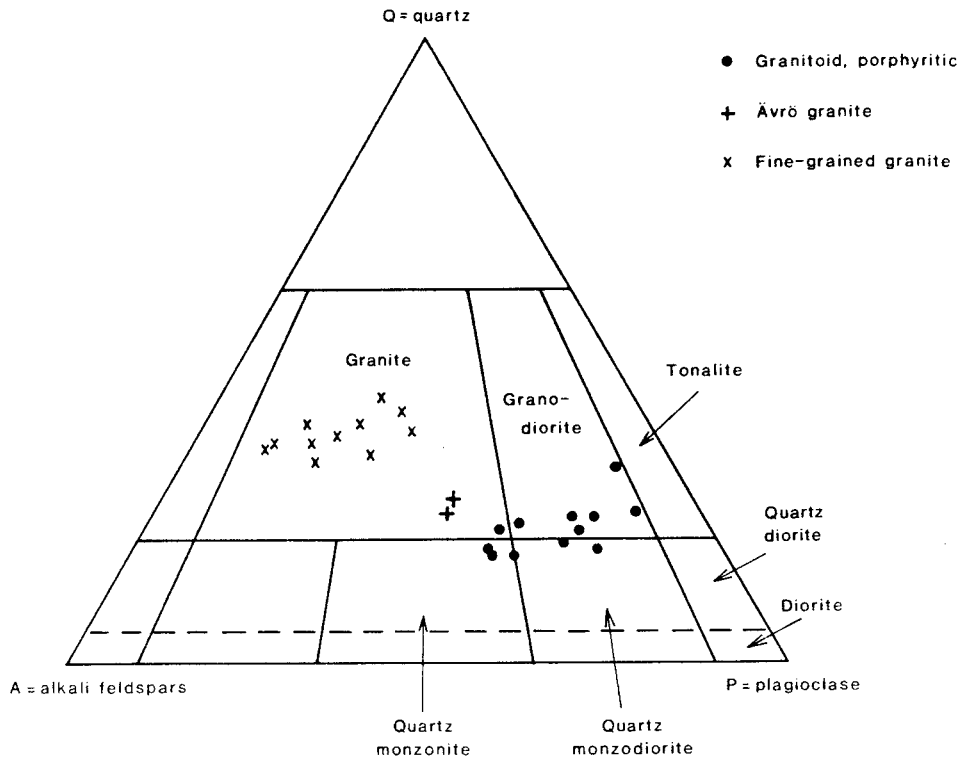
Figure 2-2. Modal classification of Äspö rocks according to their mineral (Q-A-P) content measured in per cent by volume (IUGS, 1973, 1980).

GREYISH RED TO RED, FINE-GRAINED GRANITE

Fine-grained, red to greyish red granite occurs rather frequently on Äspö island as well-defined dykes intersecting the older rocks.

The width of the dykes usually varies between a decimetre and about 5 metres. They run in various directions and vary in frequency. On the map they are marked by red strokes.

There are also much wider dykes of this rock — up to 25 metres across. The great dykes usually run NE — SW and occur above all in the central parts of the island.

Typical of the dykes of fine-grained granite is that most of them are strongly deformed. The deformation may be interpreted in the following way. After emplacement of the granite dykes along fracture planes, the block movements must have continued, resulting in a brittle deformation of the fine-grained granite in the dykes and in the country rock next to them. In thin sections this is illustrated by bands of granulated quartz and a streaky pattern of elongated clusters of mafic minerals.

The fine-grained granites can be classified as true granites. As can be seen from the modal analyses and the triangle diagrams they are rather rich in alkali feldspar (Figure 2-3). This is also evident from the chemical analyses.

From the modal analyses it is also clear that the fine-grained granite contains muscovite as well as biotite. Fluorite is missing in most samples. In an earlier report, Kornfält & Wikman (1987) supposed that they could separate possible different generations of fine-grained granites by means of their fluorite content.

11
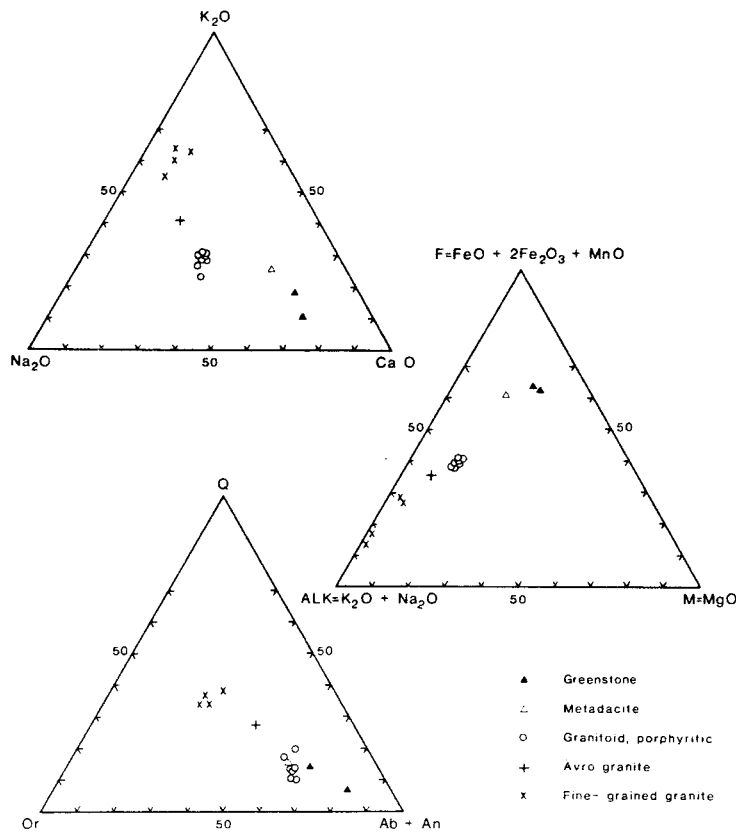
Figure 2-3. K₂O-Na₂O-CaO diagram (weight %), ALK-F-M diagram (weight %) and Q-Or-(Ab+An) diagram (CIPW norms).

It is now clear that this cannot be done as the fluorite content proved to be an uncertain property.

The age of the fine-grained granite is still uncertain. The anorogenic granites in the region are accompanied by a fine-grained granite, but this is a common feature of granite plutons of different ages.

However, as the fine-grained granites seem to be concentrated in areas bordering on the anorogenic granites it does not seem unreasonable that most of the fine-grained granites of the Äspö area could be anorogenic and related the Götemar-Uthammar granites.

The results of geophysical laboratory measurements on the core samples from Äspö /Nisca, 1988/ does not contradict the assumption that the fine-grained granite is related to the anorogenic granites.

APLITE AND PEGMATITE

Aplites and pegmatites are rare on Äspö. They occur mainly as very narrow dykes, seldom exceeding a few decimetres. Some of them have very gentle dips. As an exception, aplite and pegmatite form a kind of multiple intrusion with either the aplite or the pegmatite in the centre of the dyke. The colour of both rocks is greyish red to red.

In a few places (e.g. north of P 26 in Trench 2) diffuse pegmatitic segregations occur in the fine-grained granite.

DIABASE

Diabase (altered dolerite) has only been observed at a few localities on Äspö. It occurs as very narrow dykes seldom more than a few decimetres wide. The two dykes shown on the map of Äspö cut the foliation and run in a northerly direction. They are dark greenish grey, very fine-grained and somewhat altered. No thin-sections of the diabases have been prepared owing to the strong weathering of this rock.

The diabase may be comparable in age with the dykes observed in the Götemar massif to the north-west of Äspö /Kornfält & Wikman, 1987/. If so they will be much younger than the other rocks on Äspö.

MYLONITE

As mentioned in the previous reports of the geology of Äspö and adjacent areas strong fracturing is a prominent feature in many places. The present investigation has strengthened this impression.

Thus, fracture zones containing mylonite were observed at several localities. Most of them are rather thin, but in Trench 2 an approximately 40-m wide fracture zone with mylonite and crushed breccia was found. The zone, which runs in a east-north-easterly direction, divides the island into two halves. Within this zone the degree of mylonitization varies — from very dense (greenish white) mylonite to rocks (often greenish red) with more or less mylonitic and brecciated streaks. In the latter it is often possible to trace the original rock.

In the mylonites the original mineral assemblage and structure has changed completely to a very fine-grained mass consisting mainly of quartz and epidote. Within the crushed breccia sections, opaque minerals are often concentrated to cracks and brecciated streaks.

On Äspö there are also many, mostly thin, mylonites running in a northerly direction. One of the most prominent of these fracture zones can be observed in Trench 1, north-west of core borehole KAS 03. The mylonite is here only a few decimetres wide, but the bedrock shows strong foliation and fracturing on both sides of the mylonite, within a zone about 10 m wide.

As can be seen from the geological map of Äspö the degree of exposure is rather high. Still there are quarternary deposits and vegetation covering parts of the bedrock that are probably interesting. In order to get information of continuous bedrock sections the overburden has to be removed. This was done using an excavator. After that, the rock surface was blown clean with compressed air, followed by rinsing with high-pressure water.

The result of this work was a number of 2—5 m wide trenches (about 1500 m long in all) with cleaned surfaces, which were very suitable for studying detailed petrological and tectonical characteristics of the rock. (Figure 2-4) The trenches have numbered orientation points drilled in the bedrock and maps of the trenches to the scale of 1:1000 have been prepared.

The general foliation on Äspö and in the adjacent area is almost always between N 70° E and E-W. It is mostly weak and sometimes difficult to measure. Specially the dip is often very faint but seems to be more or less vertical in the most cases.

In certain zones the foliation is enhanced which is the case specially along the broad mylonite zone that crosses the island. It runs in the same direction as the general foliation and divides Äspö into two halves.

Figure 2-4. Section of Trench 1, where it passes west of core borehole KAS 03.
Photo H. Wikman, 1988.

Diverging foliation directions are sometimes found close to the narrow fracture and mylonite zones which run in a roughly north-south direction. These foliations are, however, very local and occur in zones not wider than 10 m.

There are also minor vertical joints running in a north-south direction. Small horizontal dislocations are sometimes found along these joints. They all seem to be younger than the general foliation and the mylonite zone. They are also younger than the numerous winding cracks filled with epidote which are characteristic, especially of north-eastern Äspö and the area to the south of the mylonite zone. Many cracks filled with a mineral, which is presumably prehnite, have also been found.

2.1.2 Shallow Reflection Seismic Profiles from Äspö

The Institute for Applied Geology of the Technical University of Denmark recorded 2 reflection seismic profiles (RS88-01 and RS88-02) on the island of Äspö in September 1988 (Figure 2-5). RS88-01 runs a total length of 1130 metres, corresponding to a subsurface coverage of 1015 metres, and is located as a straight, NW-SE line passing boreholes KAS 02, KAS 03 and KAS 04. RS88-02 runs a total length of 1010 metres, corresponding to a subsurface coverage of 875 metres, and is located approximately perpendicular to RS88-01 and passes close to KAS 03.

The aim was to use the reflection seismic method for mapping any large fracture zones in the crystalline bedrock. The target depth was from as near the surface as possible and down to approximately 1500 metres. The depth to the crystalline bedrock varies from 0 to more than 8 metres, but along most of the sections it was less than 1 metre.
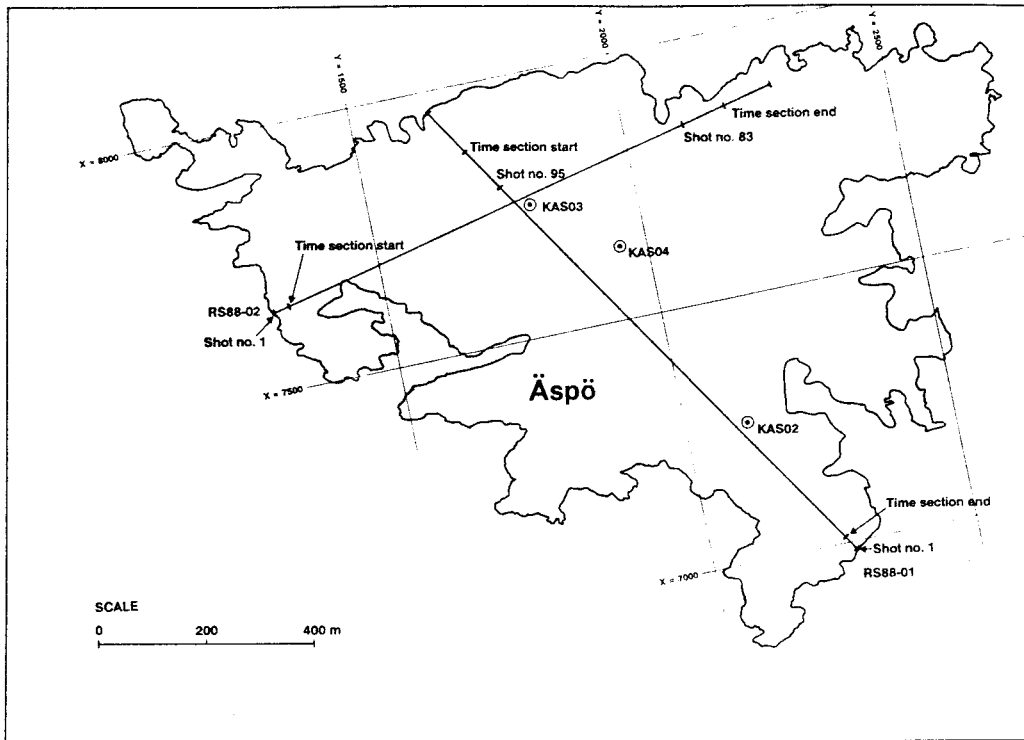
Figure 2-5. Reflection seismics location map.

Field Procedure

The parameters for the reflection seismic data acquisition were determined in accordance with the results from a test survey carried out 1987 on the island Ävrö, 1 km SE of Äspö /Plough and Klitten, 1988/.

The spread consisted of 24 geophones spaced at 10-metres centres and placed along the profile lines. The shot points were placed on the geophone line for each 10 metres, and with a 60-metres shot offset to the first geophone, resulting in a subsurface coverage of a Common Shot Point (CSP) gather on 115 metres, and in the possibility of a 12-fold Common MidPoint (CMP) stacking. In the successive shots, the source and the spread were moved in the geophone spread direction.

The energy source was 110 grams of Nobel Prime explosives, detonated electrically in boreholes drilled in advance by a local contractor. The proposed design was to drill the boreholes at least 1 metre into the hardrock with a diameter varying from 22 mm to 37 mm. The boreholes were tamped with sand and water before blasting. The depths of the boreholes varied from 1 to 8 metres according to the thickness of the overburden.

The geophones were 10 Hz single geophones placed on a 3/8 inch iron pipe situated in drilled boreholes for optimum contact with the bedrock.

The seismic instrument was a 24 channel ABEM Terraloc with a 8 bit A/D converter, which generally does not give the best resolution. However, an adequate field procedure ensured the highest possible amplifier gain in relation to the background noise, so the reflected signals could be recorded with the highest resolution.

The record time was 500 msec, providing a record nearly 1500 metres deep. The sample rate was 2000 samples/sec.

DISCUSSION

When comparing the depth sections with the observation of fractured zones in the three KAS boreholes the upper energy band (zone A) on profile RS88-01 from 300 to 500 metres depth could indicate a more or less interconnected system of heterogeneities, which can be correlated to the observed fractured zones in the three KAS boreholes between the depths of approximately 280 and 400 metres. This upper band (zone A), with reflectors, is not very pronounced in profile RS88-02, but it is there, (Figures 2-6 and 2-7).

The two very prominent reflectors in RS88-02 in the deeper energy band (zone B) are located at a depth of 1000 — 1050 metres at the intersection with profile RS88-01. On the latter profile the two reflectors can be correlated to the two strong, but irregular events from stations 0 to 200. Those reflectors as well as the main part of zone B are, however, on both profiles seated deeper than the bottoms of the two boreholes KAS 02 and KAS 03.

As regards the depth profiles it is necessary to mention that the assumed vertical velocity profile was evaluated from the variation in the time interval on the sonic logs, without being integrated or verified/corrected by reference to a well velocity log. The vertical velocity may be a little lower than the assumed 5600 — 5800 m/sec, which will result in less depth to the seismic events in the depth sections. However, the inaccuracy of the depth is much less than 10%, because a 10% reduction in depth would require a vertical velocity as low as 5200 m/sec, which is unlikely.

CONCLUSION

The investigation identified two subhorizontal zones situated at depth intervals of 300 — 500 metres and 950 — 1150 metres along both profiles and characterized by several rather short and irregular reflectors. However, two rather planar and strong reflectors do occur in the deeper zone of RS88-02 and are approximately 300 metres long. The same reflectors, but shorter and more irregular, can likely be identified in RS88-01.

Both zones are probably reflecting a system of more or less interconnected and irregular heterogeneities of fractured and weathered rock mass. Based on the much higher intensity of events in the deeper zone than in the upper one, the deeper zone must be expected to contain many more heterogeneities and to be a more strongly techtonically affected and coherent zone than the upper one. In general such large, subhorizontal techtonically affected zones cannot be expected to constitute well defined planar, regular and widespread reflector horizons as are typical of layer boundaries in sedimentary rock sequences. Instead, they will occur as more or less planar zones with varying contrast in the physical conditions along very irregular boundaries and constitute a very inhomogeneous, fractured and weathered rock mass. Consequently their "footprints" on seismic sections will be different from what is normal for sedimentary reflectors.

Figure 2-6. RS88-01, Stacked Depth Section (scale 1:7,500).

CSP processing: *Frequency filtering (10 — 230 hz), scaling (AGC 150 msec) and velocity filtering (fan 20 hz, 3000 m/s).*

CDP processing: *Residual static correction (optimized energy in time window 280 — 420 msec).*

TSC processing: *Frequency filtering (10 — 230 hz) and scaling (AGC 150 msec).*
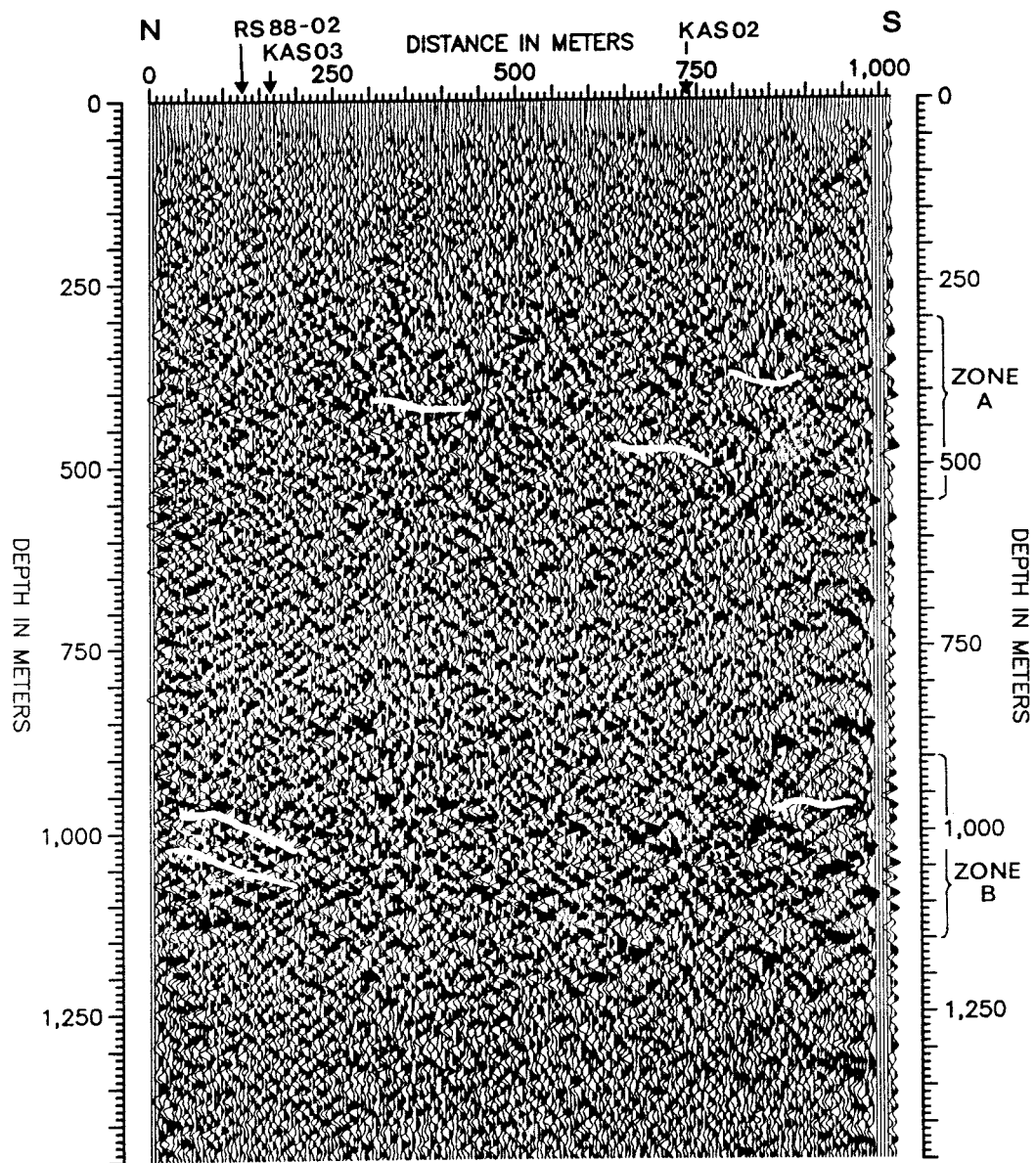
Figure 2-7. RS88-02, Stacked Depth Section (scale 1:7,500).

CSP processing: Frequency filtering (10 — 230 hz), scaling (AGC 150 msec) and velocity filtering (fan 20 hz, 3000 m/s).

CDP processing: Residual static correction (optimized energy in time window 280 — 420 msec).

TSC processing: Frequency filtering (10 — 230 hz) and scaling (AGC 150 msec).
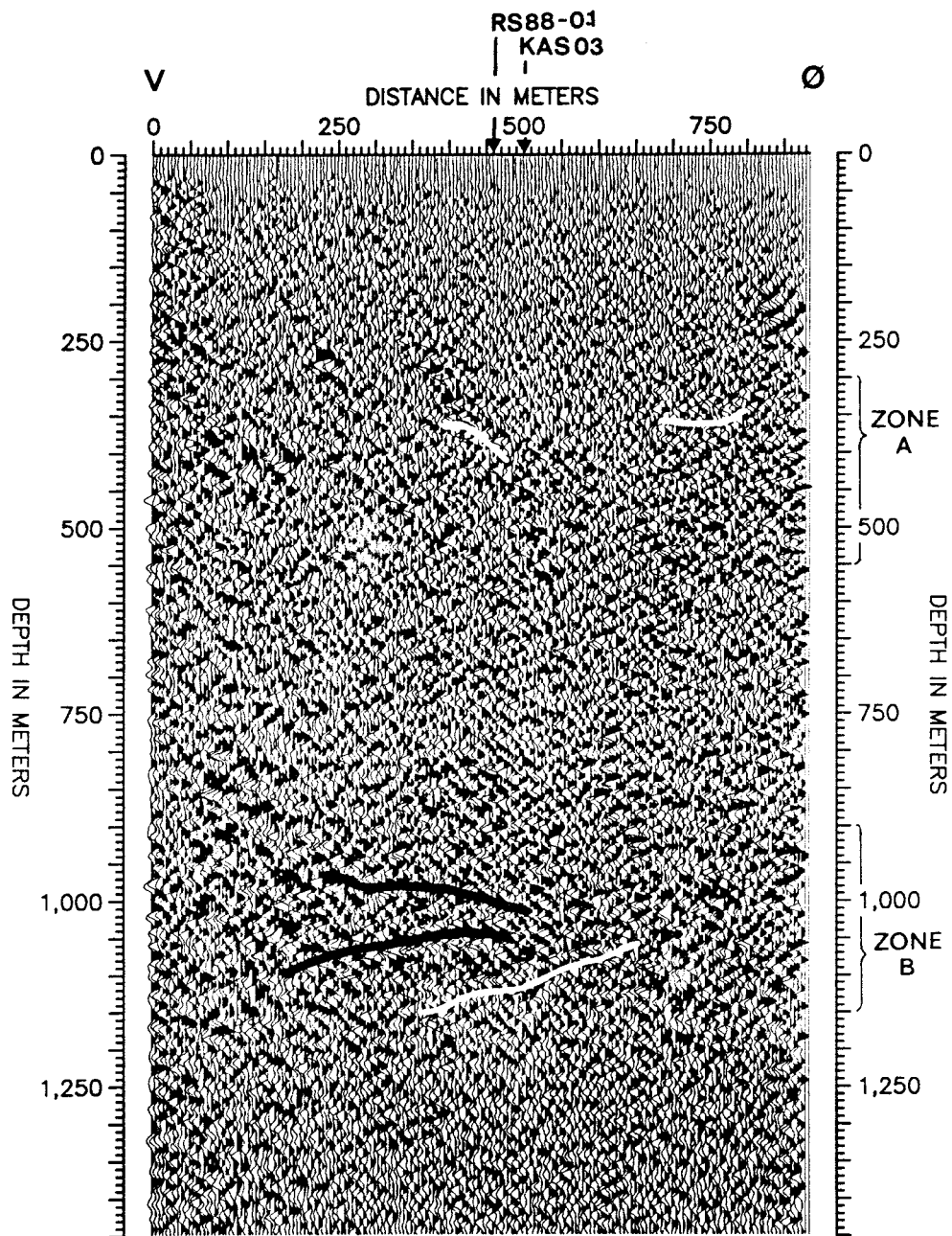
2.1.3 Structures and Tectonic History of Äspö

In 1987 Talbot-Riad reported the results of a regional study on the main tectonic zones in the Simpevarp area. In 1988 Talbot-Riad-Munier concentrated their studies of the geological deformation structures to the island of Äspö and the adjoining islands to the east of Äspö. The field results are summarized in the following short description.

Grey megacrystic granodiorite, with a few thin metabasic sheets, forms most of the surface of Äspö. The red two-mica granite is exposed on Ävrö but may extend northwards beneath a gently dipping ductile thrust to underlie parts of Äspö. Both these granitoids are Småland plutons. The aplite-veined metabasic sheets, the xenolith swarms and slight lithological variations within the granodiorite of Äspö are folded twice. Only two minor examples of the earlier folds were observed, but both are almost recumbent, with axes plunging north. The oldest foliation, S1, is axial planar to these folds.

The initial orientation of S1 was probably subhorizontal. Such an attitude may have survived in the south of Äspö, and is represented by a gentle sheet-dip over the remainder of the islands. However, S1 is steep over most of Äspö because of a second set of tight, asymmetric folds, which refold the earliest folds and are more obvious. The later folds are upright with a steep axial planar foliation dipping NNW and hinges which plunge rather gently to both the ENE and WSW. Only locally is it possible to distinguish the two early foliations. They generally combine to produce a compound gneissose fabric which varies from planar in the limbs of the later folds to almost linear near their hinges.

Strain ellipsoids describing the combined bulk effects of the compound foliation have been constructed for back-veined metabasic sheets at two localities. These are similar in orientation and shape, both to each other and isolated inclusions elsewhere on Äspö. Such data indicate that the early bulk ductile strain history involved shortening along a subhorizontal SSE axis, maximum extension along a subvertical axis and rather less extension along a subhorizontal WSW axis.

Both the first two deformations in the Småland granitoids of Äspö were remarkably ductile with unusually low competence contrasts between the aplites and the coarse-grained granitoids. They are provisionally attributed to the rise and lateral spreading at their levels of neutral buoyancy of diapirs of Götemar and Uthammar granite c.1400 Ma ago. This interpretation implies that the compound foliation should be concentric and localized around the younger diapirs. However, this does not appear to be so, the foliation appears to strike EW throughout the region at least as far south as Oskarshamn. Recent, 1840—1760 Ma zircon dates for Småland granitoids /Jarl and Johansson, 1988/ suggest that the EW tectonic grain may be due to Sveccofennian deformation.

Once the steep EW penetrative fabric was established at least 1400 Ma ago, its anisotropy appears to have influenced all subsequent deformation of the rocks on Äspö. The bulk kinematics of the first ductile shears through the younger semi-ductile vein systems and still younger brittle fracture zones appear to have been remarkably similar in general location and geometry. The major zones are subhorizontal, or subvertical with "N-S, NE, E-W and SE" trends parallel, perpendicular and approx. 45 degrees to the regional foliation; this logic implies that some fracture zones may be found with dips at about 45 degrees. Left-handed ductile shear movements changed to right-handed faults and fracture zones, but all regional displacements appear to have occurred along the same planar zones (Figure 2-8).
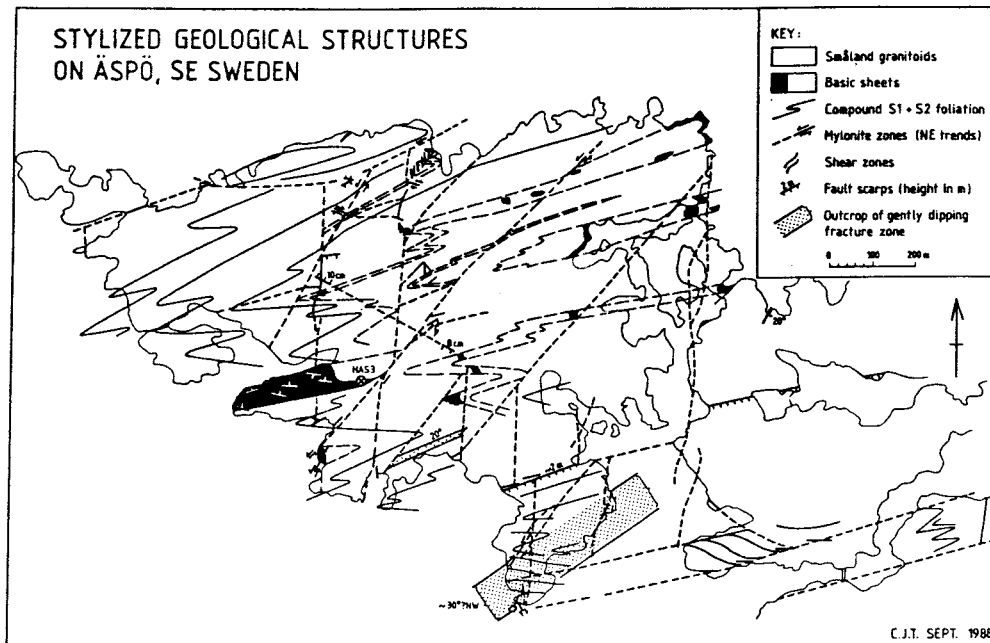
Figure 2-8. Stylized geological structures on Äspö, SE Sweden.

Details of representative examples of all the major movement zones (except the poorly exposed subhorizontal fracture zones) are in hand for their ductile, semi-ductile and brittle phases.

THE MAIN EW-ENE SHEAR AND FRACTURE ZONE

What appears at the surface to be one of the most obvious fracture zones on Äspö is developed along the southern margin of a mylonitized sheet of aplite or microgranite. The mylonite strikes N 70° E and dips steeply north. Epidotic mylonite strands, and chloritic faults define early metre-scale reversed dip-slip shear pods within this zone.

Several sets of "empty" (at surface) fractures are closely spaced in a few metre-wide zones. It is likely that the anisotropy of permeability is high along the closely spaced D (displacement) fractures which opened the steep N 70° E foliation along the zone. However, as most of the fracture sets trend NW with dips between 0 and 90 degrees the greatest permeability within the zone is expected to be along their common intersection axis. This is horizontal across the zone.

THE MAIN NNE-NE SHEAR AND FRACTURE ZONE

Steep, superposed zones of ductile shear and brittle fractures with NE strikes are common on Äspö. An example forms the major Mylonite Zone trending about N 35° E degrees through the centre of the island. This zone is several metres wide and is known to extend several kilometres to the SW of Äspö /Kornfält & Wikman 1987/. Comparatively few of the constituent fractures are actually parallel to this zone as most belong to a steep, en-echelon set striking NW. These are conjugate Riedels with respect to the N 35° E zone but reactivated part of an earlier pattern. Other fracture sets defined rhomboids with steep axes which presumably define a steep axis of high permeability within the zone.

A NW SHEAR AND FRACTURE ZONE

Fracture zones trending NW differ from the others in being rarely superposed on ductile shear zones and having few subhorizontal fractures. They generally consist of three classical fracture sets. The displacements of NW zones are too small to be certain of their sense, but they appear to be right-lateral strike-slip.

N-S SHEARS AND FRACTURE ZONE

Several zones of siliceous epidotic with semi-ductile shears <6010 cm wide, trending N-S, anastomose across Äspö. They define to a smaller scale patterns very similar to those shown by their first order equivalents of regional extent /Nisca 1987, Tirén et al 1987/. Such self-similarity persists to the outcrop scale where shear pods trending NS only decimetre-long and centimetre-wide occur. Because of their orientation, these zones are well exposed along the N-S trenches and coasts and detailed studies have revealed how they were initially ductile, became semi-ductile and then brittle. The younger, brittle zones are wider than the preceding more ductile zones and have fracture sets with orientations seen in the zones of other orientations.

As most workers on Äspö have already noted, the aplites have been particularly competent and prone to fracture much more readily than the other rock-types since the region became increasingly brittle as it cooled below temperatures of about 200 degrees C. This was the reverse of the competence contrast at higher temperatures because the aplites preferentially mylonitised and contain fewer epidote veins than other rock-types.

A well developed mature N-S fracture zone is well exposed in megacrystic granite on the southern coast of Äspö. Three sets of closely spaced R', R and D fractures (without any opening of the foliation) together indicate left-handed strike-slip shear at the brittle stage. Unexpectedly, the three sets do not share a common axis of intersection. This means that the anisotropy of hydraulic conductivity might have bimodal peaks about a horizontal axis across, rather than along, this fracture zone.

A GENTLY DIPPING FRACTURE ZONE?

Many of the fractures observed along the trench in southern Äspö have gentle dips and appear to lie in a zone trending N 60° E. They have tentatively been interpreted as lying in a zone dipping about 20 degree NNW. Variations in the dip

of the foliation measured along the same part of the trench can be interpreted in two very different ways: as due to folding or shearing. The interpretation may have to be modified in the light of further information.

ANISOTROPIC HYDRAULIC CONDUCTIVITY WITHIN FRACTURE ZONES

Structural geological observations offer some qualitative insight into how fracture zones and their internal permeabilities developed at stages labelled by different mineral infillings. As elsewhere in Sweden, the current bedrock permeability of Äspö is probably generally localized along old planar fracture zones re-opened by solution, by post-Cambrian tectonics and/or by sub-glacial hydraulics. Most but not all vein and fracture zones in Äspö reactivated old ductile shear zones. Such zones of ductile shear are not permeable as such. However, indications of ductile shear are often wider than the brittle fracture zones within them; they are therefore useful indications of nearby fracture zones. A gently dipping fracture zone in the south of Äspö was first noticed because of the gentle foliation there.

The majority of fractures within any particular zone are oblique to it. It is therefore necessary to map the envelope to the fracture tips to define the zone. This is particularly difficult for gently dipping fracture zones in an area of low relief and fracture zones which did not reactivate older zones of ductile shear. Some such zones exist on Äspö but neither their distribution nor their controls have yet been studied.

Figure 2-9 is a series of sketches indicating how the steep N-S fracture zones developed within older zones of ductile shear with different degrees of strain on Äspö. Similar processes occurred in the zones with other orientations. Single planar veins characterize most (50%?) of the areas of such zones at the stage when epidote was circulating. These planar channels dilated by fluid pressure were not in line at low strains and diffusion occurred across their offsets, the jogs, or asperities of seismologists (Figure 2-9c). Further strain led to complex zones of strongly en-echelon fractures joining the slightly en-echelon planar shears (Figure 2-9d). Such joins became strike-slip fault duplexes with further strain (Figure 2-9e centre). These duplexes have characteristic shapes on scales ranging from centimetres to tens of kilometres and represent local channels of high permeability along the generally planar zone. Unexpectedly, all fractures appear to dilate, but particularly those at large angles to the shear stresses resolved along the zone. Later, the en-echelon fractures appear to spread beyond pre-existing duplexes (Figure 2-9e) and in some cases were eventually joined by increasing numbers of fractures parallel to the whole zone (Figure 2-9f).

Assuming that the permeability of any zone relates to the orientation, aperture, spacing, length and amount of connection of constituent fracture sets implies that the permeability within each zone is anisotropic. Whether this anisotropy can be considered sufficiently homogeneous to be approximated by an ellipsoid is unknown. At every stage of development, the maximum number of fracture intersections (and therefore the vector of maximum permeability) is along the zone perpendicular to the direction of latest shear displacement. The intermediate axis of permeability lies across the zone at an early stage (Figure 2-9d) but presumably the zone after a significant number of fractures parallel to the displacement surface (Figure 2-9f).
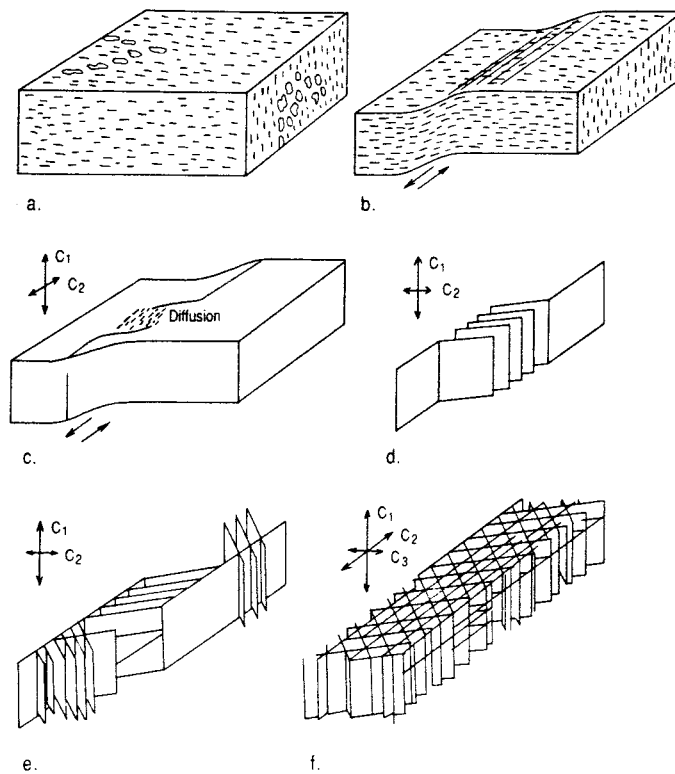
Figure 2-9. The development of a strike-slip fracture zone along a previous zone of ductile shear on Äspö. The sequence shown is based on different examples of N-S zones which have developed to different stages. Vectors of "relative hydraulic conductivity" indicate how the anisotropy of permeability within the zone changed with the strain history.

a. The steep, N 80° E compound fabric with an upright fold indicated by a xenolith train.

b. A ductile shear zone a metre or so wide may be kilometres long.

c. The first veins (epidote + quartz) dilate planar fractures which are offset. Dispersed epidote indicates diffusion from vein to vein.

d. Later fractures begin to bridge the earlier gaps in the permeability along the zone.

e. Further fractures are oblique along the zone with most intersections being vertical.

f. A mature N-S fracture zone at the surface and its "apparent anisotropy of permeability". Because open fractures may be filled at depth, the relationship between the apparent and actual permeability is unknown.

The steep zones of ductile and semi-ductile shear on Äspö were strike-slip for most of their history. As a general rule, the maximum permeability among them can therefore be expected to be vertical. (Figure 2-10).

The dip of the major, gently dipping fracture zone known at surface in the south of Äspö is not certain because no depth constraint is possible on the boundaries to the zone. Many of the internal fractures dip 80 degrees or less to the NNW, but the zone itself could dip SE like minor examples. However, whatever its dip, most of the intersections likely to define the vector of maximum permeability trend N 60° E and are horizontal. It is not yet clear whether the inter-

23
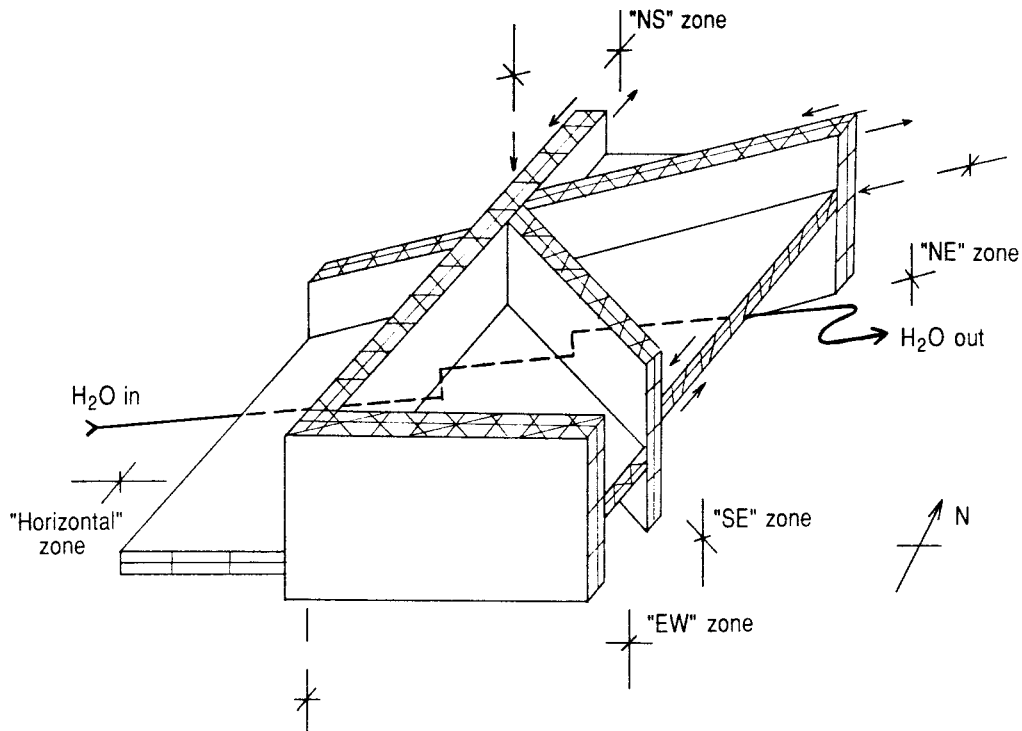
Figure 2-10. A sketch illustrating:

a. How the steep fracture zones of five different orientations could consist of diffe-
rent combinations of the same five fracture sets. This is a simplified working model.

b. Our current picture of the anisotropy of apparent permeability (based on the num-
ber of intersections in different orientations) is indicated for major fracture zones of
all five orientations. The maximum number of intersections is along the intermedia-
te stress axis. Because all the steep zones are the result of strike-slip, their vectors of
maximum permeability are expected to be vertical. Intersections of steep fracture
zones represent subvertical linear channels (pipes). Subhorizontal zones appear to
be thrusts with their vectors of maximum internal permeability parallel to their N 60°
E strike.

c. If any of the subhorizontal fracture zones have been opened (by glacial hydrau-
lics?) they are likely to be the most significant hydraulic conductors. Our work to date
indicates that the path of least resistance to groundwater flowing laterally under Äspö
would be generally N 60° E along the subhorizontal zones, with vertical sections in
any steep zones which offset them. Such a flow path is indicated.

mediate axis of permeability is perpendicular to the zone or parallel to it and
down dip. In either case, gently dipping fracture zones are the only zones recog-
nized so far to have nearly horizontal maximum permeability vectors. They are
therefore probably the most intrinsically permeable to subhorizontal
groundwater flow whether or not they were opened by glacial hydraulics.

One of the working models being considered by Raymond Munier is that the
general geometry of any fracture zone subjected to shear can be rotated in
three-dimensional space to look like any other. Figure 2-10 is a sketch illustrat-
ing this possibility for the steep zones and accounts for a large proportion of our
data (but not all observations in the subhorizontal zones).

The offsets of shear and fracture zones of one orientation by others of other orientations imply that groundwater flow will be along one zone for distances of 100 or 200 metres or so, and then move along another zone before reaching and perhaps flowing along another segment of the first permeable zone. Assuming that gently dipping fracture zones are the most permeable implies that lateral flow will rise or fall vertically in the steep fracture zones to other segments of the same fracture zone offset to other levels. Such a flow path is indicated by a heavy line on Figure 2-10.

2.1.4   Fracture Mapping

A fracture mapping programme has been carried out within the frame of the detailed preinvestigations for the SKB Hard Rock Laboratory /Ericsson, 1988/. The mapping has mainly been done on outcrops following the two cleaned N-S profiles on Äspö island. The principal aim of the fracture mapping measurements has been to produce results for geohydrological and rock mechanics model studies. The project report includes in different manners geographically integrated results, regarding strikes, dips, fracture densities, fracture lengths and spacing.

The fractures, exceeding 0.5 m, have been measured on outcrops which have surface areas from about 30 m² to 200 m². A description may thus be made for the geometric fracture structures of an outcrop, where the outcrop is considered as a geological unit. This observation scale could be considered mesoscopic.

The outcrops concerned have not been stochastically chosen on the island. The choice of outcrops mainly follows the two N-S profiles where the bedrock has been cleared of overburden.

The requirement of fractures during a surface cell mapping is about 100—150 fractures per outcrop. The assembling of data on the two rather narrow exploration profiles has implied that there is a relationship between the fracture density and the surface area. This may to some uncertain extent influence the evaluation of data (see Figure 2-11).

Summarized rosette diagrams shows predominant sectors around N 60° W, N 5° W and N 60° E. E-W fractures are more scarce but still occur in a more narrow, prominent peak (see Figure 2-12). About 85% of the 4500 mapped fractures are steep with dips in the interval 70°—90°. The relatively few observed inclined fractures with dips in the interval 0°—65° show predominant strikes around N 60° E and dip mainly to the north. The foliation is common in N 60° E — N 80° E and has implied a fracture frequency increase within the sector in question (see Figure 2-13).

The apertures have not been measured but fractures with widths of millimetres have been noted. The so-called open fractures verify the brittle pattern with a predominant peak at N 55° W. An obvious similarity between the rosette diagrams of the open fractures and the red-stained fractures has been found (see Figures 2-14 and 2-15). Quartz-filled fractures strike N-S and E-W.

Within the exploration profiles, twentyfive fracture zones, have been observed. These zones strike mainly E-W and coincide with the Mylonite Zone direction at N 55° E.

A distribution fitting test (Chi-square) showed that the data are log-normal distributed in respect of fracture density. The log-normal behaviour also includes the fracture lengths.
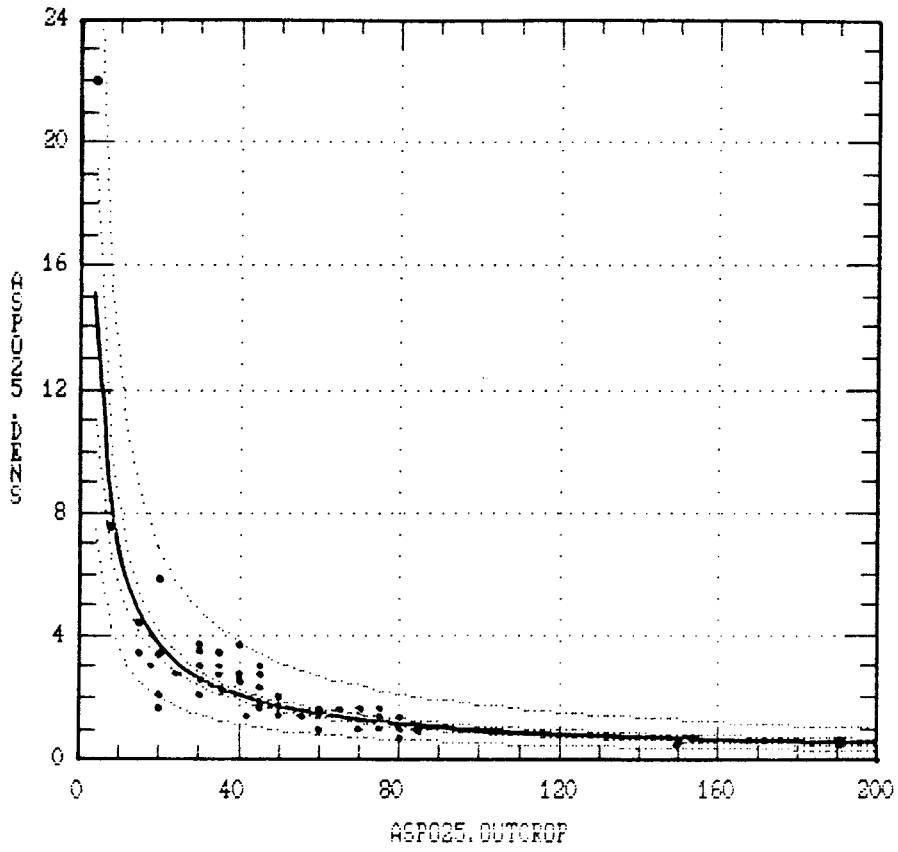
Figure 2-11. Fracture density (all 52 outcrops) versus outcrop area, (Y=46.5 x X$^{-0.84}$).

3666 FRACTURES

282 FRACTURES CORRESPOND TO RADIUS
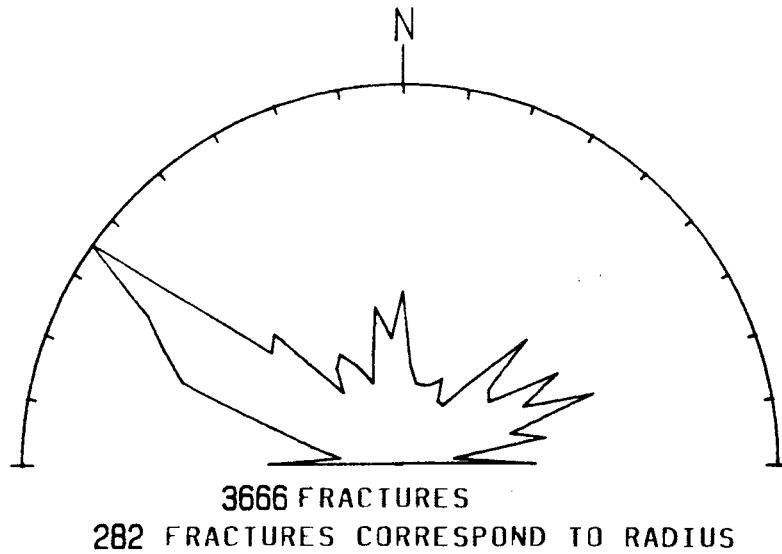
Figure 2-12. Rosette diagram for all mapped outcrop fractures with dips 70°—90° (cell 141—176, 179—194) on Äspö island.

279 FRACTURES
69 FRACTURES CORRESPOND TO RADIUS
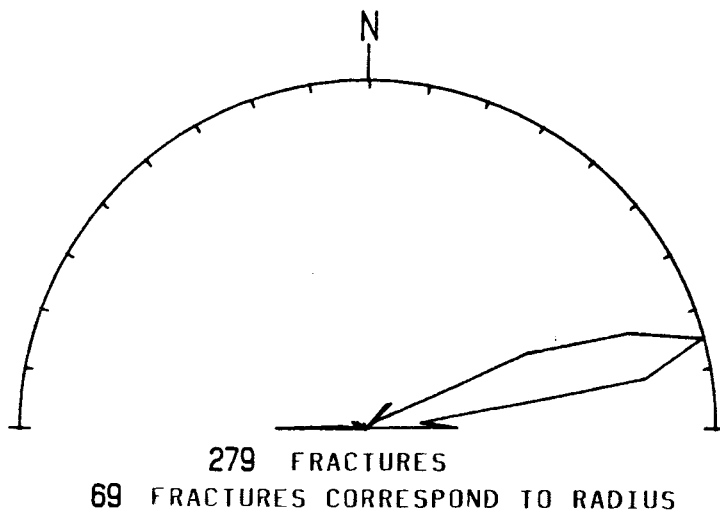
Figure 2-13. Foliation fractures, dips 0° — 90°.

QUARTZ

70 FRACTURES
6.75 FRACTURES CORRESPOND TO RADIUS

EPIDOTE

388 FRACTURES
21.75 FRACTURES CORRESPOND TO RADIUS

RED STAINING

499 FRACTURES
41.75 FRACTURES CORRESPOND TO RADIUS
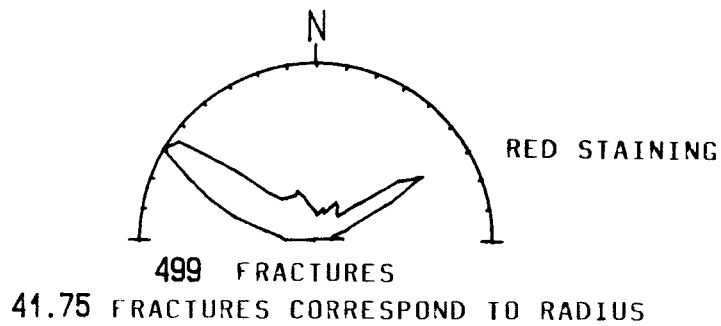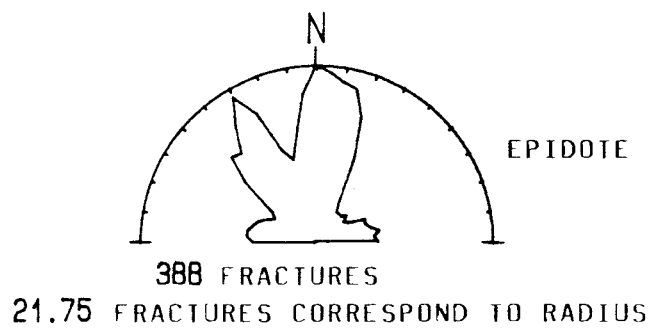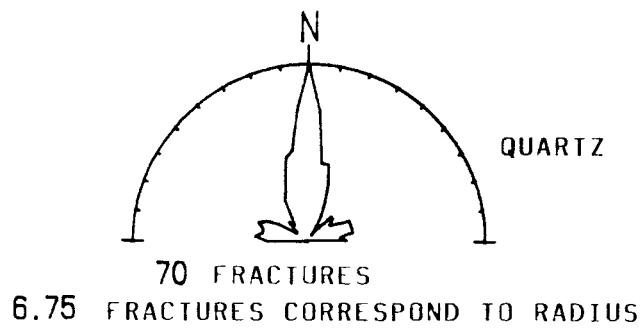
Figure 2-14. Rosette diagram, filtrated and summarized for Äspö island with fillings of quartz, epidote, and fractures surrounded by red hematite staining. Dips 0° — 90°.
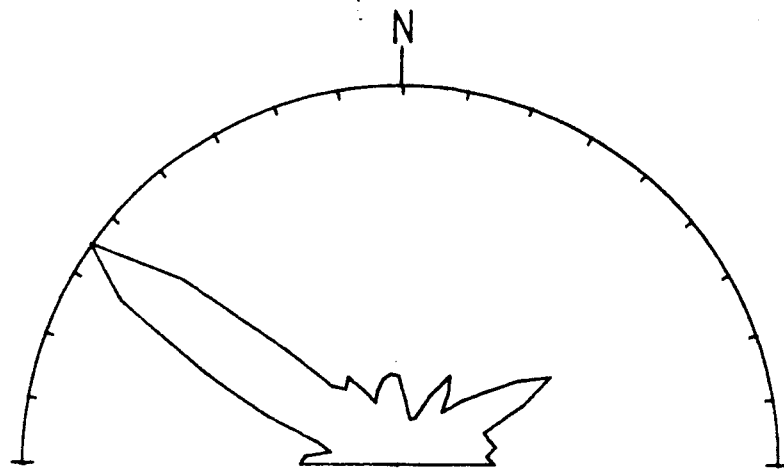
837 FRACTURES

75 FRACTURES CORRESPOND TO RADIUS

Figure 2-15. Observed open fractures, filtered values, dips 0 — 90°.

In respect of the bedrock type, the longest fractures are found in the porphyritic granite and the shortest ones in the mylonite. The fracture density of the fine-grained granite is significantly higher than that of the porphyritic granite (level of significance = 1%) (see Tables 2-1 and 2-2).

Table 2-1. Fracture lengths in different rock types.

Bedrock type	Amount No.	Geom mean x metre	Confidence interval for geom. mean (median) 95% level	Estimate stand. dev. $\log^{\wedge} \sigma$
Granite to granodiorite, porphyritic greyish-red to red	3494	1.05	1.01 − 1.08	0.35
Greenstone	198	0.80	0.72 − 0.89	0.35
Granite fine-grained, greyish red to red	768	0.90	0.85 − 0.95	0.35
Mylonite	53	0.40	0.31 − 0.51	0.39

Table 2-2. Fracture density data, different rock types.

Bedrock type	Number of out-crops	Mean (median) numbers per m^2	Confidence interval for mean 95% conf. level number per m^2	Estimate of stand. dev. log$^\wedge \sigma$
Granite to grano-diorite, porphy-ritic greyish red to red	39	1.75	1.45 − 2.12	0.25
Granite fine-grained, greyish-red to red	9	3.44	1.74 − 6.80	0.38

The outcrops have been grouped into three classes according to their situation on Äspö island, i.e. the Northern Block, the Mylonite Zone and the Southern Block (see Figure 2-16). The Mylonite Zone has a predominant sector around N 60° E. Within the Southern Block the N 55° W fractures dominate strongly. The Northern Block is relatively more homogeneous but four conspicuous sectors appear around E-W, N 60° W, N 5° W and N 60° E. The Mylonite Zone has a higher fracture density (85% conf. interval for the geometric mean)
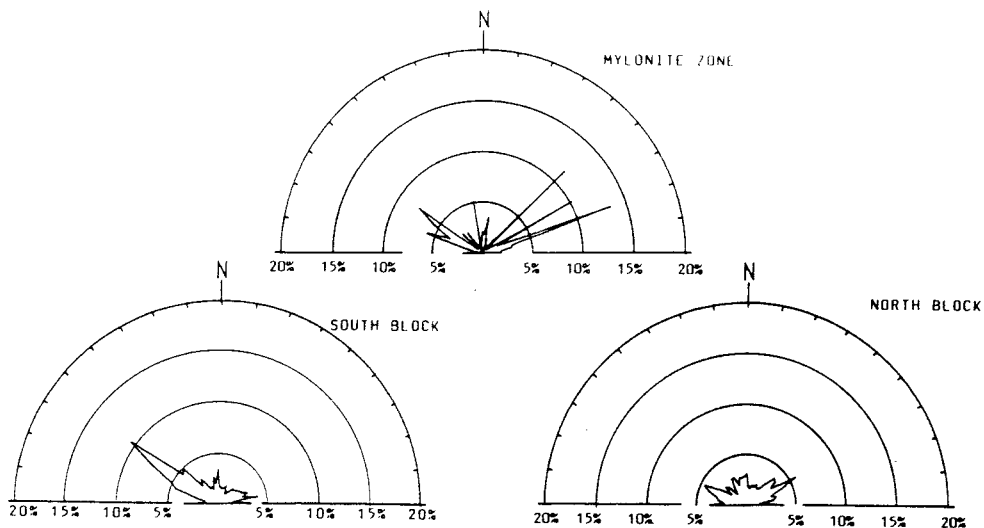
Figure 2-16. Tectonic fractures in samples from the northern and southern parts of Äspö island as well as samples from to the Mylonite Zone.

than the surroundings and the Southern Block is more fractured than the Northern Block.

Figure 2-16 shows the corresponding normalized rosette diagrams. The Mylonite Zone has a main peak which coincides with the direction of the Mylonite Zone. The Southern Block has one predominant peak at N 55° W. The Northern Block has a somewhat greater fracture intensity within the sector N 40° E — N 65° E.

For the values of the Northern Block, Mylonite Zone and the Southern Block a stepwise multiple linear regression shows only a few possible significant relationships in respect of how the fracture density and sector frequency percentage are dependent on the geometry. At this moment no tectonic conclusions can be recommended according to these regression results.

By way of conclusion some mean spacing estimates were made within the four sectors, E-W, N 45° W, N-S and N 45° E, for the tectonic blocks. The spacing results reflect what was earlier mentioned about the fracture lengths and sector frequencies, i.e. the Northern Block is rather homogeneous, with mean spacings around 2.0 m. The fractures in the Mylonite Zone are more dense and shorter, with mean spacing from 0.50 m to 1.80 m. The Southern Block seems to be the most heterogeneous, with mean spacings of 0.90 m in the NW direction and up to 2.0 m in the NE direction.

Compared with the previous results in the regional study this analysis shows confident determinations and estimations regarding strikes, dips, lengths and fracture densities. The former conductive fracture mean spacing evaluations of Äspö /Ericsson, 1987/, seem, however, to be somewhat overestimated because fractures which are crossed by more than two other fractures were neglected.

2.1.5 Detailed Geomagnetic and Geoelectric Mapping of Äspö

This report presents a detailed analysis of the total ground magnetic total field measurements and resistivity profiling over Äspö and puts the results in a regional to semi-regional perspective /Nisca-Triumph, 1989/.

Measurements were made every fifth metre along profiles in an east-west direction, with profiles at 10-metres centres in the geomagnetic survey and at 40-metre centres in the geoelectric survey.

Magnetic Surveying

In magnetic measurements, variations in the natural magnetic field of the earth are measured. Anomalies in the total magnetic field are caused by the fact that magnetization of different types of rock is different, resulting from contrasts in magnetic susceptibility or remanence within the rocks.

The variation in magnetic susceptibility is, in principle, proportional to the volume content of magnetic minerals, mainly magnetite and magnetic pyrrhotite, in the rock. The distribution of these magnetic minerals in a rock introduces a pattern of anomalies characteristic for the rock type.

Magnetic dislocations (fractures, faults) are interpreted from distortions and magnetic minima in the magnetic anomaly pattern.

A local decrease in the magnetic susceptibility within a magnetite bearing rock unit, causing the magnetic minima, is due to low-temperature alteration of magnetite to hematite. In general these minima, including disturbed anomaly patterns, indicate both open and closed fracture zones.

Geoelectric Surveying

In geoelectrical mapping the variations in electrical resistivity are measured along profiles. An electrical current is transmitted into the earth through two current electrodes from a transmitter circuit. The resulting potential field in the earth is measured by means of a receiver circuit containing two non-polarizable potential electrodes. The transmitting and receiving electrodes may be arranged in several different geometrical configurations.

Apparent resistivity is calculated on the basis of transmitted current, potential difference between receiver electrodes and a correction factor, which is depending on the geometrical configuration of the electrodes. This apparent resistivity is dependent on the distribution of electrically conducting material in the earth.

Fracture zones in crystalline rock may be sealed or open. In open fractures, water is often found provided that the groundwater level is high enough. Since water is a good conductor in comparison to fresh granite, as present at Äspö, low-resistivity anomalies should be encountered near vertical/sub-vertical fracture zones. Clay is also common in fracture zones as filling material. It is, however, normally difficult to distinguish clay from water solely by electrical mapping. Thus if a low-resistivity zone exists it is interpreted as open, but with water or clay as filling material.

As mentioned above several different geometrical arrangements of current and potential electrodes can be used in geoelectrical mapping. In order to effectively map relatively narrow zones (2- m thick), and low-resistivity zones near the surface, a 5-10-5-metre dipole-dipole configuration was used.

Analysis of Geomagnetic Data

Principal bedrock and tectonic analysis from geomagnetic data.

The detailed ground-magnetic measurements are shown in different types of processed map to a scale of 1:5000 (Figure 2-17), magnetic colour map and horizontal magnetic gradients (Figure 2-18).

A principal interpretation of the magnetic data is presented in Figure 2-19, showing the main bedrock units and fracture zones. The island of Äspö is divided into three main magnetic or bedrock units, the Northern Block (granite), the Central Block (Mylonite Zone) and the Southern Block (granite). The Northern and Southern Blocks exhibit show similar magnetization, indicating that they consist of the same bedrock type, granites.

According to the interpretation map (Figure 2-19) the width of the Mylonite Zone crossing the island of Äspö is estimated at about 300 metres. The dip of the Mylonite Zone at the northern boundary is calculated to about 80°N. The dip of the E-striking, southern boundary is calculated to be about 55°—70° towards the north.

The main E-W fracture zone (Figure 2-19) is about 70 metres wide with a calculated dip of about 60°—75° towards the north.

The most significant vertical and lateral displacements are observed along the E-W fracture zones. From the analysis of both aerial-magnetic and ground-magnetic data, it is obvious that a dextral movement along the E-W fracture zones has displaced the northern and southern parts of the Mylonite Zone approximately 200 metres (Figure 2-19). The main fracture zones are outlined in Figure 2-20.

31
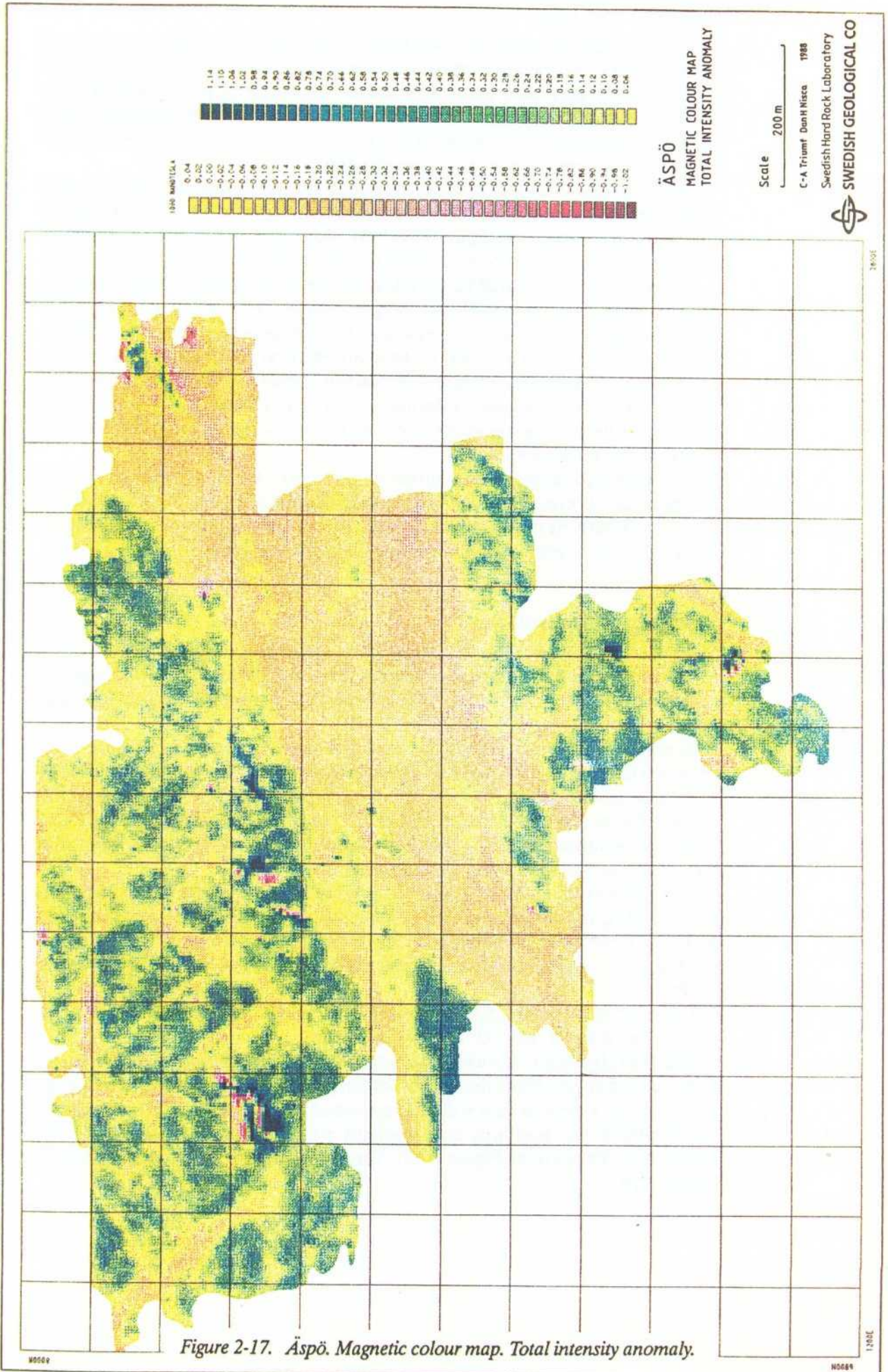
Figure 2-17. Äspö. Magnetic colour map. Total intensity anomaly.

Figure 2-18. Äspö. Horizontal magnetic gradients. Colour composite.

North-South, green illumination from south
East-West, red illumination from west

Steeper gradients give higher intensity

(red-magenta)   N   black

(red)   W   +   E

(yellow)   S   (green-cyan)

(green)
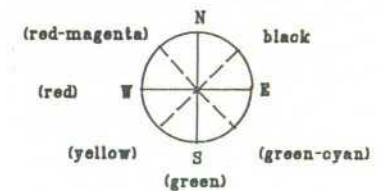
ÄSPÖ

HORISONTAL MAGNETIC
GRADIENTS

COLOUR COMPOSITE

Scale ⌐   200 m   ⌐

Image Data Analysis -1988

Swedish Hard Rock Lab

SWEDISH GEOLOGICAL CO

33
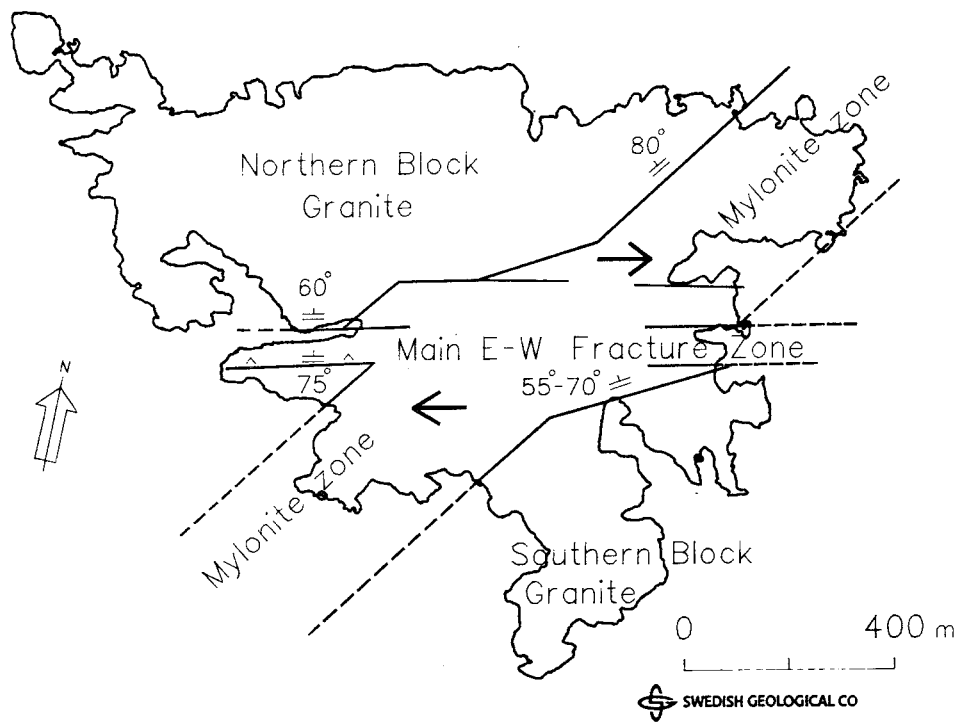
Figure 2-19. Principal magnetic interpretation map with main bedrock units.
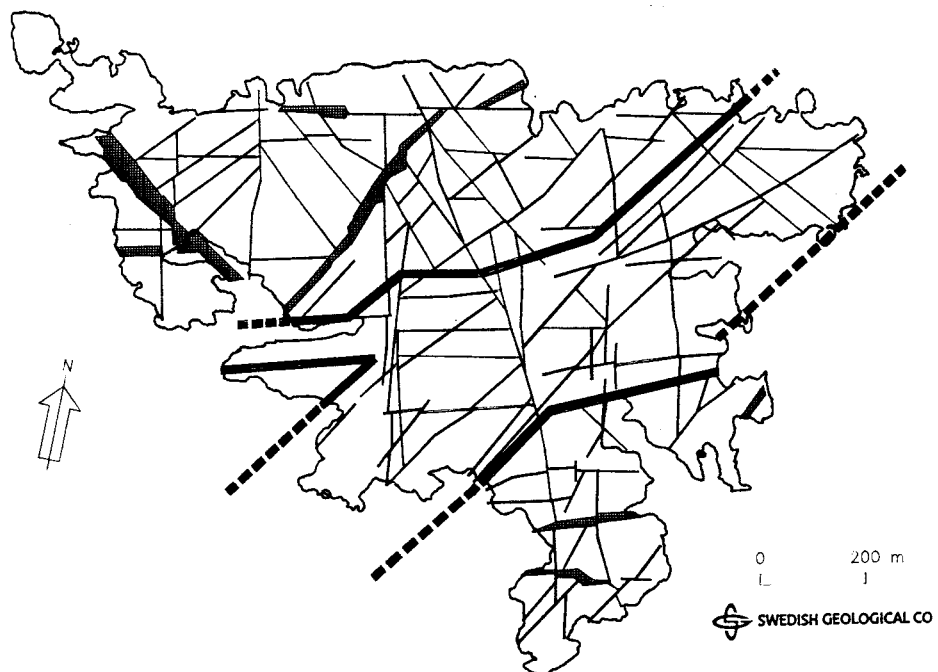
Figure 2-20. Principal magnetic interpretation map with main fracture zones.

Detailed Bedrock and Tectonic Analysis from Geomagnetic Data

A detailed bedrock and fracture interpretation based on ground-magnetic data is presented in Figure 2-21.

Fracture zones and fractures in Figure 2-21 are shown with their estimated widths. The accuracy in the determination of localization and width is closer than 5 metres in the case of structures more or less perpendicular to the profile direction, and closer than 10 metres in the case of structures almost parallel to profiles.

According to the ground-magnetic measurements the island is divided into three main units, the Northern Block, the Mylonite Zone and the Southern Block. The Northern and Southern Blocks have similar magnetizations (Figure 2-17), and the main rock type in both blocks is granite (Figure 2-21).

In the Northern Block, two highly magnetized units are outlined, probably consisting of greenstone (diorite-gabbro). In addition, two semi-rounded magnetic bodies (diameter approx. 25 m) with high magnetizations were detected in the Northern Block. A speculative interpretation of these latter bodies is that they are old pipes or feeding channels from earlier basic magmatism in the area.

The main rock type within the Mylonite Zone is altered granite. Three bodies are outlined within the Mylonite Zone, interpreted as remnants of less altered granite. In the northern part of the Mylonite Zone a highly magnetized body was detected and interpreted as a greenstone remnant.

According to the geological mapping, there are two main strike directions found among the granitic dykes, one parallel to the strike of the Mylonite Zone, and one following the E-W fracture zones. A comparison of the geological mapping and the geophysical interpretation shows that most of the granite dykes in the area are situated in the Mylonite Zone. Granitic dykes appearing outside the Mylonite Zone are generally coupled to fracture zones trending E-W. This indicates two generations of granite dyke.

In the Southern Block three low magnetic areas are isolated and interpreted as greenstones. Two small semi-rounded magnetic anomalies are also outlined.

A large number of fractures and fracture zones are interpreted from the magnetic data, as presented in Figure 2-21. Special data processing was used to distinguish magnetic features within the low-magnetic Mylonite Zone. Both quantitative and qualitative dip estimates as well as vertical and lateral displacements are presented in Figure 2-21.

Fracture Orientation Based on the Magnetic Survey Results

The most frequent fracture orientations found in this study are 10°W and 80°E, which should be compared with the results obtained in the semi-regional study /Nisca, 1987 a,b/. The prominent fracture orientation N-S/E-W found in the semi-regional study indicates that the same fracture set is independent of scale. The conclusion is that the N-S/E-W fracture set is self-similar.

Two fracture populations, N55°W and N35°E, were also found in data from the whole area (Figure 2-22), forming an orthogonal fracture set. The Mylonite Zone and the extensive brittle fracturing within it belongs to the NE fracture population, with a peak value at N35°E.

The fracture orientation within the Mylonite Zone and the Southern Block exhibits local variations from the data for the entire area. The orientation data from the northern and southern boundaries show that almost all fractures affect the boundaries of the Mylonite Zone.

Figure 2-21. Äspö. Magnetic bedrock and tectonic analysis.

36

LEGEND

Bedrock boundary
GA Granite
M   Mylonite zone, altered granite
G   Greenstone (diorite to gabbro)
GAM Granite, less altered granite
    remnants (Mylonite zone)
GM Greenstone, Mylonite zone

Fractures

Fracture, fracture zone with estimated width
Fracture, thin
Faults (fractures) with relative
vertical displacements, arrow indicate downthrown
Faults (fractures) with estimated
relative lateral displacements in metres
Deep seated structure
Dips
Calculated dip, bedrock contact and fracture
Qualitative bedrock contact dip estimation,
steep and intermediate dip angles
Qualitative fracture (fault) dip estimation
steep and intermediate dip angles

ÄSPÖ

MAGNETIC BEDROCK AND
TECTONIC ANALYSIS

Scale

0   100 m

Dan H Nisca C-A Triumf -1989

Swedish Hard Rock Laboratory

SWEDISH GEOLOGICAL CO

Figure 2-22. Fracture orientation (magnetic survey).
Whole of Äspö, Northern Block, Mylonite Zone, Southern Block and the two main block boundaries.

37

Combined Analysis of Geomagnetic and Geoelectric Data

As described earlier, open fractures/fracture zones are probably encountered in areas where the bedrock is covered with till, sediments and organic material. An interaction between apparent resistivity anomalies caused by the relatively low-resistivity overburden and, water or clay-filled fracture zones, could then be expected. In the survey design this inherent problem in the detection of open fracture zones is an important factor to be accounted for, parallel to factors governing the economic effectiveness of the survey. By using complementary information provided by magnetic data, it is possible to make a meaningful connection between low-resistivity zones between profiles, in spite of the large profile distance. Magnetic data also provide information important for the extraction of overburden induced anomalies from anomalies induced by fracture zones.

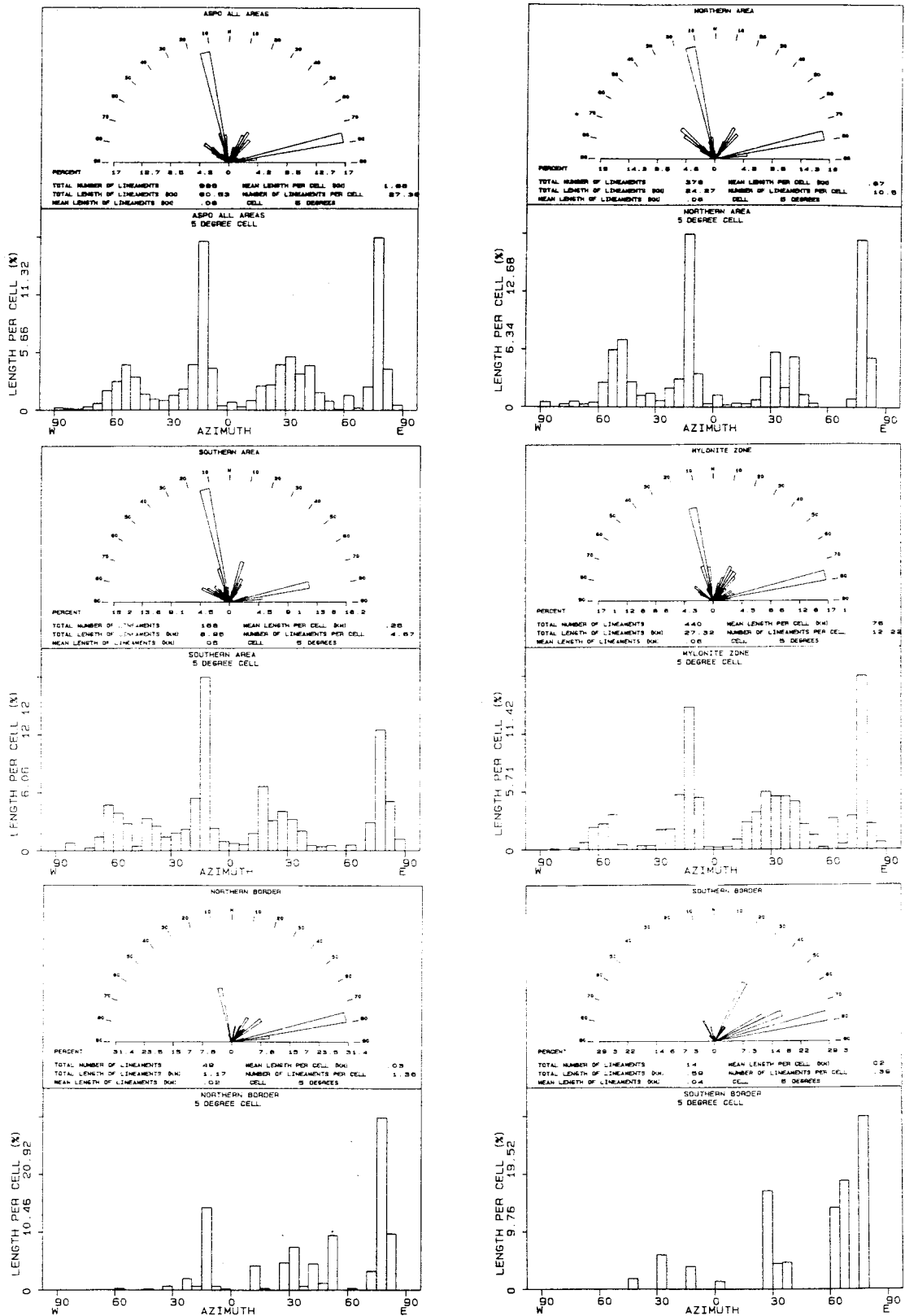Figure 2-23 presents a generalized map of the fractures/fracture zones indicated by both electric and magnetic measurements. Fractures/fracture zones interpreted as open, but filled with water and/or clay, were delineated by combinating geoelectric and geomagnetic data.

It is evident from Figures 2-23 and 2-24 that low-resistivity zones differ somewhat in length and orientation within the Mylonite Zone, in comparison to the Northern and Southern Blocks. Low-resistivity zones are more common in the Mylonite Zone. Furthermore, the mean length of a low-resistivity zone is slightly larger within the Mylonite Zone than elsewhere in the area.

In addition to the low-resistivity zones connected between profiles, several low-resistivity cross-overs are marked along the profiles (Figure 2-24). A part of them are probably caused by overburden effects, but it is also probable that some of them are due to the presence of fractures not indicated by the geomagnetic survey.

It is obvious that a similar principal trend, with two orthogonal sets of fractures as presented for the magnetic data, can be found. This is not surprising as magnetic data has largely controlled the connection of low-resistivity zones between the profiles.

The orthogonal fracture set N-S/E-W (Figure 2-25) is almost consistent in all the three sub-areas, the Northern Block, the Mylonite Zone and the Southern Block. The direction of the second orthogonal fracture set, however, varies from area to area. The fractures in the Northern Block and Mylonite Zone run in similar directions, though the directions of fractures within the Mylonite Zone are more scattered around N35°E. In the Southern Block, however, a shift is obvious in the dominating angle to about N15°E for the same fracture set. Furthermore, the concentration of fracture directions around N55°W, recognizable in the Northern Block and Mylonite Zone, are lacking.

CONCLUSIONS

Fracturing occurs in rocks at all scales, from the micro scale (micro-cracks) to the continental scale (mega-faults) and can be observed under the microscope as well as in ground-geophysical, aerial-geophysical and satellite data.

It is quite obvious that these various scales of fracture are closely related to each other. The orthogonal fracture set N-S/E-W was outlined in the regional scale /Nisca 1987a/ and in the semi-regional scale /Nisca 1987b/. Now the same orthogonal fracture set is outlined in the detailed scale, mostly on the basis ground-magnetic measurements. A 10 degree anticlockwise rotation was observed, however, which is probably explained by local disturbances, diapirs and superposition of other fracture sets.
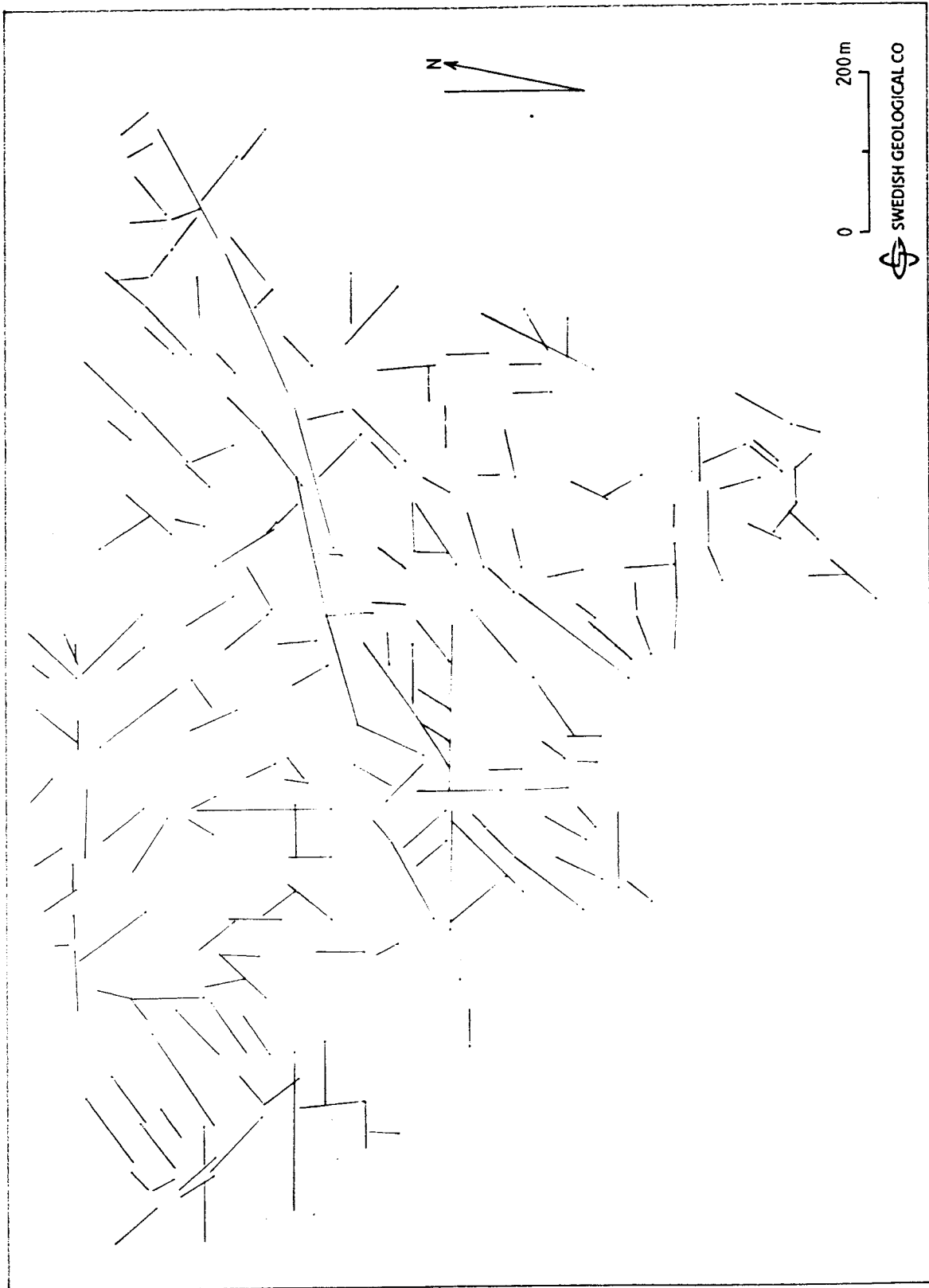
Figure 2-23. Fractures based on electric and magnetic measurements, Äspö.

Figure 2-24. Äspö. Combined analysis of magnetic and electric mapping.

LEGEND

▣ Low resistive zone, distinct
▣ Low resistive zone
▱ Connected low resistivity zones
▰ Low resistivity zone
   semi parallel to profiles
▰ Boundary, main lithological unit

ÄSPÖ

COMBINED ANALYSIS OF
MAGNETIC AND ELECTRIC
MAPPING

Scale

0   100 m
⊢_____⊣

Dan H Nisca C-A Triumf -1989

Swedish Hard Rock Laboratory

SWEDISH GEOLOGICAL CO

40
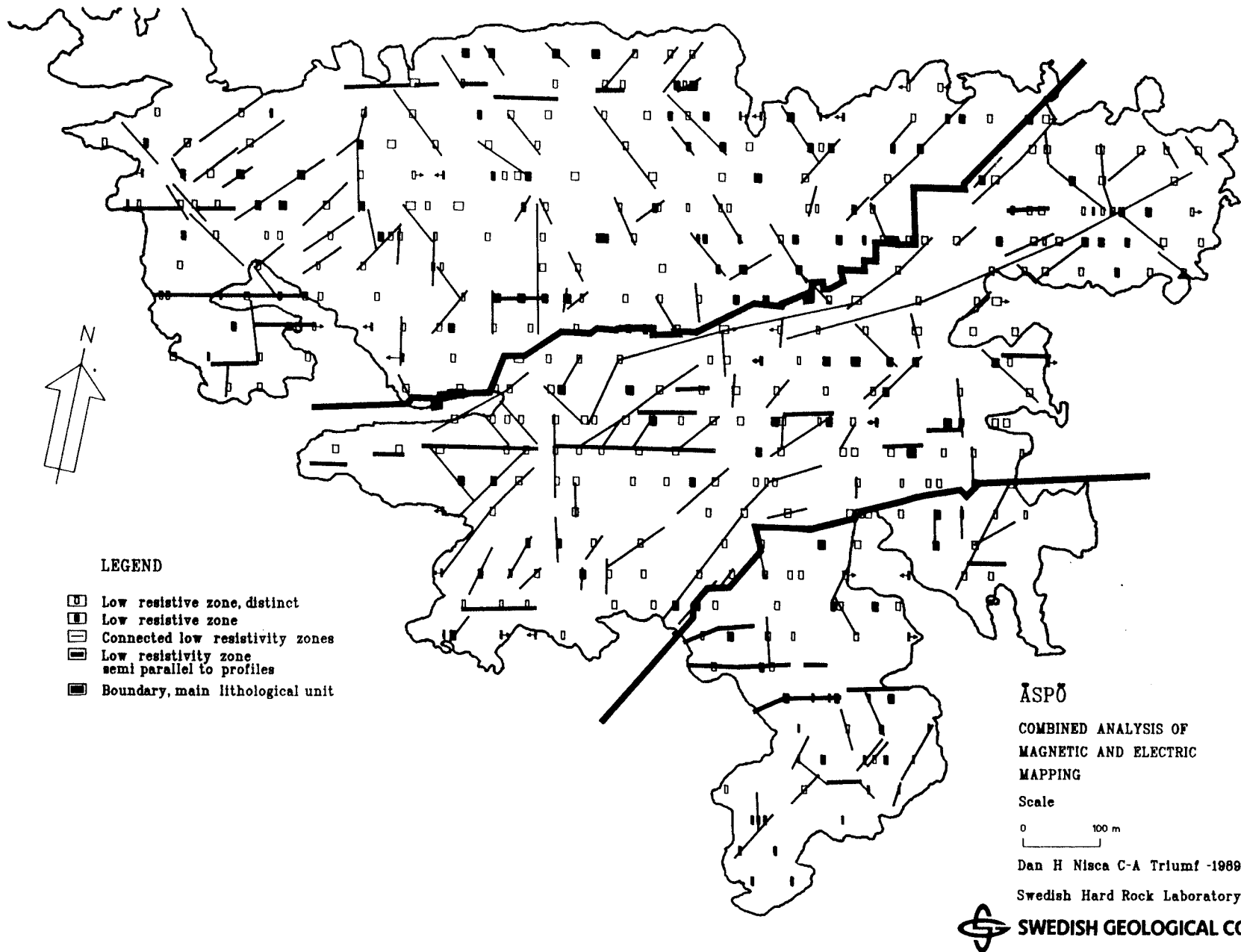
Figure 2-25. Fracture orientation (combination of electric and magnetic surveys). Whole of Äspö, Northern Block, Mylonite Zone and Southern Block.

41

In summary, the bedrock and tectonic analysis conducted on the basis of the geophysical measurements, produced the following results:

1. The island of Äspö is divided into three main bedrock blocks, the Northern Block (granite), the Mylonite Zone (altered granite) and the Southern Block (granite).

2. The interpreted width of the Mylonite Zone on the island of Äspö is about 300 metres. The Mylonite Zone, together with the E-W fracture zones, occupies about 40 percent of the area of the island. The Mylonite Zone is sub-vertical with a small dip-angle toward the north. The computed dip-angles for the E-W fracture zones are 55°—70° towards the north.

3. The largest lateral and also vertical displacements were observed along the fracture zones trending E-W. The main E-W fracture zone, together with other E-W fracture zones in the central part of Äspö, exhibits dextral lateral displacement. Thus, the Mylonite Zone has been displaced in a dextral sense at least about 200 metres.

4. Fracture orientation data for the whole of Äspö show four orientation populations. These can be grouped into two orthogonal fracture sets, N-S/E-W and NW/NE.

5. The N-S/E-W orthogonal fracture set is **self-similar** (independent of scale).

6. The NW/NE orthogonal fracture set is older than the N-S/E-W fracture set. The Mylonite Zone itself is the oldest fracture, or deformation zone in the study area. Two other fracture zones were found in the Northern Block, one NW and the other striking NE, much wider than the other fracture zones within the block, and also affected by them.

7. By combining the geological mapping of the granite dykes with the magnetic fracture interpretation it is quite obvious that most of the granite dykes are situated in the Mylonite Zone and the main E-W fracture zone, striking in both directions. There are probably two dyke generations.

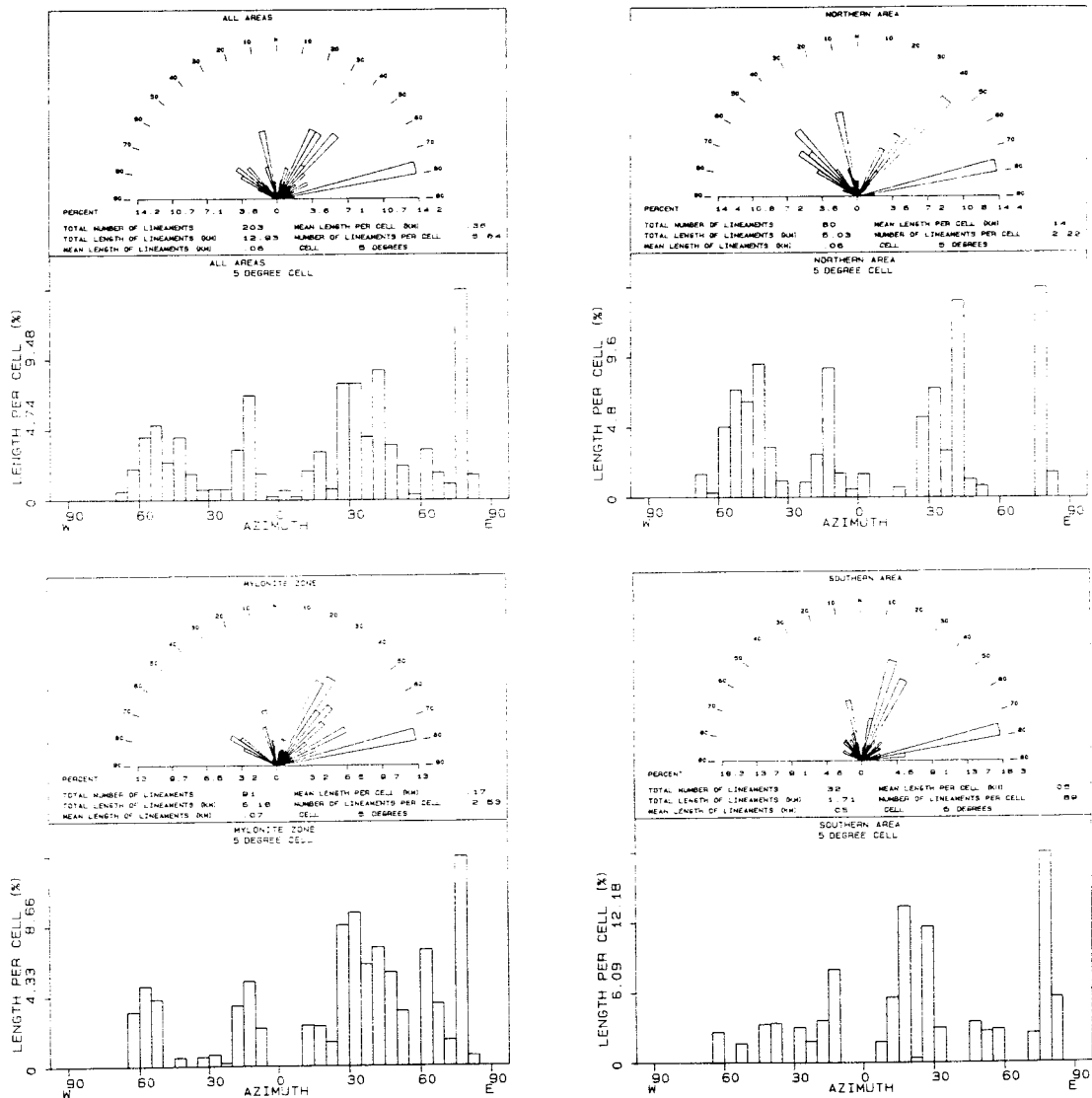8. Fractures/fracture zones interpreted as open, but filled with water and/or clay, were delineated by combining geoelectric and geomagnetic data.

9. Low-resistivity zones differ somewhat in length and orientation within the Mylonite Zone, in comparison to the Northern and Southern Blocks. Low-resistivity zones are more common within the Mylonite Zone. Furthermore, the mean length of a low-resistivity zone is slightly larger within the Mylonite Zone, than elsewhere in the area.

10. From orientation data for fractures interpreted as open, a similar principal trend, with two orthogonal sets of fractures as presented for the magnetic data, can be found.

11. The N-S/E-W orthogonal fracture set, identified from geoelectric/geomagnetic data is almost consistent in all the three sub-areas, the Northern Block, the Mylonite Zone and the Southern Block. The direction of the second orthogonal fracture set is, however, varyies from area to area. The directions in the Northern Block and Mylonite Zone are similar, though directions of fractures within the Mylonite Zone are more scattered around N35°E. In the

Southern Block, however, a shift is obvious in the dominating angle to about N15°E for the same fracture set. Furthermore, the concentration of fracture directions around N55°W, recognizable in the Northern Block and the Mylonite Zone, is absent.

12. A part of the low-resistivity zones detected on single profiles are probably caused by overburden effects, but it is also possible that some of them indicate the presence of fractures not delineated by the geomagnetic survey.

2.1.6 Geological Borehole Description

During the first phase of the drilling programme for the Hard Rock Laboratory four core boreholes, KAS 02, KAS 03, KAS 04 and KLX 01, were sunk in 1987 — 1988. The results of many different borehole investigations are summarized in this section.

The boreholes referred to were sited in preliminary geological and geohydrological models of Äspö and Laxemar (Figure 2-26). At an early stage of the investigation it was found that Äspö consisted of two comparatively undisturbed blocks separated by a major tectonic zone. Borehole KAS 02 was sited in the central part of the SE block of Äspö and borehole KAS 03 in the NW block of Äspö. Borehole KAS 04 is an inclined (60° SE) hole across the tectonic zone — the Mylonite Zone. Borehole KLX 01 was sited in the central part of a major block in the Laxemar area. This report summarizes the most important data from the geological evaluation of the four core boreholes mentioned above.

Aim of the Boreholes

The aim of the boreholes was to obtain basic information on the bedrock composition, orientation and characteristics of the local fracture zones and the hydraulic properties of the rock mass at increasing depth.

DESCRIPTION OF METHODS OF INVESTIGATION AND GENERAL RESULTS

When drilling was finished geophysical logging involving many different methods was performed and the drill cores mapped and investigated in great detail.
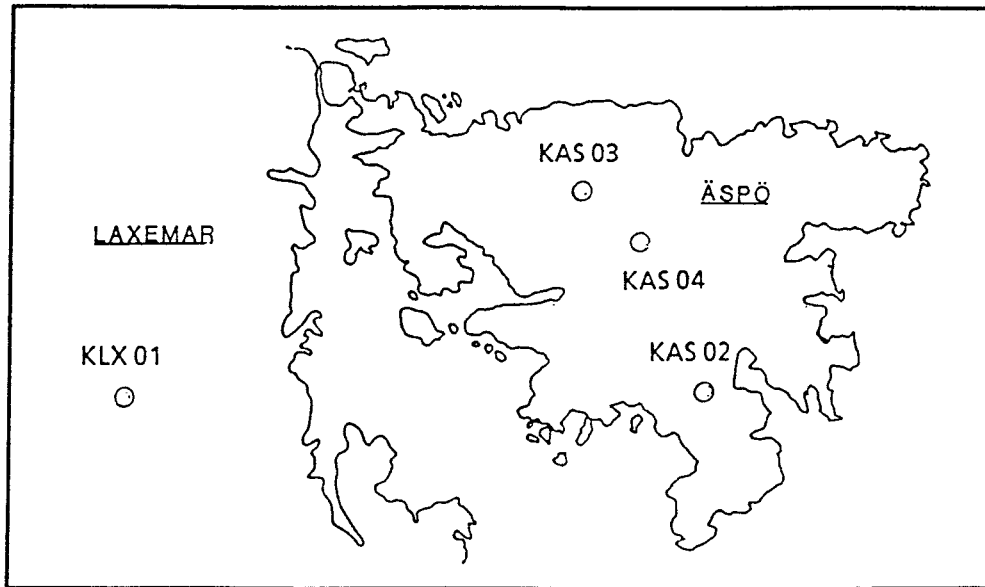
Figure 2-26. Borehole locations on Äspö and Laxemar.

Technical Data

		KAS 02	KAS 03	KAS 04	KLX 01
Coordinates (national grid)	X:	7261.986	7758.228	7636.826	7267.000
	Y:	2125.224	1805.250	1955.060	595.000
	Z:	7.68	8.79	11.5	16.81
Altitude (m.a.s.l.)		~8	~9	~11	~17
Direction:		330°	330°	135°	350°
Dip:		85°	85°	60°	85°
Borehole length:		924 m	1002 m	481 m	702 m
Borehole diameter:		56 mm	56 mm	56 mm	76 mm

Geophysical Logging

In order to investigate lithological, tectonic and hydrogeological conditions at Laxemar and Äspö, geophysical logging was performed in core boreholes KLX 01, KAS 02, KAS 03, and KAS 04 /Sehlstedt — Triumf, 1988/. The logging programme carried out in the core boreholes generally comprised measurement of:

— borehole deviation
— caliper
— sonic
— natural gamma rays
— single-point resistance
— self-potential
— magnetic susceptibility
— normal resistivity 1.6 m
— lateral resistivity 1.6 — 0.1 m
— temperature
— borehole fluid resistivity
— radar measurements

The gradient of the temperature and the equivalent content of sodium chloride were calculated from the temperature and the borehole fluid resistivity methods.

In KAS 04 problems with the instrumentation resulted in lack of confident data from the first hundred metres using the caliper and magnetic susceptibility methods.

The aim of the interpretation was to describe the geophysical logging data in terms of lithology, fracturing and hydrogeology. The logging methods applied make their specific contributions to the different subjects above, the amount varying strongly with the physical property measured.

For the interpretation of the rock type based purely on the combination of diagnostic physical properties, the magnetic susceptibility, natural gamma ray measurements and sonic logs from boreholes were used. The lack of magnetic susceptibility in KAS 04 (0—100 m), however, implied a strong bias of natural gamma radiation on the rock classification.

The sonic logging, single-point resistance, normal resistivity, caliper and the self-potential methods were mainly used for delineation and classification of fracturing in core borehole walls.

Observations of water movements and temperature signatures in boreholes were obtained mainly from temperature measurements and borehole fluid-resistivity logs.

Water transport in a borehole is common and occurs when the borehole serves as a connection between water-bearing fractures/fracture zones with different hydraulic heads.

The interpretation was aimed at distinguishing zones with influx and efflux of water, relative to the borehole. A special type of influx is also distinguished that originates from water injected into fractures during drilling. During drilling with reversed drilling fluid injection, fracture zones may serve as receptors of the cold fluid, and thereby induce temperature anomalies with negative relative amplitudes.

Major salinity changes are only commented on in the text and not displayed in the illustration of the interpretation.

Borehole radar measurement were carried out, both as single-hole reflection measurements and as VRP (Vertical Radar Profiling) measurements. The VRP measurements were carried out to determine the radar pulse velocity in the rock at the different sites. The radar measurements were performed with a mid-frequency of 22 MHz /Niva-Gabriel, 1988/.

The single-hole reflection measurements were performed between the logged depths shown in Table 2-3.

Table 2-3. Logged depths during radar measurements.

Borehole	Start depth (m)	Stop depth (m)	Point spacing (m)
KAS 02	14.23	909.23	1
KAS 03	14.23	979.23	1
KAS 04	110.23	469.23	1
KLX 01	14.23	684.23	1

The field data was stored on floppy disks on the field computer and backup copies were made of all data collected in the field. Additional data processing was carried out at the main office in Uppsala. This has comprised of RD- DC filtering and band-pass filtering. A moving average filter was also applied to the filtered data for the interpretation process. The interpreted structures are displayed on the band-pass filtered plots in the figures.

Geophysical Laboratory Measurements on Core Samples

Measurements on physical properties were performed on core samples from the two boreholes KLX 01 (Laxemar) and KAS 02 (Äspö), as a subproject within a comprehensive investigation programme. The following physical properties were determined in the laboratory: density, magnetic susceptibility, remanent magnetization, resistivity, and induced polarization. Laboratory spectrometry measurements of uranium (U), thorium (Th) and potassium (K) were made on samples from one of the boreholes, KAS 02 (Äspö).

The total number of measured samples was 212, 90 samples from borehole KLX 01 and 122 samples from KAS 02. The samples were collected at a distance of about 10 metres from one another, thus, some geological units are represented by only a few samples. The spectrometry measurements of U, Th and K have been converted to equivalent ppmU, ppmTh and percentage K contents and are also presented as different ratios. The measured and presented U, Th and K values are not absolute ones (about 10—15% to a high), because the cylindrical drill core samples were measured and calibrated according to the formula for cubic samples. However, when using different ratios of U, Th and K

contents the absence of absolute values is of no importance and the measurements can be compared with other spectrometry measurements.

The results of the measurements of the physical properties are shown in two-variable diagram, single property versus borehole length, as different ratios and also in tables with arithmetic mean values and standard deviations.

To provide a general information and understanding of the usefulness of the petrophysical measurements, the results of a general analysis and interpretation of the measurements are also presented. The results and most obvious trends and findings from the analysis of petrophysical measurements are shown in the summaries and more in detail in the conclusions of the two separate reports. /Nisca 1988/

Drill Core Mapping

The drill cores were mapped with the highest precision possible using the Petro Core System from Petro Bloc AB. Since the central component of the fracture hydrology programme is the calculation of the directional permeability from measured fracture orientation, spacing and apertures, considerable attention has been devoted to the characterization and mapping of the fractures. Basic data on fracture orientations, fracture spacing and the surface characteristics of the fracture planes, including mineral filling and coatings, were obtained by logging the drill cores. Rock types and alteration variation along the cores were also mapped. The mapping data are plotted in coloured pictures to two scales, 1:200 and 1:1000 /Stråhle, 1988/.

Different orientation methods were used to obtain information on the location of the fractures intersecting the boreholes. During the core mapping procedure the drill core was reconstructed and the relative orientation of longer or shorter orientation sections obtained.

The absolute orientation of the relatively oriented sections was obtained using a TV-logging device in KAS 02, KAS 03 and KAS 04. In KAS 04 absolute orientations were also defined by the drillers using an iron rod indentor with a wire. As KAS 04 is inclined at an angle of 60 degrees, it was possible to slide the indentor down the borehole and make an impact mark at the lowest part of the bottom stub.

The oriented natural fractures are plotted on Schmidt stereo-nets (lower hemisphere).

Petrological Characteristics of the Rocks in the Drill-cores

The examination of the colour, grain-size and structure of the cores, together with the results of the chemical and mineralogical analyses has led to a division of the rocks in the following groups according to Wikman-Kornfält in /Wikman et al, 1988/:

GREYISH BLACK, FINE-GRAINED GREENSTONES

The greyish black to dark-grey, fine-grained greenstones (Group 1 rocks) were presumably originally supracrustals of volcanic origin. Their modal and chemical composition corresponds to a basalt to andesite and they are thus more basic than the andesitic to dacitic metavolcanics encountered during mapping of the Simpevarp area. The greenstones occur as a rule as remnants within the

47

dioritoids and granitoids and are thus older. The age of the metavolcanics is unknown and we do not know yet whether they belong to the older Svecokarelian supracrustals or to the younger, post-orogenic volcanics.

DARK-GREY, FINE-GRAINED DIORITOIDS

Group 2 rock comprises dark-grey, fine medium-grained dioritoids. They occasionally contain red, rather idiomorphic megacrysts of microcline. At least some of the megacrysts are metamorphic.

As can be seen from the modal analyses, the rocks in this group can be classified as quartz monzodiorites, quartz diorites or diorites. Some parts of the dioritoids are rather heterogeneous and seem to be affected by younger granitoids. This has resulted in hybridic rocks which are difficult to classify. Irregular and winding foliation is sometimes typical of these rocks.

Rocks of this kind (Group 2) were not encountered during the previous mapping of the bedrock in the Simpevarp area, which is quite remarkable.

Assigned to this group is a quartz diorite from the top of borehole KAS 04, which occurs as a dyke-like formation and has a doleritic texture.

REDDISH GREY TO GREYISH RED, FINE MEDIUM-GRAINED TO MEDIUM-GRAINED MAINLY GRANITOIDS

Group 3 rock is composed of two, fine medium-grained to medium-grained granitoid varieties, one of which is reddish grey and more basic (3a), while the other is greyish red and less basic (3b).

There are generally megacrysts of microcline in Subgroup 3a, whereas they are less frequent in 3b. A characteristic feature of these granitoids is also the unusually high content of sphene.

The rocks can as a rule be classified as granite, granodiorite or quartz monzodiorite. There is, however, one sample which appeared to be a tonalite.

Rocks of especially Subgroup 3a are the most common at the surface in the Simpevarp area which is clear from the mapping.

The rocks in Group 3 usually exhibit some kind of weak foliation. In some cases it can be so strong that the final result is mylonites.

These observations show that the postorogenic granitoids have suffered from some stress influence after their emplacement. This may be due to the anorogenic, intrusive activity during the formation of the Götemar, Uthammar and Virbo granites. The interesting, secondary growth of some of the unusually common sphene crystals may also indicate heat supply during this period.

GREYISH TO RED, FINE MEDIUM-GRAINED GRANITES

Group 4 rock comprises greyish red to red, fine medium-grained granites. They are redder than the granites in the Group 3b and they are not so fine-grained as the granites in Group 5. Rocks belonging to Group 4 contain no microcline megacrysts.

The granites of this group which can be divided in two subgroups — one greyish red (4a), and one red (4b) — are completely absent from 2 of the drill cores.

The greyish red to red granite (4a) occurs in the core from the Laxemar drilling (KLX 01). It is also found at the surface in the area north-west of Laxemar.

This granite also resembles to some extent the greyish red, fine medium-grained granite on Ävrö and restricted parts of southern Äspö. The red granite (4b) is more rare and occurs only in a few sections of drill core KAS 03.

FINE-GRAINED GRANITES, OCCASIONALLY FOLIATED

The last and youngest rock-group (5) is composed of red or more seldom reddish grey, fine-grained granites. The somewhat varying colours have been the basis for a further division into the following 4 subgroups:

5a. Reddish grey, fine-grained granite.

5b. Greyish red to red, fine-grained granite.

5c. Dark-red, fine-grained granite.

5d. Dark-red, fine-grained, strongly fractured granite, with cavities.

During the geological mapping of the Simpevarp area it was noticed that the fine-grained granites occurred in small massifs and dykes in the older rocks. Typical of the dykes at the surface is, that some of them are strongly deformed. This is also evident from the thin-sections of fine-grained granites, which show not only intense parallel, mylonitic structures, but also strong fracturing and crushing.

The fine-grained granites in the drillcores can be classified as true granites. As can be seen from the modal analyses and the triangle-diagrams they are rather rich in alkali feldspar. This is also evident from the chemical analyses.

The age of the fine-grained granites is uncertain. We know that the anorogenic granites in the region are accompanied by a fine-grained granite, but this is a common feature of granite plutons of different ages.

However, it does not seem unreasonable that most of the fine-grained granites in the Äspö area could be anorogenic and related to the neighbouring Götemar-Uthammar granites.

Ductile Structures

An analysis of the ductile structures in cores KAS 02, 03 and 04, has been performed by Riad-Munier, /Wikman et al, 1988/ to investigate the ductile structures at depth in the bedrock of Äspö and to seek relationships between these early ductile structures and later brittle fractures (Figure 2-27).

Variations in the intensity and orientation of foliation is indicative of the presence of structures such as folds and shear zones, for which reason this report will deal precisely with the foliation.

The interpretation is here limited to two dimensions; variations in the dip borehole of structures are considered but not variations in strike. As long as the borehole is vertical, the dip of the structure in relation to the core axis will be identical to the dip of the structure in the bedrock. This will, however, not be the case when the borehole is inclined. Furthermore, since the cores are not oriented in three dimensions it will be almost impossible to distinguish a ductile shear zone, defined by distorted foliation, from a fold. The foliations therefore give the false impression of an overall dip toward the same direction.

The foliation in the core varies in intensity from rarely detectable to very strong or mylonitic. It is generally more intense close to mylonites. Abrupt
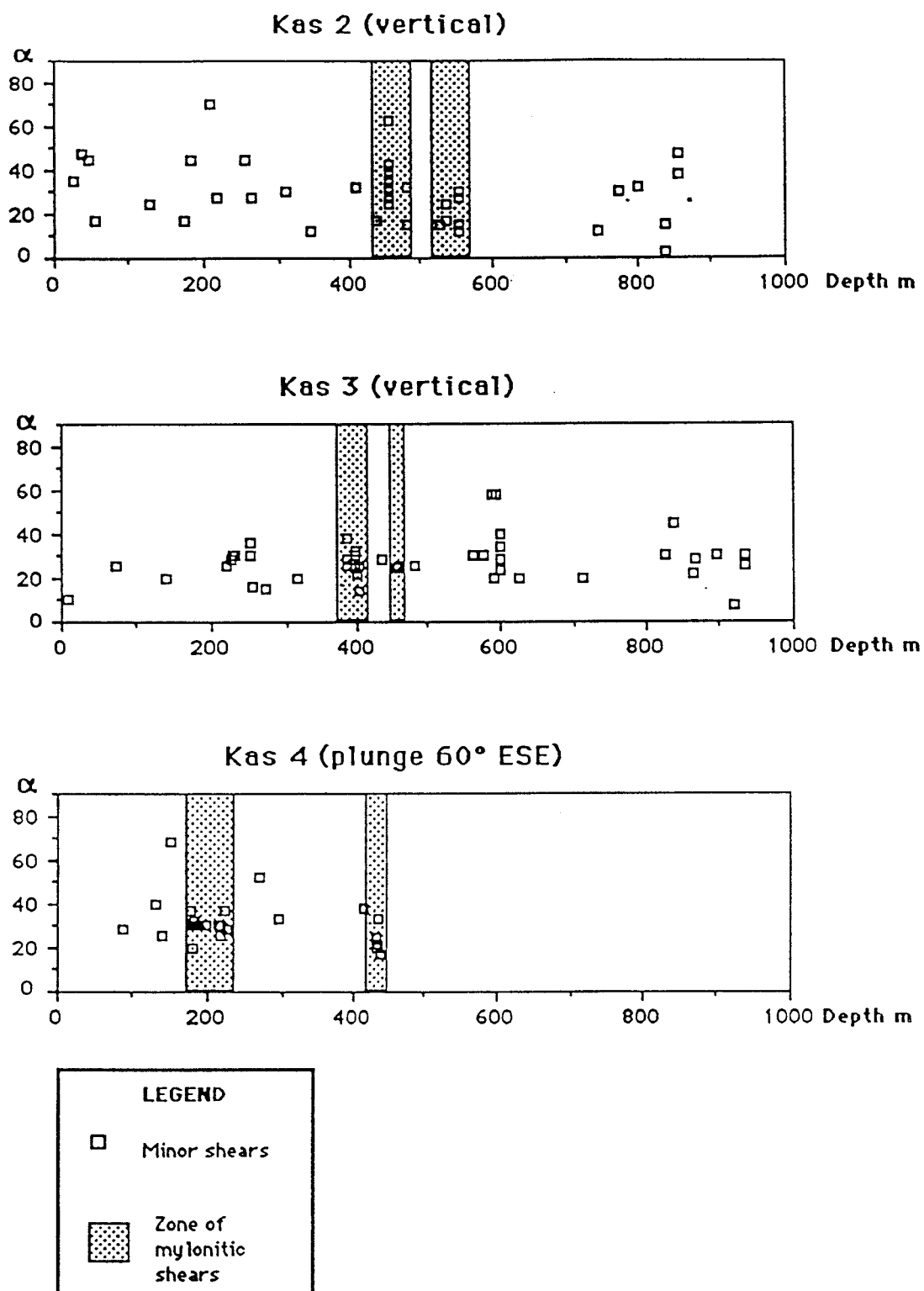
Figure 2-27. All measured shear zones and mylonites (respective of size) are plotted against the core length. Shaded areas indicate zones consisting of mylonites of different sizes (1 cm — 1 m). A mylonitic zone is defined as a part of the core, consisting of impressive mylonites and shear zones, which distort the general foliation. However, clusters of shear zones are detectable in the diagrams but they only affect the bedrock foliation locally and could not be labelled mylonitic zones.

changes in foliation with regard to intensity and/or orientation are due either to a change of rock type or the occurrence of narrow (centimetre-wide) shear zones. Ductile shearing is also common along lithological boundaries.

A second, very weak, subvertical foliation occurs in fractured sections of the cores. This may be interpreted as indicating the vicinity of a fold hinge, where the general foliation dips 55° — 60° (true dip) would be an axial planar foliation. In other fractured parts of the cores no foliation is recognizable. Apart from the possibility of the rock not being foliated, the lack of foliation may be due to the difficulty in identifying any foliation in a fracture zone or the foliation having vanished in a later cataclastic process.

Finally, it should be remembered that from a borehole, with it's very small diameter, conclusions drawn about regional features will be very uncertain.

In the following description, the dips of structures will be referred to in terms of the angle 90° -α. α is defined as the angle between the core axis and the structure. The depths of structures referred to measured from the surface, down the borehole and only coincide with the true depth whenever the borehole is vertical.

Fracture Mineral Study

The fracture mineralogy, as observed in the cores from Äspö and Laxemar, is dominated by chlorite, calcite, hematite and epidote but also minerals like quartz, muscovite, laumontite, prehnite, fluorite and pyrite are frequent, as well as low-temperature minerals like Fe-oxyhydroxide and clay-minerals. These minerals are also represented in the core from the reference area at Laxemar /Tullborg 1988/.

Results from the core mapping correspond well with the results from the XRD-analyses and most of the unidentified mineral phases from the core mapping appeared to be colour- or textural varieties of chlorite, hematite, fluorite, clay minerals or quartz.

A fracture filling history based on textural studies of thin sections (Table 2-4) resulted in the following sequence (all of which postdates the foliation (1) in the granite/granodiorite):

(2) Mylonitisation with growth of fine-grained quartz, epidote and muscovite.

(3) Growth of iron-rich, idiomorphic epidote and fluorite.

(4) Formation of idiomorphic quartz, muscovite, hematite, fluorite, calcite, spherulitic chlorite and possibly some Fe-oxyhydroxide.

(5) Mineralizations of prehnite, hematite-stained laumontite, calcite and fluorite.

(6) Formation of gypsum, chlorite, illite and probably clay-minerals like kaolinite.

Ages for listed mineralizations above are suggested to range from Middle Proterozoic (1660 Ma) to the present. A detailed account of the relative ages of the mineralizations is given in Table 2-5.

Studies of the frequency of calcite coated fractures (Figure 2-28) as well as fractures containing Fe-oxyhydroxide indicate a relatively shallow penetration of surface water on Äspö (10 to 30 m). This is in accordance with the detected calcite saturation within the analysed water sample from 40 to 70 m depth in the percussion boreholes on the island. However, a deeper penetration of surface

water is suggested in the fracture zone penetrated at approx. 60 m core depth in borehole KAS 04.

The frequency of hematite and Fe-oxyhydroxide show good correlation, which indicates that these minerals are in one way or another related to each other. Two possibilities are indicated:

1) The Fe-oxyhydroxide constitutes the last phase of the hydrothermal event responsible for the hematite mineralization.

2) The Fe-oxyhydroxide is a product of groundwater/hematite interaction, i.e. a result of repeated dissolution/precipitation in the water-conducting fractures.

Table 2-4. Relative ages of minerals in fracture fillings.

Sample	Ep	Qz	Fl	Ca	La	Pr	He	Fe	Py	Mt	Mu	Clay	Cl	My
KAS 02														
18.00b				2										1
24.08b	1,2i													
31.55	1			2	2									
51.87				2									1	
74.95f							1						1	
95.64	1		2		2								2	
97.16					1		1	2					2	
130.33	1		2	2										1
139.84			1										1	
178.48	1,2i	1	2,3	3	3		3							1
189.33	1	2	3	2			2							
191.64	1,2i		3									3		1
200.05f	1,2i		4		3									1
200.68	1,2,3i	1,2	3	3					3,4					
240.90	1,2i		2											1
263.89	1,2i	1		3	3		3							
315.67				2,3	1									
318.50	1	1		2	2									
322.20	1	1		2	2		2							1
387.65	1	1		2		2							3	1
404.47	1	1			2									1
459.74	1,2i													
513.42	1	1	3	2		2								
563.87	1	1		3,4	2			4						
578.67	1		1	2									3	
667.40f			2		2	1	2							
691.49				1							2			
696.83f	1	1		2	2								2	1
755.38				2	1									
824.70	1			3	3	2,3	3							
836.79				1		1								
843.00				1	1	1							1	
843.73	1			2	2	2	2							1
869.53f		1			2									
874.67f				2		2					1			
876.10f				1	1		1			2	2			
878.00f		1									1			
880.12		1	1				1							
889.12		2		3									3	1

Table 2-4: continued.

Sample	Ep	Qz	Fl	Ca	La	Pr	He	Fe	Py	Mt	Mu	Clay	Cl	My
KAS 03:														
33.31	1			2	2	2	2							
46.36f				1	1		1							
57.15	1i	1							1					
74.61			1	1									1	
79.59					1	1	1							
115.80			2								1-2		2	
126.19f				2	1		1							
149.75				1	1		1							
153.32				2							1	3	1	
259.45				1	1		1						1	
304.03	1	1								1-2			1	
312.87					1		1							
334.39			1	1	1,2									
421.05	1	1												
438.77													1	
466.19			1				2						2	
510.09				3			1					2	1	
617.11		1			1								2	
622.64			1,2				1				1		2	
KAS 04:														
159.86	1,2	1				3								

Ep = Epidote, Qz = Quartz, Fl = Fluorite, Ca = Calcite, La = Laumontite, Pr = Prehnite,
He = Hematite, Py = Pyrite, Mt = Magnetite, Mu = Muscovite, Clay = Clay minerals,
Cl = Chlorite, My = Mylonite
b = fracture in basite, f = fracture in fine-grained granite, i = idiomorphic crystals,
1,2,3 = indicate relative ages; 1 = oldest

Rock Quality

Rock Quality Designation (RQD) values are commonly used for technical descriptions of cores and evaluation of rock masses for engineering purposes. In order to eliminate local, abnormal peaks of RQD values, Z (RQD) values are calculated for a longer section (zone) of the core. A zone may be more or less homogeneous regarding fracturing alterations and permeability. To get a rough estimation of the Rock Quality of the cores four different Z (RQD) classes were used:

1. Z (RQD) >0.75
2. Z (RQD) = 0.50 — 0.75
3. Z (RQD) = 0.25 — 0.50
4. Z (RQD) <0.25

Table 2-5. Sequence of events within the granitoids at Äspö.

1)	Regional deformation resulting in the E-W to ENE-WSW foliation	Cf. the D3-event in SW-Sweden 1660-1400Ma.(1,2)
2)	Mylonites or "shear-bands" containing fine-grained epidote, muscovite and recrystallized quartz.	Some mylonites probably belongs to the last phase (shearing) of D3 above (1)
3)	Iron-rich, idiomorphic epidote and fluorite.	Intrusion of the anorogenic Götemar-granite c. 1400 Ma (2,3) Tension.
4)	Growth of idiomorphic quartz, muscovite, hematite, fluorite, calcite and spherul - itic chlorite.	Post-magmatic hydrothermal circulation from the anorogenic granite (s).
5)	Prehnite, hematite-stained laumontite, possibly Fe-oxyhydroxides,calcite and fluorite	Burial metamorphism c. 1100 Ma. (4,5)
6)	Gypsum, chlorite, illite, probably calcite and possibly Fe-oxyhydroxides.	Burial metamorphism c. 300 to 400 Ma (3,6)
7)	Calcite, Fe-oxyhydroxides and clay-minerals like kaolinite.	Results of present ground-water circulation?

According to Tullborg in Wikman et al, 1988 - SKB, PR 25-88-11

In general terms "Group 1", may be regarded as fresh and good rock (mean, 1—3 fracture/m, "Group 2" comprises cores with somewhat increased fracturing (normally 4 — 6 fractures/m) and "Group 3" highly fractured cores (7 — 12 fractures/m) more or less altered. In "Group 4" the cores are highly fractured — crushed and more or less completely altered.

Geohydrologically a rock mass comprising "Group 1" may be regarded as tight — slightly permeable and "Group 2" and 3 as moderate — highly permeable. A zone comprising "Group 4" may be very complex as a result of mineral alteration (clay) in parts of the zone which may be tight — moderately permeable. Heavy flows may occur in highly fractured, less altered sections of the same zone.
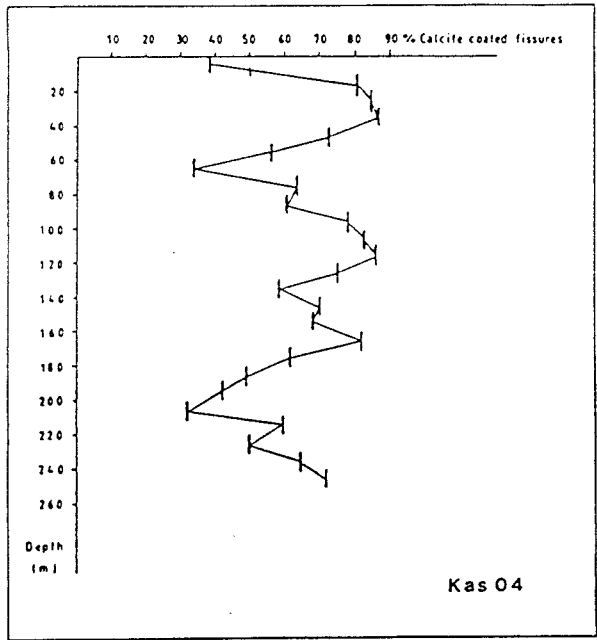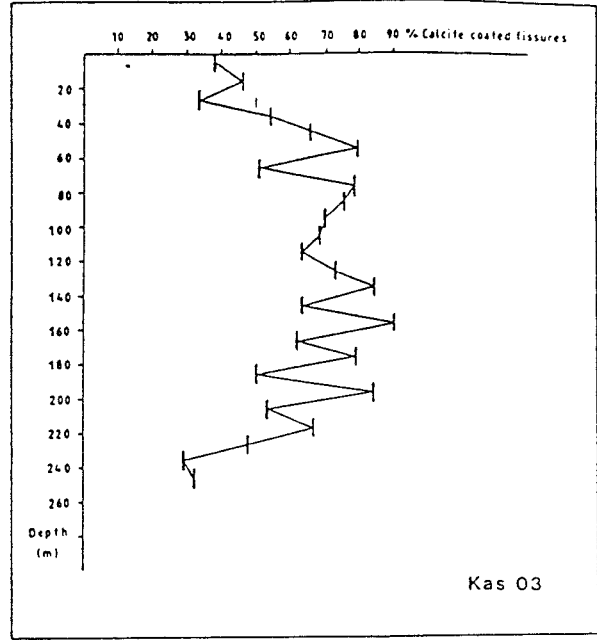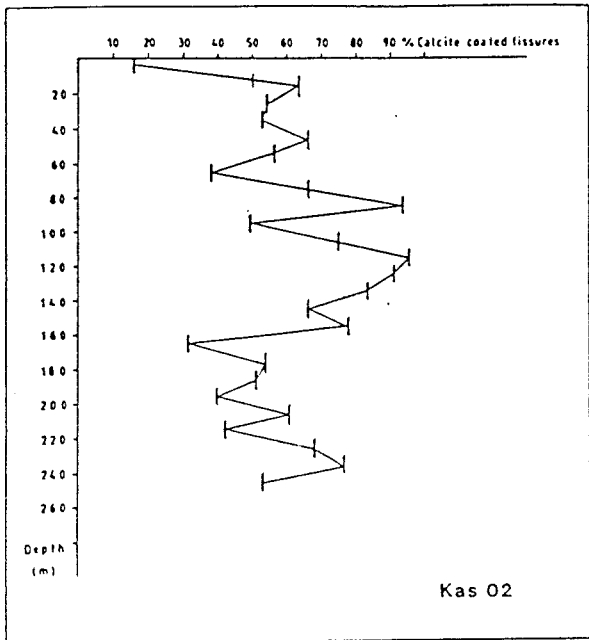
Figure 2-28. Percentage of calcite coated fractures versus depth for the upper 250 metres of cores KAS 02, KAS 03 and KAS 04.

55

Core Mapping Data KAS 02

Some basic data from the examination of borehole KAS 02 are presented in Figures 2-29 — 30 and Table 2-6.
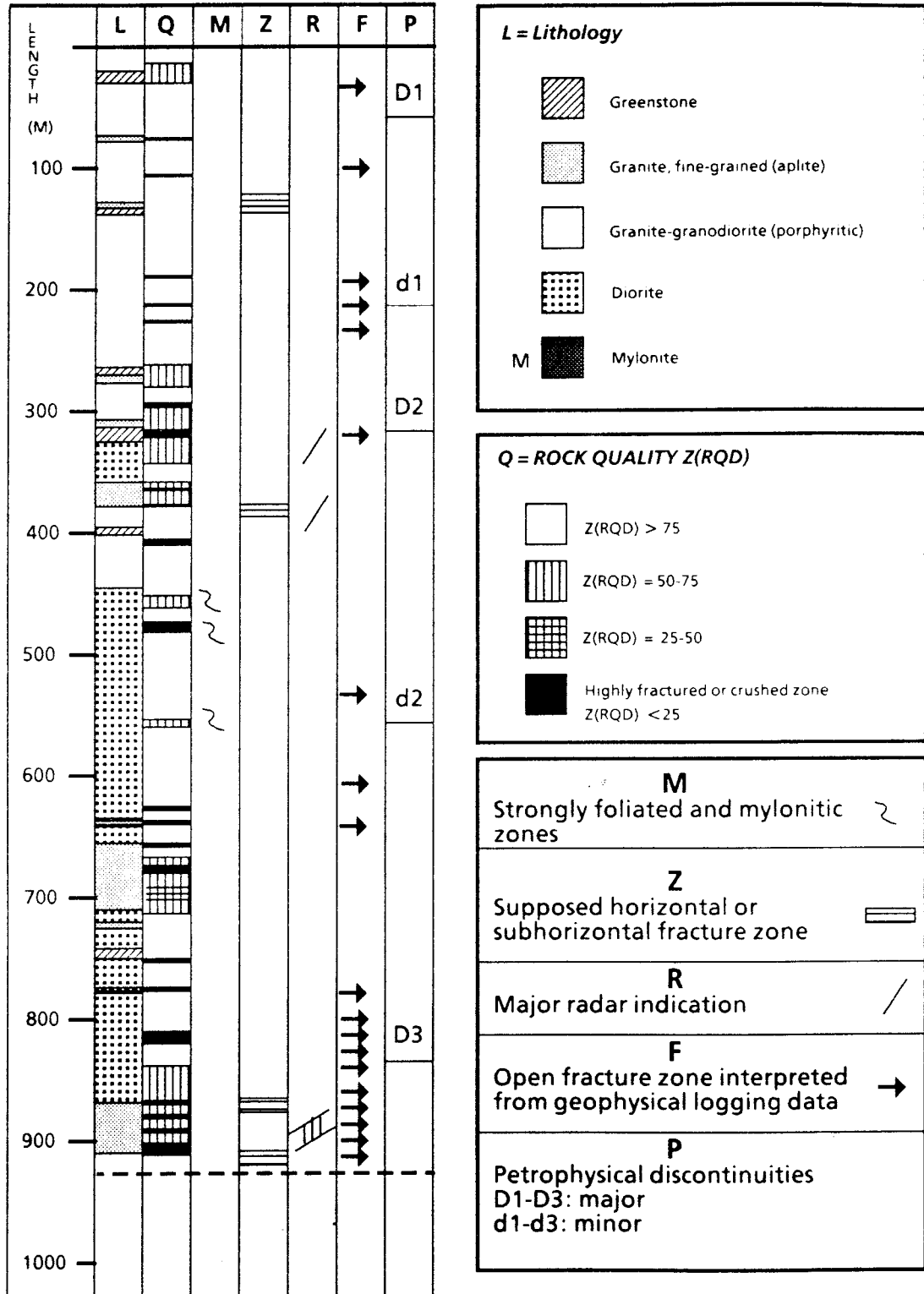
SUMMARY OF DATA FROM BOREHOLE KAS 02

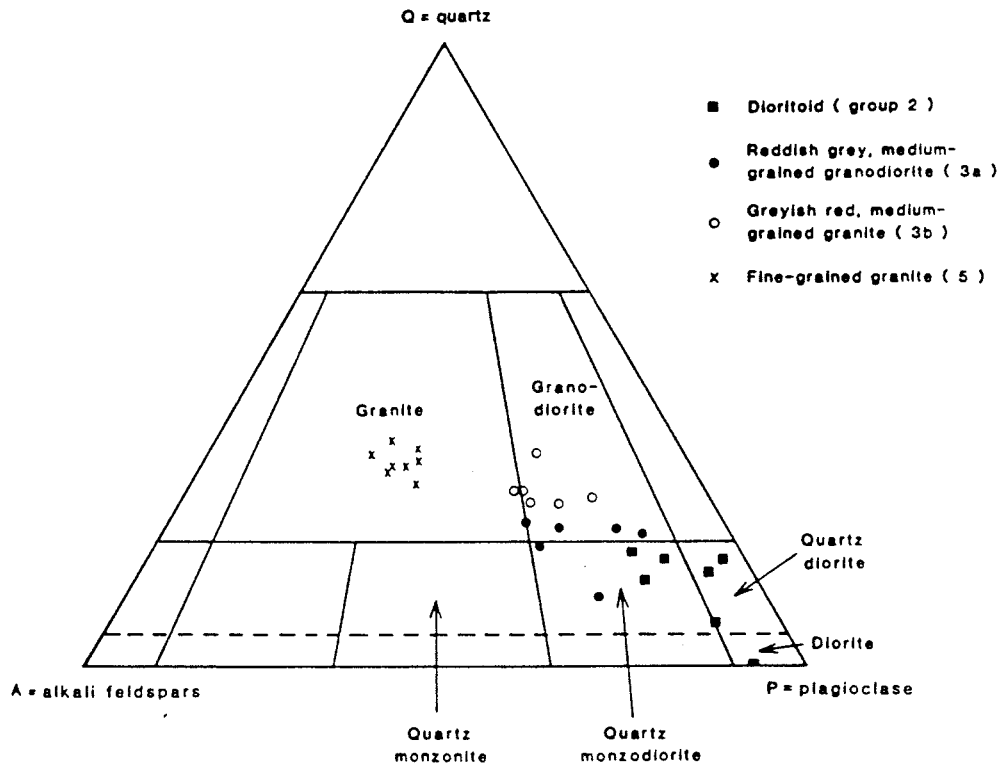Figure 2-29. Summary of borehole data from KAS 02.

Q = quartz

■ Dioritoid (group 2)

● Reddish grey, medium-grained granodiorite (3a)

○ Greyish red, medium-grained granite (3b)

x Fine-grained granite (5)

Granite

Grano-diorite

Quartz diorite

Diorite

A = alkali feldspars

P = plagioclase

Quartz monzonite

Quartz monzodiorite

Figure 2-30. Modal classification of rocks from KAS 02 according to IUGS (1973, 1980).

Table 2-6.

Rock distribution in the borehole	
Rock type	%
Småland granite	40
Diorite	42
Fine-grained granite	14
Greenstone	4

Indications of main fracture zones	
Borehole length	75, 315, 510, 670-710 and 810-925 m

Indications of subhorizontal fracture zones	
Borehole length	120-150, 370, 870 and 910 m

Number of natural and sealed fractures within the rock mass (crush-zones excluded)	
Natural fractures "/m	3373 3.65
Sealed fractures "/m	437 0.47
Total number of fractures "/m	3820 4.12

57

Core Mapping Data KAS 03

Some basic data from the examination of borehole KAS 03 are presented in Figures 2-31 — 32 and Table 2-7.
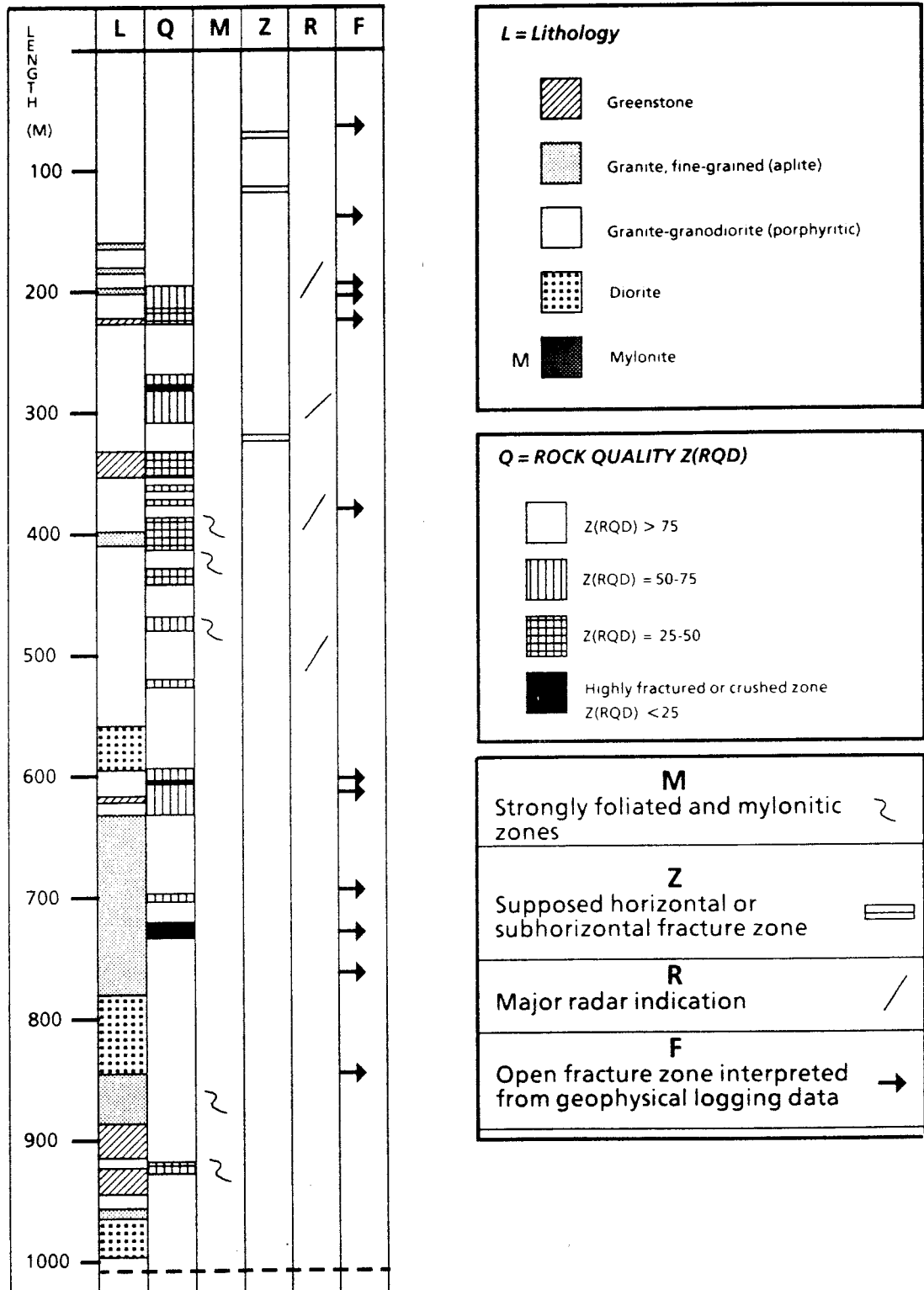
SUMMARY OF DATA FROM BOREHOLE KAS 03

Figure 2-31. Summary of borehole data from KAS 03.
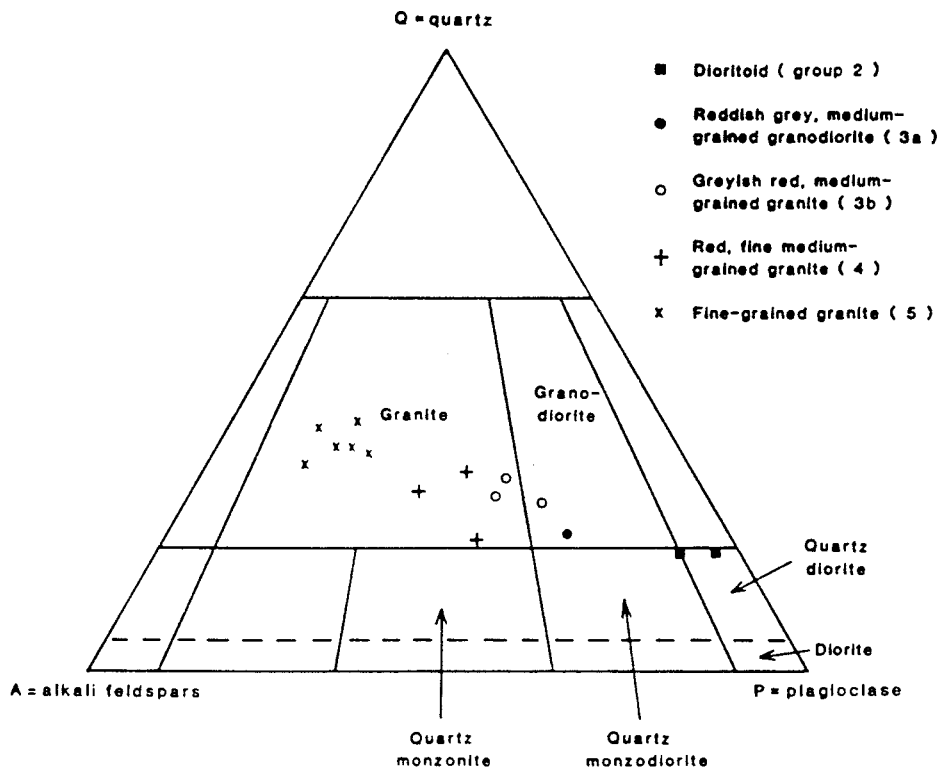
Figure 2-32. Modal classification of rocks from KAS 03 according to IUGS (1973, 1980).

Table 2-7

Rock distribution in the borehole	
Rock type	%
Småland granite	62
Diorite	12
Fine-grained granite	23
Greenstone	3
Indications of main fracture zones	
Borehole length	290, 39-420, 620 and 710-740 m
Number of natural and sealed fractures within the rock mass (crush-zones excluded)	
Natural fractures " " /m	3718 3.71
Sealed fractures " " /m	1762 1.76
Total number of fractures " " /m	5480 5.47

Core Mapping Data KAS 04

Some basic data from borehole KAS 04 are presented in Figures 2-33 — 34 and Table 2-8.

SUMMARY OF DATA FROM BOREHOLE KAS 04

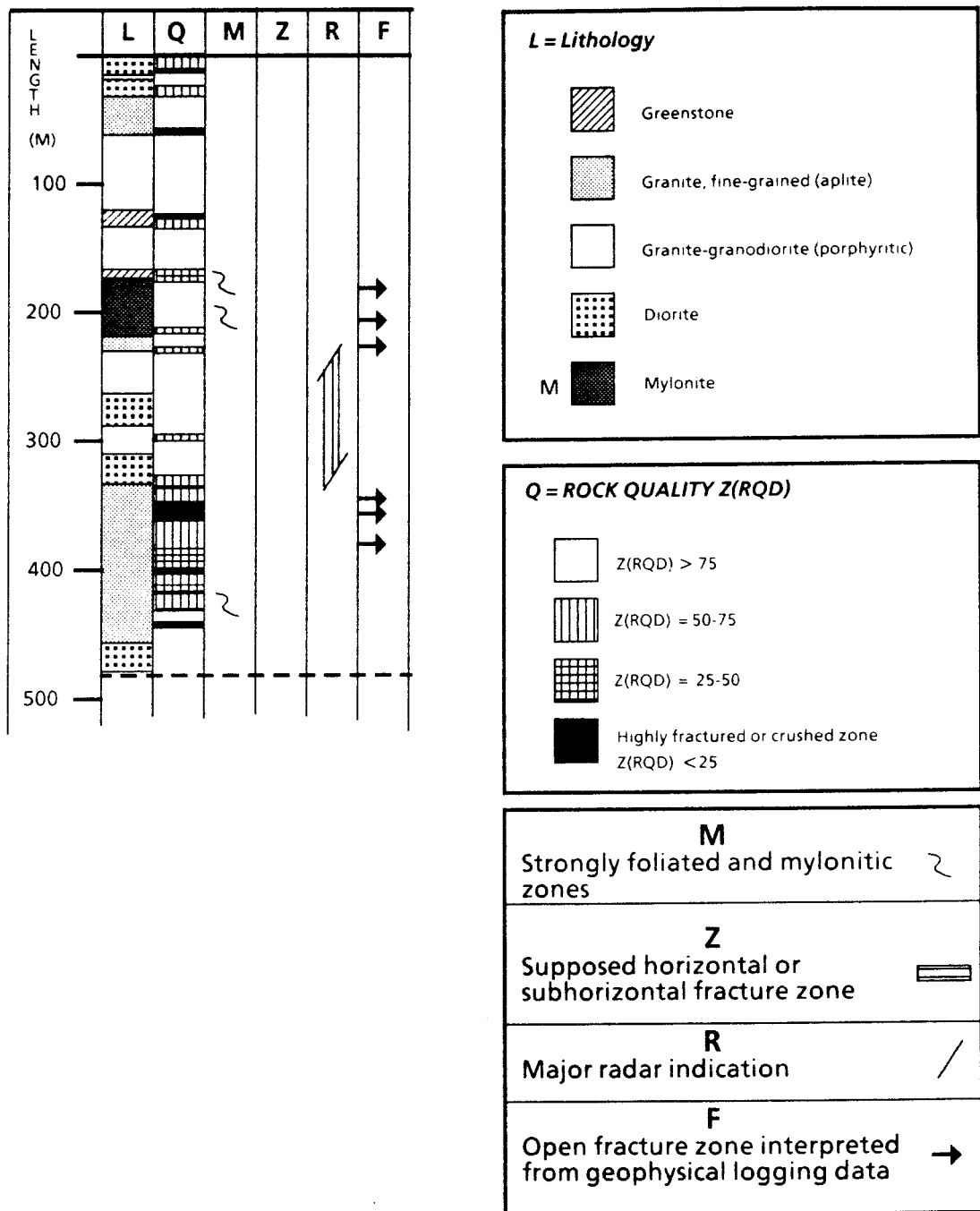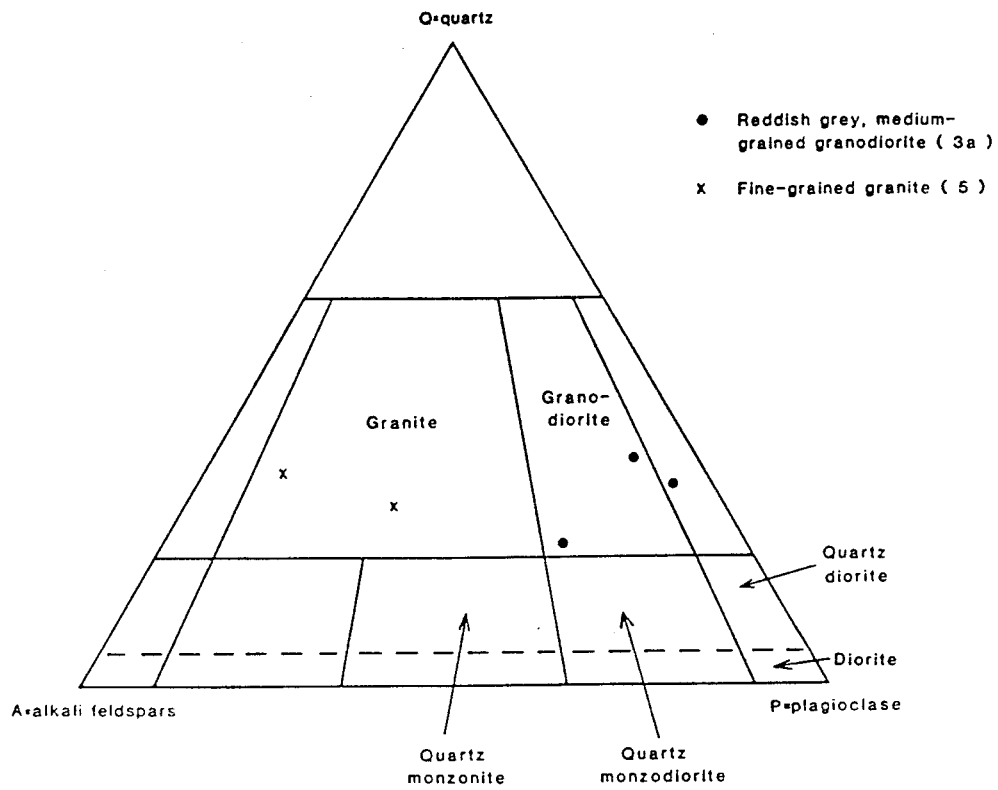Figure 2-33. Summary of borehole data from KAS 04.

O=quartz

● Reddish grey, medium-grained granodiorite (3a)

X Fine-grained granite (5)

Grano-diorite

Granite

X

X

Quartz diorite

Diorite

A=alkali feldspars

P=plagioclase

Quartz monzonite

Quartz monzodiorite

Figure 2-34. Modal classification of rocks from KAS 04 according to IUGS (1973, 1980).

Table 2-8

Rock distribution in the borehole	
Rock type	%
Småland granite	37.5
Diorite	20
Fine-grained granite	32
Greenstone	0.5
Mylonite	10

Indications of main fracture zones	
Borehole length	50-70 and 380-440 m

Number of natural and sealed fractures within the rock mass (crush-zones excluded)	
Natural fractures " " /m	2890 6.0
Sealed fractures " " /m	787 1.64
Total number of fractures " " /m	3677 7.64

61

Core Mapping Data KLX 01

Some basic data from borehole KLX 01 are presented in Figures 2-35 — 36 and Table 2-9.
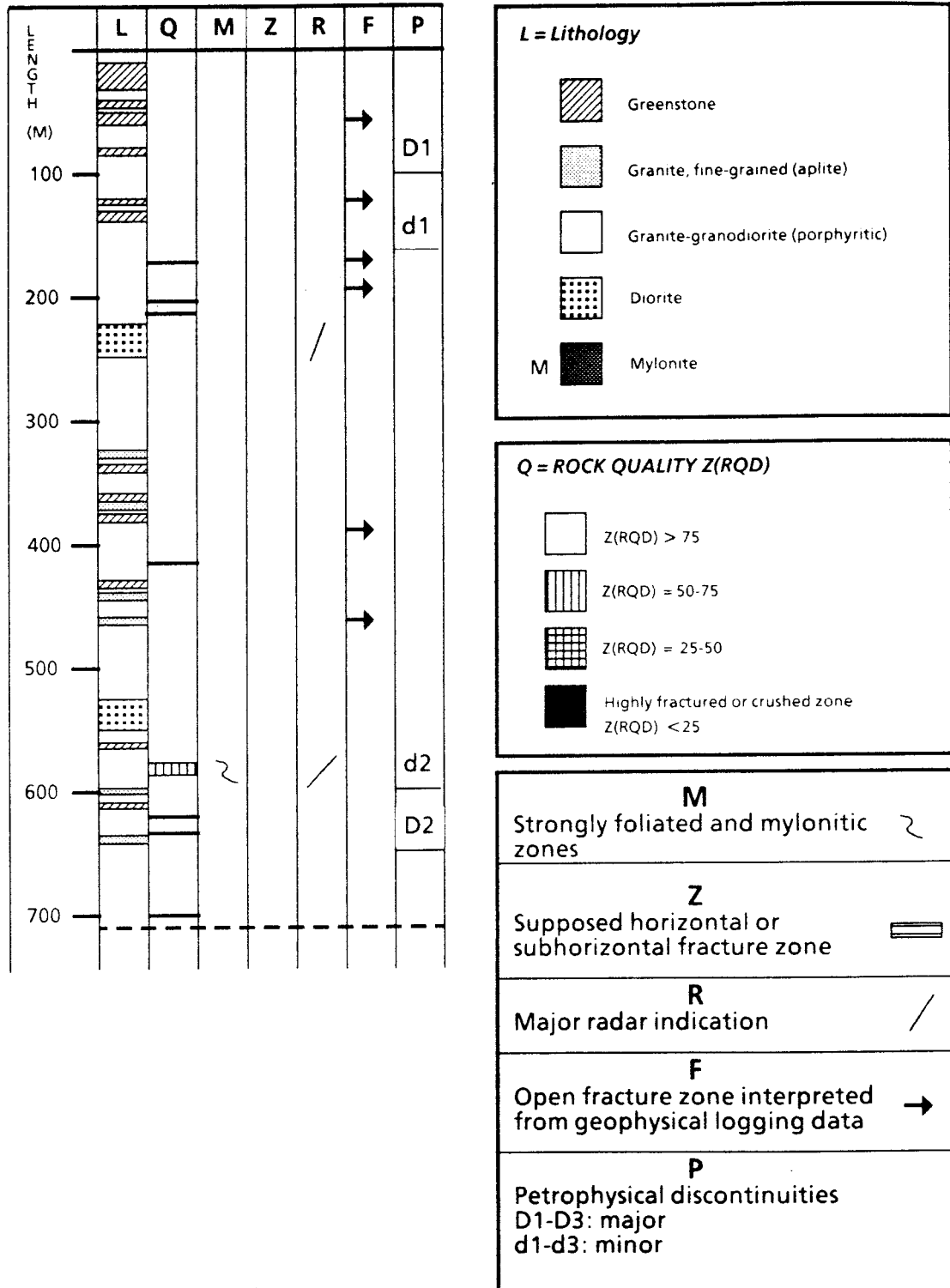
SUMMARY OF DATA FROM BOREHOLE KLX 01

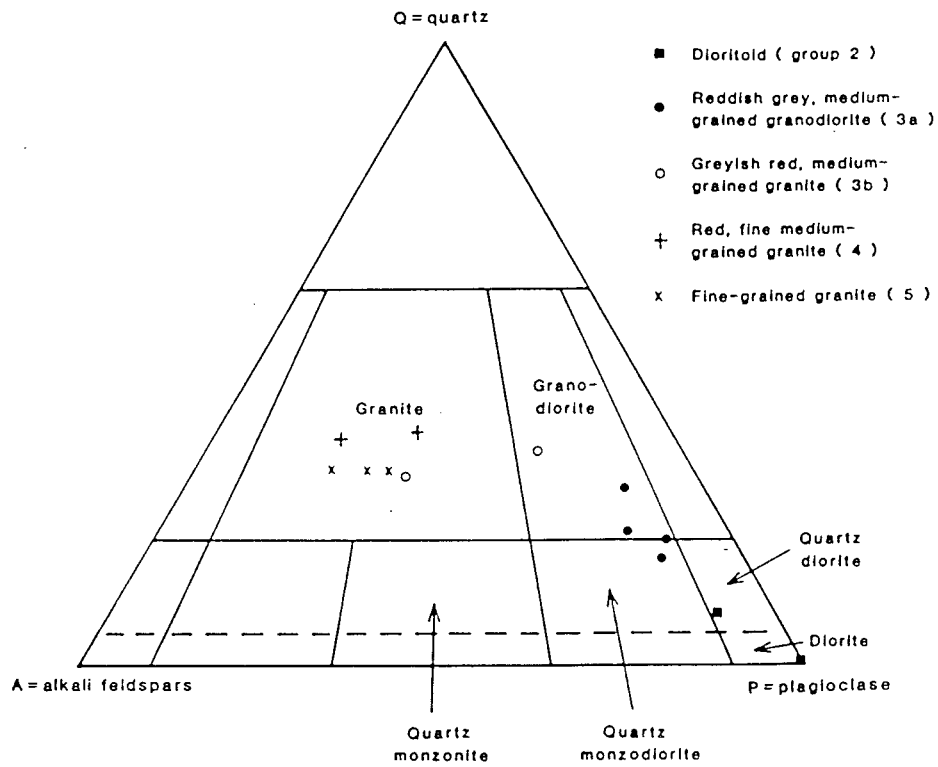*Figure 2-35. Summary of borehole data from KLX 01.*

Figure 2-36. Modal classification of rocks from KLX 01 according to IUGS (1973, 1980).

Table 2-9

Rock distribution in the borehole	
Rock type	%
Småland granite	72
Diorite	13
Fine-grained granite	5
Greenstone	10
Indications of main fracture zones	
Borehole length	590 m
Indications of subhorizontal fracture zones	
Borehole length	
Number of natural and sealed fractures within the rock mass (crush-zones excluded)	
Natural fractures " " /m	1807 2.57
Sealed fractures " " /m	895 1.27
Total number of fractures " " /m	2702 3.85

2.2 GEOLOGICAL-TECTONICAL MODELS OF ÄSPÖ

For the planned modelling work it is important to establish rock mass descriptions on different scales.

Based on present knowledge of the geological conditions on Äspö it seems possible to make rock mass descriptions on the following three scales:

Site scale	(approx. 500 x 500 m)
Block scale	(approx. 50 x 50 m)
Detailed scale	(approx. 5 x 5 m)

2.2.1 Site Scale

Based on lineament interpretation /Tirén et al., 1987/ and aero-geophysical measurements /Nisca, 1987/ at an early stage of the investigation it was found that Äspö consisted of two comparatively undisturbed blocks separated by a major very complex tectonic zone — the Mylonite Zone (Figure 2-37). Geological mapping /Kornfält et al., 1988/ and geophysical ground measurements /Nisca et al., 1989/ on a detailed scale, supported by a first batch of boreholes, confirmed this first preliminary geological model.
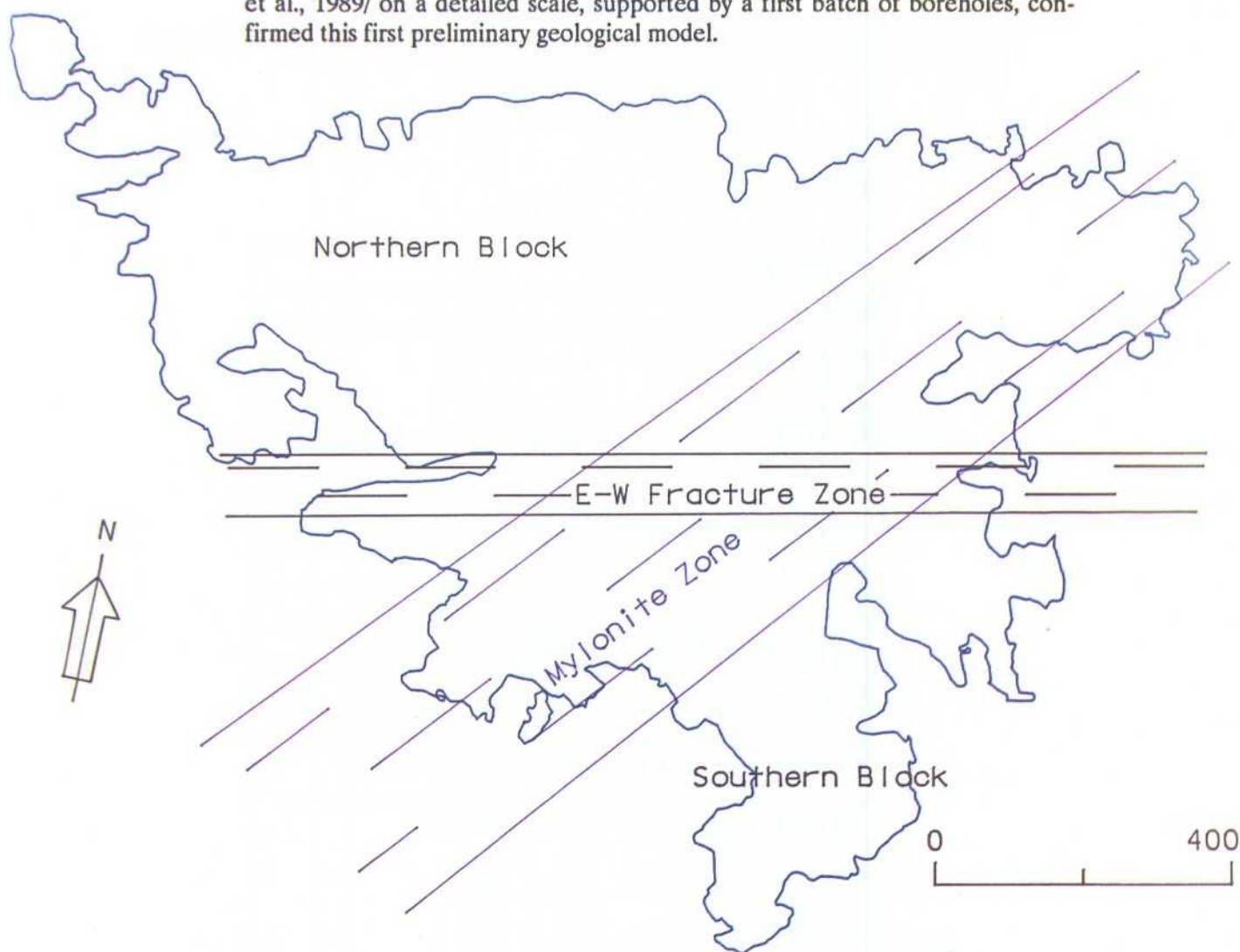

Figure 2-37. Geological-tectonical model of the island of Äspö.

Lithology

The predominating rock on the island of Äspö is a reddish grey medium-grained granitoid with megacrysts of red microline /Kornfält et al., 1988/. A redder, fine medium-grained granite with few, smaller megacrysts (Ävrö granite) occurs in the southern part of Äspö. Both these granite varieties are usually called Småland granites.

A fine-grained greenstone (metabasalt) seems to be the oldest rock. This rock has been intruded by different kinds of granitoids.

Fine-grained granites, as well as rare pegmatites and aplites, penetrate the above mentioned supracrustals and granitoids.

A few dykes of diabase (altered dolerite) were observed.

The dioritoids, found at depth in the core boreholes on Äspö, seem to be absent at the surface, which is rather remarkable. Based on the results of mineralogical and chemical analyses the following divisions of the rock on Äspö seems to be suitable:

1. Greyish black, fine-grained greenstones, probably metavolcanics (GREEN-STONE)

2. Dark-grey, fine medium-grained dioritoids (quartz monzodiorite, quartz diorite and diorite). Occasionally with red megacrysts of microcline. (ÄSPÖ DIORITE).

3. Reddish grey to greyish red, fine medium-grained granitoids (granite, granodiorite). Generally with megacrysts of microcline. (SMÅLAND GRANITE).

   a. Reddish grey, fine medium-grained to medium grained granodiorite.

   b. Greyish red, fine medium-grained to medium-grained granite to granodiorite.

4. Greyish red to red, fine medium-grained granites. (ÄVRÖ GRANITE).
   a. Greyish red, fine medium-grained granites.
   b. Red, fine medium-grained granites.

5. Fine-grained granites, occasionally foliated. (FINE-GRAINED GRANITE).
   a. Reddish grey, fine-grained granite.
   b. Greyish red to red, fine-grained granite.
   c. Dark-red, fine-grained granite.
   d. Dark-red, fine-grained granite, strongly fractured, with cavities. The medium-grained granodiorites and granites may have been formed by normal crystallization differentiation from a (quartz) dioritic magma.

Ductile Structures

Strong foliation and fracturing, resulting in mylonites, are common in certain zones of the island. Two fracture directions are specially pronounced, one about W.S.W.—E.N.E. and the other about SSW—NNE.

According to /Talbot et al 1988/, the steep planar fabric trending in the Småland granitoids of Äspö is the result of superposition of two foliations generated during early phases of ductile penetrative strain. Once the steep "E-W" penetrative fabric was established, it influenced all subsequent deformation of the rocks on Äspö and subsequent regional strains became increasingly local-

ized in zones of shear which have simple geometries in relation to the ductile fabric. Such zones are subhorizontal, or steep with "N-S, NE, E-W and SE" trends.

Brittle Structures — Fracture Mapping Data

The brittle tectonic conditions on Äspö are documented by fracture mapping /Ericsson, 1988/. Fracture orientation in N60°W, N5°W and N60°E are predominant. E—W fractures are more scarce but they occur in a more narrow, prominent peak.

About 85% of the 4500 mapped fractures are steep, with dips in the interval 70°—90°. The relatively few observed inclined fractures with dips in the interval 0°—65° exhibit predominant strikes around N60°E and dip mainly to the north. The foliation is common in N60°E — N80°E and has implied a fracture frequency increase within the sector in question.

The open fractures verify the brittle pattern with a predominant peak at N55°W. An obvious relationship similarity between the rosette diagrams of the open fractures and the red-stained fractures has been found. Quartzfilled fractures strike in NS and EW. Epidote-filled fractures are more scattered.

The fracture zones that have been observed strike mainly E-W as well as coinciding with the Mylonite Zone direction at N55°E.

In respect of bedrock type, the longest fractures are found in the porphyritic granite and the shortest ones in the mylonite. The fracture density of the fine-medium grained granite is significantly higher than that of the porphyritic granite.

In the Mylonite Zone the fracture orientation is predominantly around N60°E. Within the Southern Block the N55°W fractures dominate strongly. The Northern Block is relatively more homogeneous but four conspicuous sectors appear around E-W, N60°W, N5°W and N60°E. The fracture density of the Mylonite Zone is higher than that of the surrounding rock and the Southern Block is more fractured than the Northern Block.

Tectonic Analyses Based on Geophysics

According to the bedrock and tectonic analyse conducted on the basis of the detailed ground geophysical measurements the island of Äspö is divided into three main bedrock blocks, the Northern Block, the Mylonite Zone and the Southern Block /Nisca et al., 1989/.

The interpreted total width of the complex Mylonite Zone is about 300 metres. The Mylonite Zone is sub-vertical, with a small dip-angle towards the north. The computed dip-angles for the E—W fracture zones are 55°—70° towards the north.

The largest lateral and also vertical displacements are observed along the E-W fracture zones trending.

Geophysically interpreted fracture orientation data for the whole of Äspö show four orientation populations. These can be grouped into two orthogonal fracture sets, N-S/E-W and NW/NE.

The NW/NE orthogonal fracture set is older than the N-S/E-W set. The Mylonite Zone itself is the oldest fracture, or deformation zone in the study area. Two other fracture zones were found in the Northern Block, one striking NW and the other striking NE, with widths much greater than those of the other fracture zones in the block.

Low-resistivity zones differ somewhat in length and orientation within the Mylonite Zone, in comparison to the Northern and Southern Blocks. Low-resistivity zones are more common in the Mylonite Zone. Furthermore, the mean length of a low-resistivity zone is slightly longer in the Mylonite Zone, than elsewhere in the area.

The orthogonal N-S/E-W fracture set, delineated from geoelectric/geomagnetic data is almost consistent in all the three sub-areas, the Northern Block, the Mylonite Zone and the Southern Block. The direction of the second orthogonal fracture set, however, varies. The directions of fractures in the Northern Block and Mylonite Zone are similar, though the directions of fractures within the Mylonite Zone are more scattered around N35°E. In the Southern Block, however, a shift is obvious in the dominating angle to about N15°E for the same fracture set. Furthermore the concentration of fracture directions around N55°W, recognizable in the Northern Block and the Mylonite Zone, is absent.

Rock Stress Measurements

Results from two different rock stress measurements are presently available /Bjarnason and Strindell in Olsson—Stille, 1989/. Measurements were made in borehole KAS 03 and KAS 05. The first one is located in the Northern Block and the second in the Southern Block.

The first measurements were made by hydraulic fracturing in borehole KAS 03. The results for all levels above 550 m are presented below. (Table 2-10)

The relationships $\sigma H/\sigma v$ and $\sigma h/\sigma v$ have been calculated for each level. Mean values for the measured values are 1.5 and 0.9.

Table 2-10. Stress measurements in borehole KAS 03.

Vertical depth (m)	σv (MPa)	σh (MPa)	σH (MPa)	$\sigma h/\sigma v$	$\sigma H/\sigma v$
128.0	3.4	3.6	5.0	1.1	1.5
149.7	4.0	4.5	6.8	1.1	1.7
338.1	9.0	5.5	7.7	0.6	0.9
468.5	12.4	10.7	19.5	0.9	1.6
481.5	12.8	10.9	20.7	0.9	1.6
501.3	13.3	11.8	19.4	0.9	1.5
519.7	13.8	11.8	25.1	0.9	1.8
521.6	13.8	12.4	24.4	0.9	1.8
531.2	14.1	10.7	20.2	0.8	1.4
533.2	14.1	9.8	17.7	0.7	1.3
536.1	14.2	9.8	18.0	0.7	1.3
			mean value	x = 0.9	x = 1.5

σv = assumed vertical stress, depth(m) x 0.0265(MPa)
σh = smallest horizontal stress, measured
σH = largest horizontal stress, measured

The second set of measurements were made in borehole KAS 05 using the overcoring technique. Three measurements were made at the 195 m level in medium-grained granite and four at 355 m in diorite. (Table 2-11)

The stresses in the horizontal plane show a very obvious uniform pattern, with the greatest magnitude in the E-W direction and the smallest magnitude in the N-S direction. Two of the values at the 355 m level are negative, tensile stresses for σh and low values for σH. These figures seem peculiar and may be caused by local residual stresses. In further calculations these two values will not be considered.

The mean values for all measured levels are 2.0 for $\sigma H/\sigma v$ and 0.4 for $\sigma h/\sigma v$.

Table 2-11. Rock stress measurements in borehole KAS 05.

Vertical depth (m)	σv (MPa)	σh (MPa)	σH (MPa)	$\sigma h/\sigma v$	$\sigma H/\sigma v$
195.3	5.2	2.4	9.8	0.5	1.9
196.6	5.2	7.6	9.3	1.5	1.8
197.4	5.2	5.0	12.9	1.0	2.5
			mean value	x = 1.0	x = 2.1
355.0	9.4	1.9	17.0	0.2	1.8
355.9	(9.4	-2.6	10.3	-0.3	1.1)
356.8	(9.4	-0.6	10.6	-0.1	1.1)
357.7	9.4	2.3	17.7	0.2	1.9
			mean value	x = 0.2	x = 1.8

The measurements in the two boreholes show rather similar results for the $\sigma H/\sigma v$ relationship. This value is of interest when predicting deformations and possible rock burst problems in the tunnel.

As mentioned before, the two measurements were made in the two different blocks which Äspö, from a structural geological point of view, is divided into.

However, the results do not show any tendency which would indicate that different rock stress conditions are appropriate for different parts of the island.

Borehole Data

The three core boreholes, KAS 02, KAS 03 and KAS 04, were sited in a preliminary geological and geohydrological model of Äspö, Figure 2-37:

KAS 02: A sub-vertical borehole to approx. 1000 m depth in the Southern Block.

KAS 03: A sub-vertical borehole to approx. 925 m depth in the Northern Block.

KAS 04: An inclined (60°SE) borehole across the Mylonite Zone.

Granitic rocks (Småland granite) are the most common in all the cores except KAS 02, where dioritic rocks (Äspö diorite) are by far the most common from about 315 m to the bottom of the hole, (Figure 2-38). Dioritic rocks are much more rare in the other cores and its also interesting to note that this rock type has not been observed during the surface mapping within the Äspö area.

Fine-grained granite is represented in dykes and veins in the three cores but is much more common (approx. 30% of the core length) in KAS 03 and KAS 04 than in KAS 02 (only 15%). There is a very evident radiometric correlation
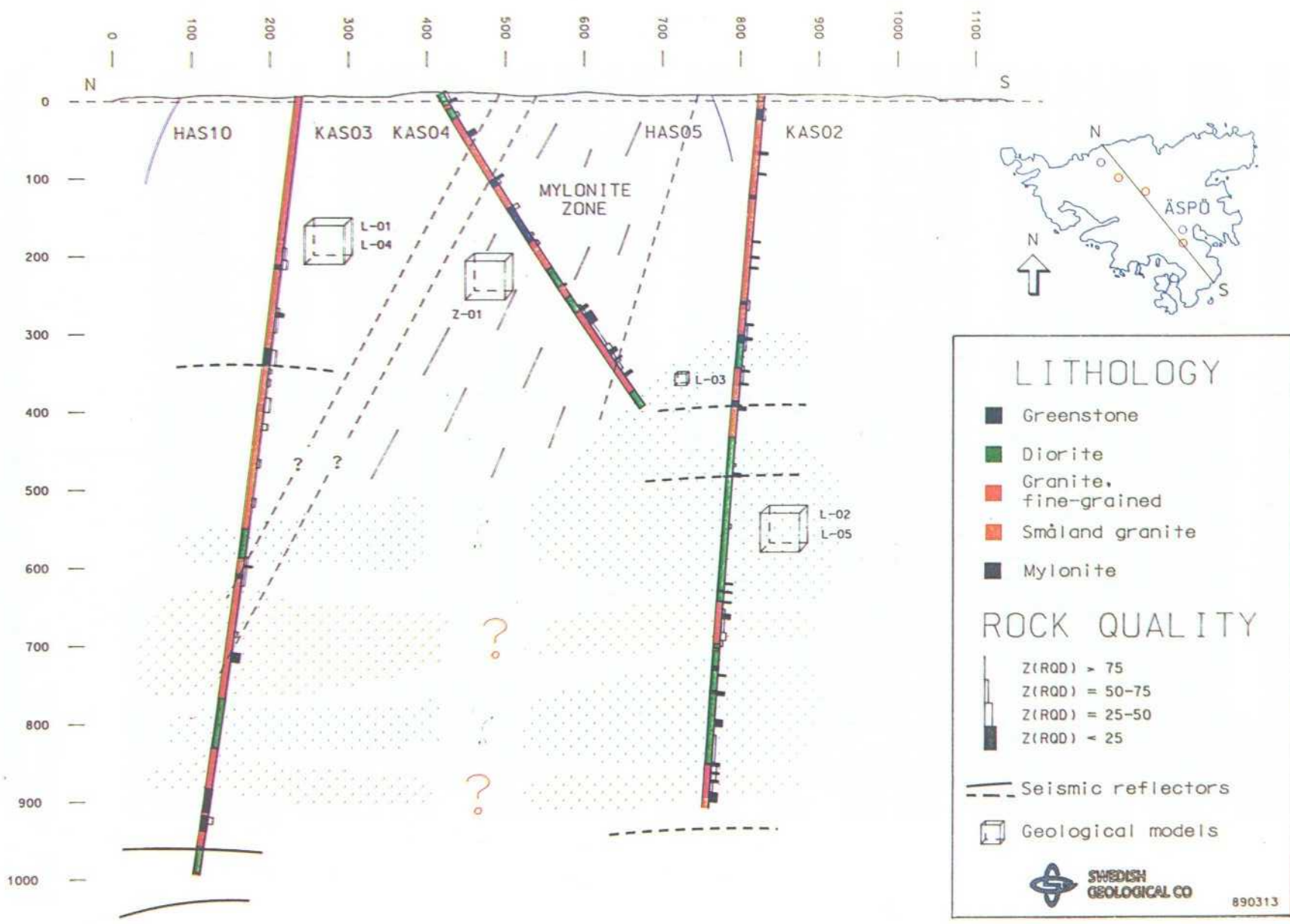
Figure 2-38. Cross section through the island of Äspö. Generalized lithological interpretation.

69

LITHOLOGY

- Greenstone
- Diorite
- Granite, fine-grained
- Småland granite
- Mylonite

ROCK QUALITY

Z(RQD) > 75
Z(RQD) = 50-75
Z(RQD) = 25-50
Z(RQD) < 25

Seismic reflectors

Geological models

SWEDISH GEOLOGICAL CO

890313

between two large sections of fine-grained granite at the depths of approx. 700 and 875 m.

Dark, fine-grained greenstone occur as some metre-wide remnants — often strongly altered — in the younger granitic and dioritic rocks. The greenstone constitutes 4% of the total core length in all the boreholes.

The foliation of the rocks in the cores varies in intensity from rarely detectable to very strong or mylonitic. It is generally more intense close to mylonites. Ductile shearing is also common along lithological boundaries. Concerning the relationship between ductile and brittle structures there is a good correlation between shear zones — especially wide mylonitic zones — and intense fracturing. The fracture frequency is also greater in sections of the cores where two foliations are present.

Major Mylonite Zones were observed, especially in KAS 04 at 170—182 m and 214—217 m. In KAS 02 mylonitic zones occur at 455—485 m and a 550—570 m depths, both associated with 1—2-m wide crushed zones. In KAS 03 approx. 1-m wide mylonites are intersected at 397, 403, 456, 865 and 920 m depths. These zones correspond to increased fracturing.

The fracture frequency is generally higher in KAS 03 than in KAS 02 down to approx. 750 m. Below this level the core in KAS 02 is highly fractured. In KAS 04 the core on the whole show signs of strong mechanical deformation.

Fractures dipping steeply-moderately seem to be more frequent than low-dipping fractures in all the boreholes. The natural surfaces of the fractures are mostly rough and uneven in KAS 02 while smooth and often slickensided surfaces dominate in the other boreholes.

Calcite and chlorite are the most frequent fracture minerals throughout all the cores. Hematite and epidote are concentrated to distinct zones. There seems to be agreement between the open fractures detected in the geophysical logging and the frequency of Fe-oxyhydroxide and hematite. These Ferroan-minerals are much more frequent in KAS 03 than in KAS 02, where there is a very large increase of Ferroan-minerals which can be correlated to the main fracture zone in the bottom of this borehole. Tullborg in /Wikman et al 1988/.

Sections with increased fracturing and crushed zones (normally only 1—2 m wide) are more or less evenly distributed throughout the three boreholes — but are most frequent in KAS 04 and KAS 02 and least in KAS 03. Core losses are very rare and more complete alteration is normally noticed only in the greenstones. Fine-grained granite appears to be more brittle and more highly fractured than the Småland granite and diorite.

Main fracture zones occur in KAS 02 at approx. 300—370 m and below approx. 800 m, in KAS 03 at approx. 300—350 m and approx. 725—750 m, and in KAS 04 at approx. 325—450 m (Figure 2-38).

Crosshole correlations of single-hole radar results indicate one structure between boreholes KAS 02, KAS 03 and KLX 01. This intersects the holes at the depths 863, 579 and 577 metres, resulting in a strike of N54°E dipping 27° towards SE /Niva, 1988/.

2.2.2 Block Scale

Rock mass descriptions to such a detailed scale as about 50 x 50 x 50 m can, of course, only be of a rather preliminary character until the descriptions can be based on results from more detailed geological investigations (especially core drilling). Descriptions based on the present knowledge may, however, be of in-

terest as a test of predictive ability in this second stage of the preinvestigation programme.

Six rock volumes are described. L-01—L-03 are more general examples of the lithological distribution and Z-01—2-03 are examples of different possible fracture zones in the rock mass on the island of Äspö (Figure 2-39a-i).

L-01

This is an example of lithological distribution — especially at the level 0 — approx. 300 m — in the Northern as well as in the Southern Block of Äspö (according to surface mapping and core boreholes KAS 02 and KAS 03). The dominating rock type is a medium-grained, reddish-grey granite-granodiorite, often porphyritic, called "Småland granite".

It is a dark grey, fine-grained rock type which occur as lenses and narrow dykes in the granite mass. This rock is called "Greenstone" and normally regarded as being of volcanic origin. The rock mass described is extensively intruded by a red, fine-grained granite (aplite) in form av veins and dykes. This rock type is called "Fine-grained granite".

L-02

This is an example of lithological distribution at deeper levels, especially in the Southern Block. Below the level of approx. 300 m a dark grey, medium-grained, sometimes porphyritic, more basic rock type is very frequent. This rock which, according to mineralogical and chemical analysis, has a composition from monzodiorite to diorite, is called "Äspö diorite".

L-03

This is a single open fracture in a rock mass of Småland granite. Open fractures (centimetre to decimetrewide) occurring irregularly in a homogeneous and isotropic granitic rock mass are often highly permeable and very hard to predict.

Z-01

This is an example of fracture zone in mylonite. Fracture zones of many different kinds may occur in the approx. 300 m wide "Mylonite Zone" crossing the central part of Äspö in a ENE-NE direction. The "Mylonite Zone" is very complex, with highly fractured and permeable parts alternating with more or less unaffected parts in tight units.

Z-02

This fracture zone is of a more general nature in the Småland granite connected to areas of increased shear in the granite blocks of Äspö, considered to be moderately to highly permeable.

SKB
Hard rock laboratory - Äspö.
Geological model on a block scale (L-01).
Level approx. 0-500 m.
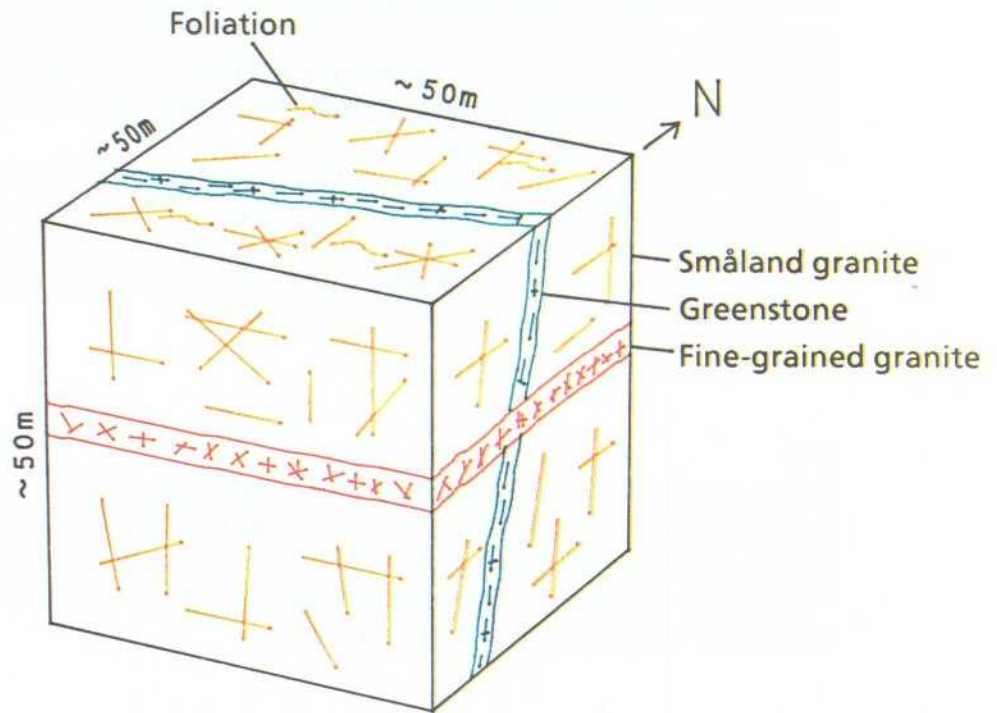
|	Greenstone	Sm. granite	Fine-gr. granite
J_v (number of fractures per m3):	5.6-16	4.8-8	7.2-16
Fracture length:	0.5-1 m	1-2 m	0.5-1 m
Fracture filling:	Chlorite-Clay	Calcite-Fe-oxy-hydroxide	Calcite
Permeability: (estimated)	Low (contact zones may be high-permeable)	Low-medium	High

Figure 2-39a. Rock block L-01.

SKB
Hard rock laboratory - Äspö.
Geological model on a block scale (L-02).
SE block area (level approx. 300-600 m).

ÄSPÖ

Äspö diorite

Fine-grained granite
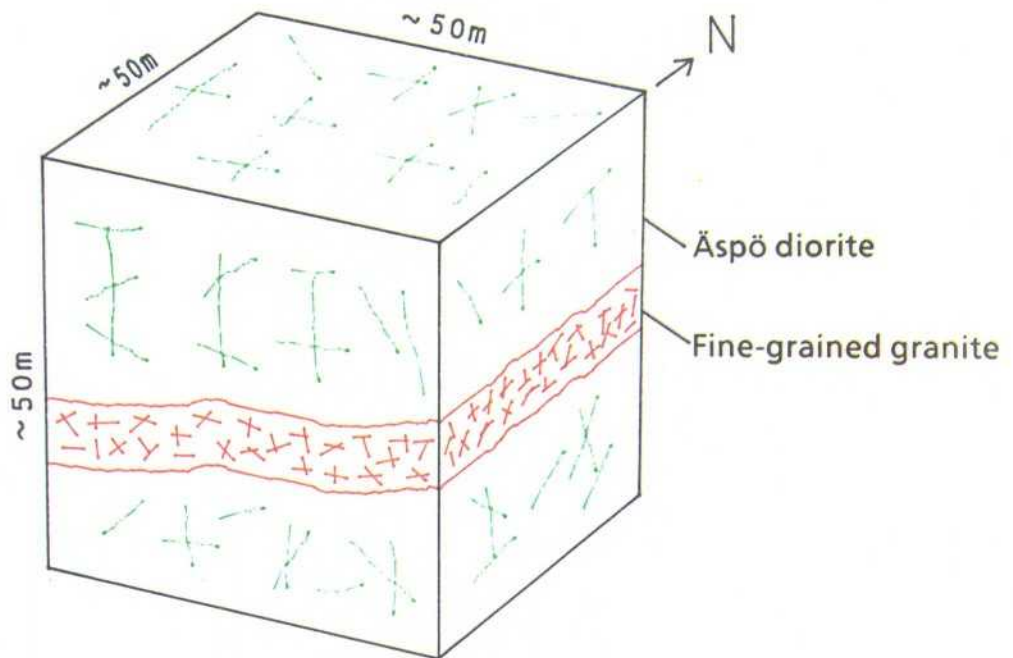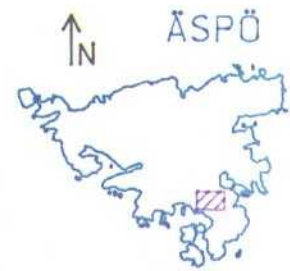
	Diorite	Fine-grained granite
J_v (number of fractures per m³):	3.3-6	7.2-16
Fracture filling:	Chlorite	Chlorite, Fe-oxy-hydroxide
Permeability: (estimated)	Low	High

Figure 2-39b. Rock block L-02.

SKB
Hard rock laboratory - Äspö.
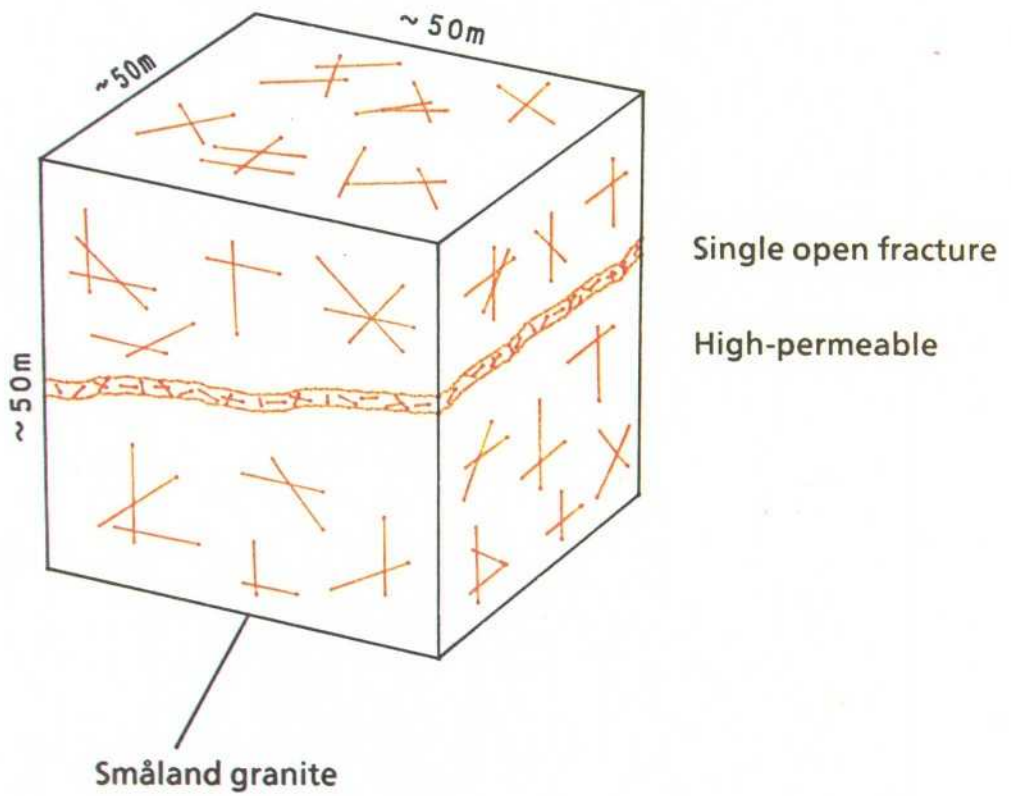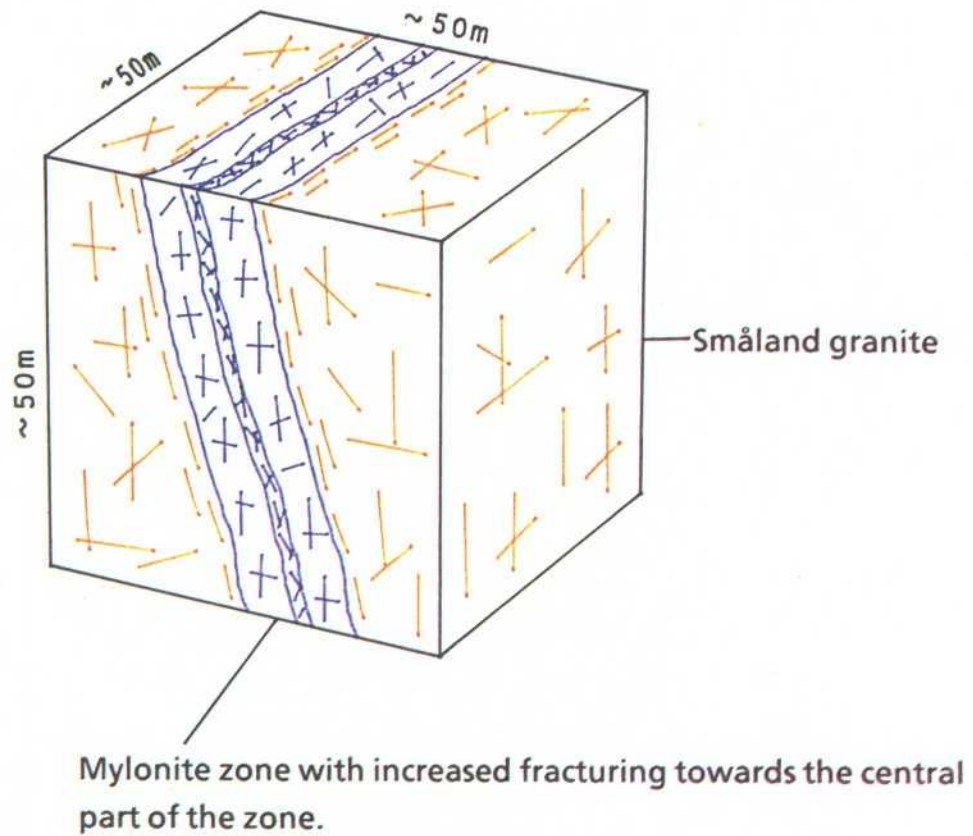Geological model on a block scale (L-03).
Single open fracture.

Figure 2-39c. Rock block L-03.

SKB
Hard rock laboratory - Äspö.
Geological model on a block scale (Z-01).
Fracture zone: Mylonite.

Mylonite zone with increased fracturing towards the central part of the zone.

Fracture filling: Mostly calcite and Fe-oxy-hydroxide.
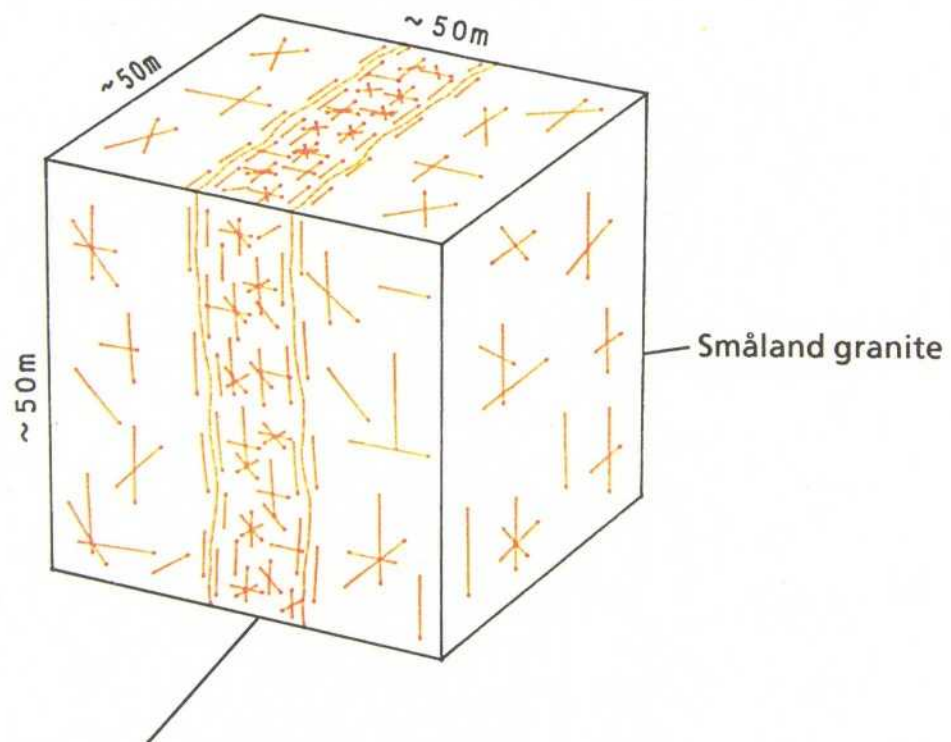
Permeability: Increasing towards the centre of the zone.

Figure 2-39d. Fracture zone Z-01.

SKB
Hard rock laboratory - Äspö.
Geological model on a block scale (Z-02).
Fracture zone: Water bearing.

~ 50m

~50m

~ 50m

Småland granite

Fracture zone with increased shearing and fracturing in Småland granite.

Fracture filling: Chlorite, calcite and Fe-oxy-hydroxide.

Permeability: Medium-high!
    May be irregular along the extension of the zone!

Figure 2-39e. Fracture zone Z-02.

SKB
Hard rock laboratory - Äspö.
Geological model on a block scale (Z-03).
Fracture zone: slightly permeable - dry.

Figure 2-39f. Fracture zone Z-03.
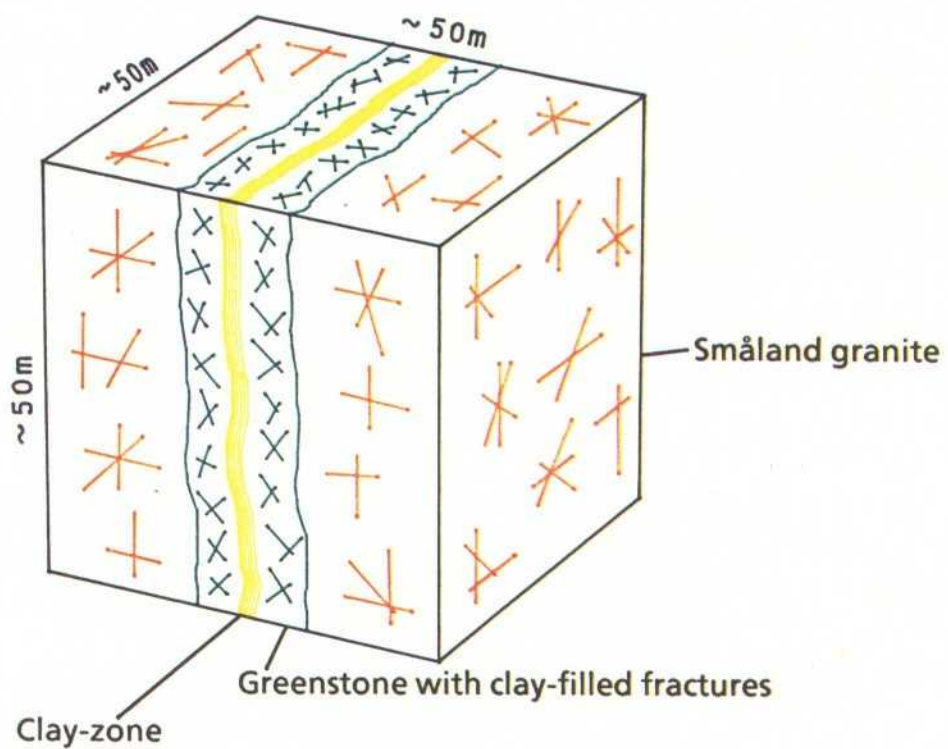
Permeability: The central clay-filled zone is normally dry. The surrounding greenstone, with partly clay-filled fractures, may be slightly permeable - dry.

SKB
Hard rock laboratory - Äspö.
Geological model on a detailed scale (L-04).
SE block area (level 0-300 m).

Småland granite
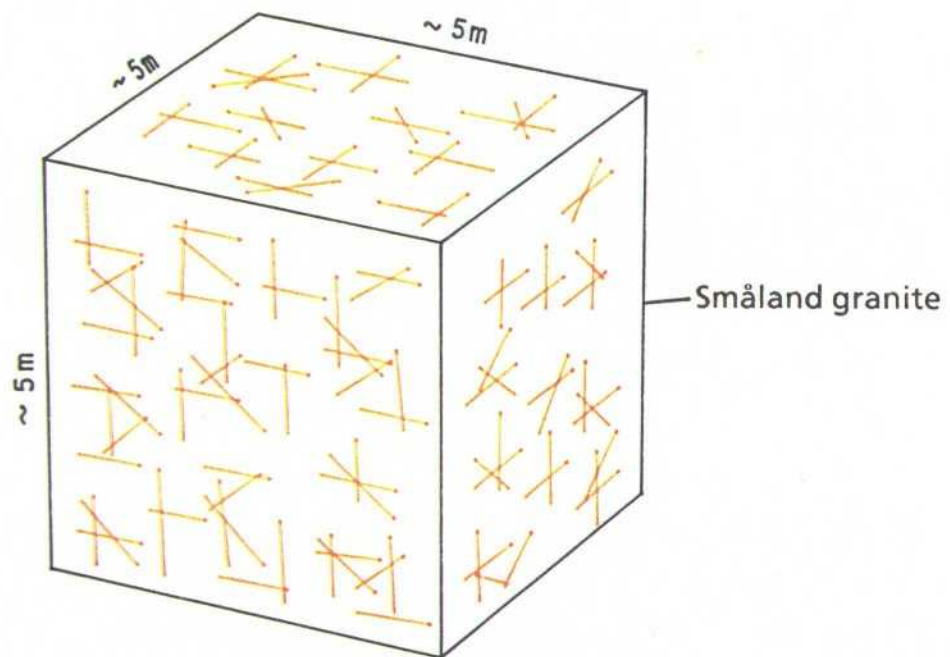
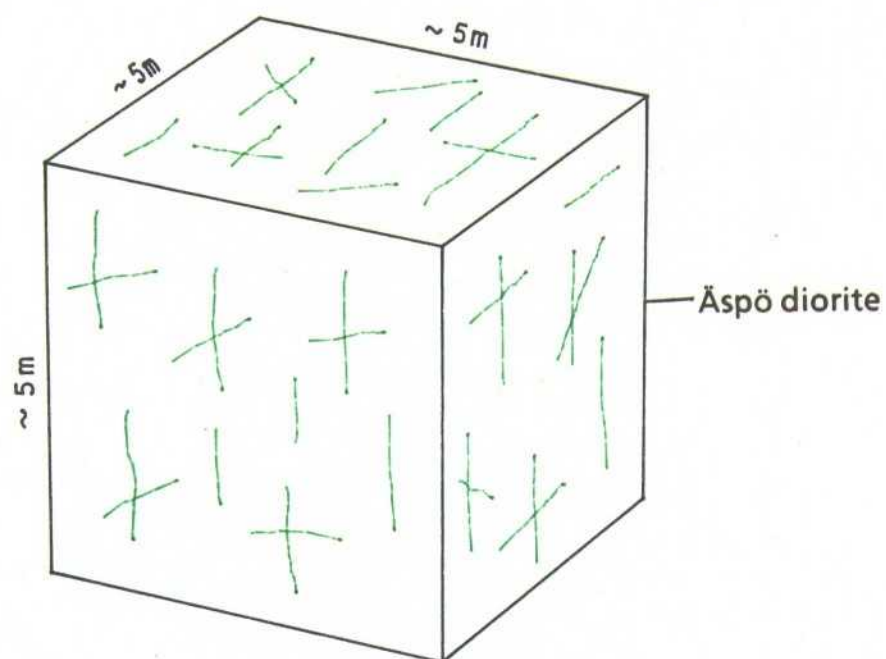| J_v (number of fractures per m³):	4.8
Fracture length (surface):	1-2 m
Fracture filling:	Chlorite, Fe-oxy-hydroxide
Permeability (estimated):	Low-medium

Figure 2-39g. Rock block L-04.

SKB
Hard rock laboratory - Äspö.
Geological model on a detailed scale (L-05).
SE block area (level approx. 300-600 m).

~ 5 m
~ 5 m
~ 5 m
Äspö diorite

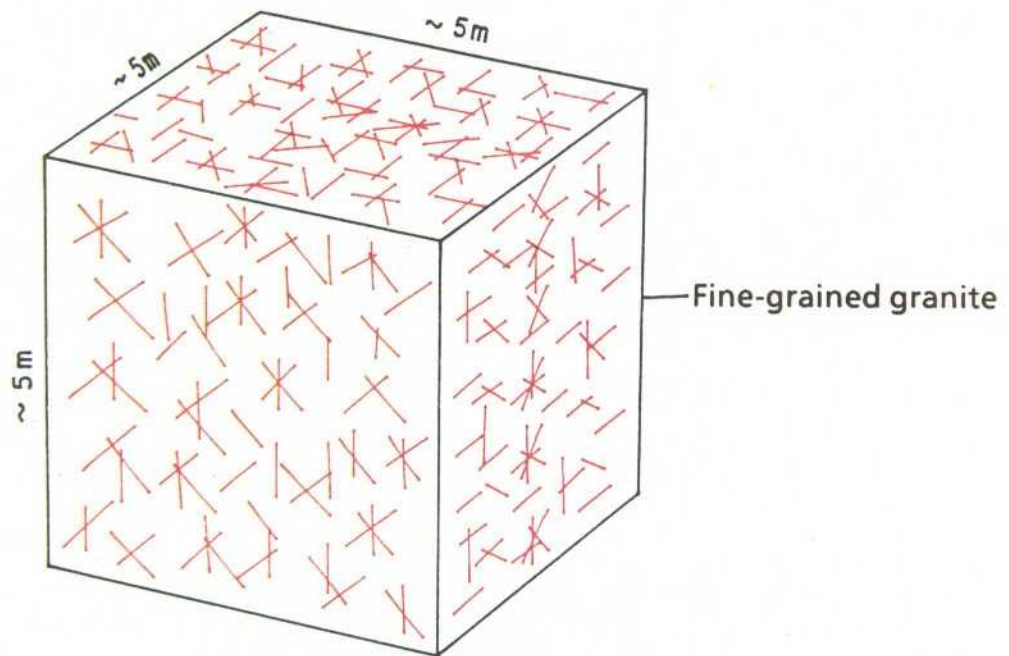| Jv (number of fractures per m³):	3.3
Fracture filling: :	Chlorite
Permeability (estimated):	Low

Figure 2-39h. Rock block L-05.

SKB
Hard rock laboratory - Äspö.
Geological model on a detailed scale (L-06).
SE block area (level approx. 0-500 m)

~ 5m

~ 5m

~ 5m

Fine-grained granite

J_v (number of fractures per m3):	7.2
Fracture length (surface):	0.5-1 m
Fracture filling:	Chlorite, Fe-oxy-hydroxide
Permeability (estimated):	Medium-high

Figure 2-39i. Rock block L-06.

Z-03

This fracture zone in the Småland granite on Äspö is of a more complex nature. The central part of this zone is estimated to be less permeable than the marginal parts due to increased altering and clay-filling.

2.2.3 Detailed Scale

Three rock mass descriptions in the detailed scale of about 5 x 5 x 5 m are presented on the basis of information from detailed surface mapping and core logging.

L-04

Homogeneous "Småland granite" not affected by fracture zones.

L-05

Homogeneous "Äspö diorite" not affected by fracture zones.

L-06

Homogeneous "Fine-grained granite" — not affected by more intense fracturing.

2.3 VALIDATION OF THE PRELIMINARY GEOLOGICAL-TECTONICAL MODELS OF THE SIMPEVARP AREA

The geological-tectonic models of the Simpevarp area in report SKB-TR 88-16, were made as rock mass descriptions on three different scales.

Regional scale	(approx. 5000 x 5000 m)
Site scale	(approx. 500 x 500 m)
Block scale	(approx. 50 x 50 m)

The validity of these models — based on our present knowledge — is discussed below.

2.3.1 Regional Scale

The greater part of the geological description is still considered to be valid. Further information has become available mainly from core drilling and geophysical measurements in the Äspö and Laxemar areas.

Seismic reflection profiles on Äspö indicated two subhorizontal fracture zones at depth of 300—500 metres and 950—1150 metres. Both zones are probably reflecting a system of more or less interconnected and irregular heterogenetics of fractured rock mass which very probably extend outside Äspö. According to Nordenskjöld (1944) thrust zones especially trending NW and with low dips to the WSW occur i.e. in the area to the west of Simpevarp.

Information from all the boreholes in which dioritic rocks were observed indicate large bodies of mafic rocks (diorite-gabbro) formed in a continuous magma-mingling and magma-mixing process /Wikström, 1989/.

2.3.2 Site Scale

THE LAXEMAR AREA

Core borehole KLX 01 was sited in the central part of a rock block, (Figure 2-40). Homogeneous Småland granite, with xenoliths of greenstone intersected by fine-grained granite and flat-lying pegmatites, was predicted in the rock mass description. Only minor local fracture zones were expected. The core description in Figure 5-1 is in rather good accordance with the rock mass prediction, except for the pegmatites, which are almost absent.

THE ISLAND OF ÄSPÖ

At an early stage of the pre-investigation the island of Äspö was subdivided in three geological-tectonic units: The Northern Block, the Southern Block and the Mylonite Zone (greenstone lenses) in between them, (Figure 2-37). This subdivision is still valid. Later geophysical measurements have indicated the width of the Mylonite Zone to be about 300 m dipping approx. 70° to the north.

NW Äspö

Information from borehole KAS 03 indicates that the lithological distribution, down to the 500-m level, and the increased fracturing at the 300—400-m level valid except the for low-dipping pegmatites, which are rare (Figure 2-38).

The Mylonite Zone

The inclined core borehole, KAS 04, reveals a lithological distribution in rather good accordance with the rock mass description except for the pegmatites. The dip of the Mylonite Zone was predicted to be almost vertical and to extend not so far to the south.

SE Äspö

In core borehole KAS 02 the occurrence of basic rocks is less frequent at the 100—300-m level than predicted. At the 300—500-m level they are in rather good accordance with the preliminary model. Low-dipping pegmatites are almost absent. The dip of the fracture zone about 100 m south of the borehole was predicted to be southwards.

2.3.3 Block Scale

Based on present knowledge most of the information from the geological models on the block scale still seems to be valid.
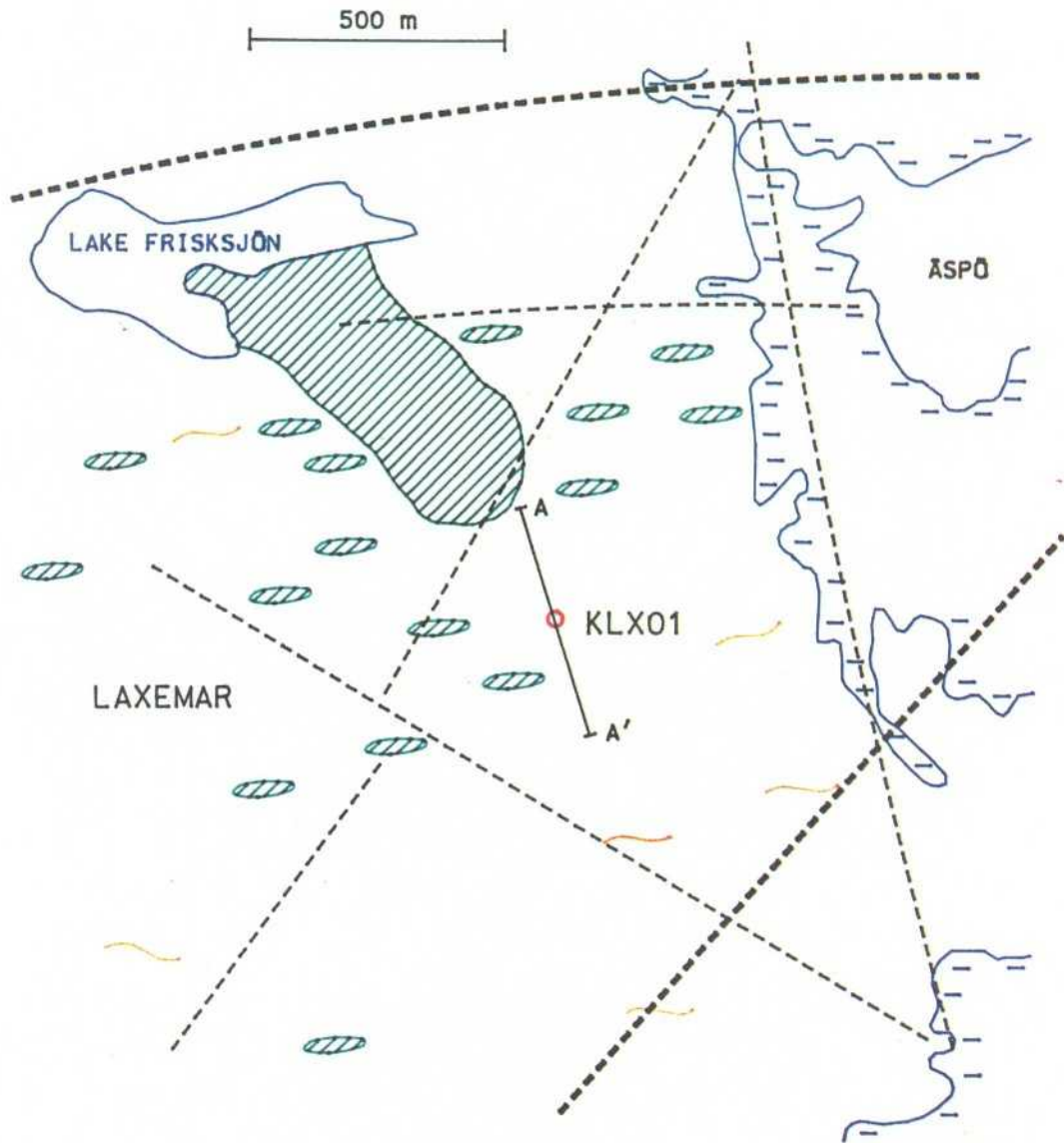
Figure 2-40. Geological-tectonical model of the Laxemar area.

3 GEOHYDROLOGY

3.1 GEOHYDROLOGICAL STUDIES

3.1.1 Hydraulic Tests in the Boreholes

In connection with the drilling operations hydraulic tests were performed in the boreholes. The tests were made at different stages in the operation and on different scales. The tests are evaluated and reported by /Nilsson 1988/. Based on the test results some conductive sections of the boreholes were selected for transient interference tests. These are summarized in Section 3.1.2.

Section 3.1.3 presents the hydraulic parameter evaluation based on the lithology and the geophysical logs in the borehole combined with the hydraulic tests. A short summary of the tests performed and their results are given below.

AIR-LIFT TESTS

Air-lift tests were performed in percussion borehole HAS 08-12 and, in connection with water sampling during drilling, one test in borehole KAS 02 and two in borehole KAS 03. The tests in the percussion boreholes were performed as one-hour of air-lift pumping followed by a recovery period. In the core boreholes a packer is set above 100 m above the bottom of the hole, and the air-lift test was done through the packer string.

The percussion boreholes of the second batch, HAS 08-12, all had a very low transmissivity, so low that the well bore storage in the boreholes made conventional transient analysis impossible. The specific capacity of the boreholes can, however, be related to the previous boreholes (see Figure 3-1).

The air-lift tests in the core boreholes were too few to be related to other tests. However, in themselves they give relevant information, thus making the test procedure interesting for subsequent investigation phases.

PACKER TESTS OVER 3-M SECTIONS

Packer tests over 3-m sections were performed in all core boreholes. Due to some trouble with the equipment it was not possible to test the full depth of all holes. The sections tested are summarized in Table 3-1.

Each test was performed as a 10-minute injection period at 200 kPa followed by a 10-minute fall-of period before the packer set was moved.

Data were evaluated in two steps. First a conventional steady-state evaluation was performed for the sections where a reliable flow could be measured using the flow gauge. Based on these data and a regression on the after-flow determined from the pressure decline periods, a new set of flows was calculated. In the second run both steady-state and transient evaluations were performed. Data was found to exhibit approximately log-normal distribution and an example from borehole KAS 03 is shown in Figure 3-2. The results are summarized in Table 3-1.
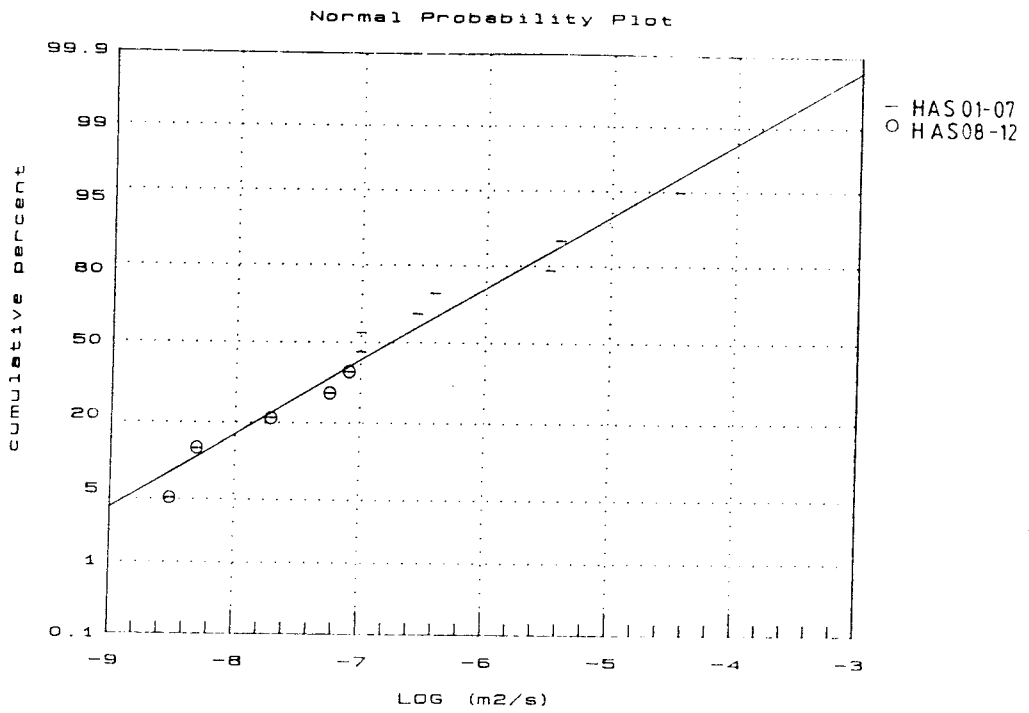
Figure 3-1. Cumulative plot of specific capacities for percussion boreholes on Äspö.
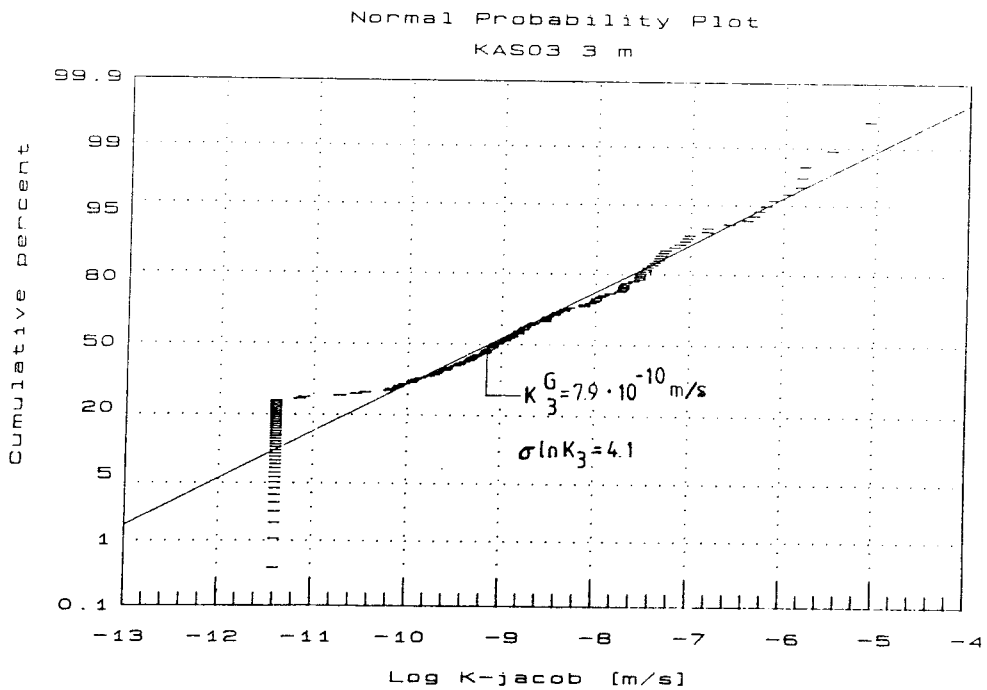

Figure 3-2. Cumulative plot of hydraulic conductivities for 3-m sections in KAS 03.

Table 3-1. Conductivity distribution for 3-m sections.

Borehole	Section (m)	Arithmetic mean K^A(m/s)	Geometric mean K^G(m/s)	Std. dev. S_{lnK}
KAS 02	102—801	$1.7 \cdot 10^{-8}$	$1.3 \cdot 10^{-11}$	4.48
KAS 03	103—547	$2.2 \cdot 10^{-8}$	$8.0 \cdot 10^{-10}$	4.25
KAS 04	133—454	$7.8 \cdot 10^{-8}$	$8.9 \cdot 10^{-10}$	3.93
KLX 01	106—688	$2.2 \cdot 10^{-8}$	$1.0 \cdot 10^{-10}$	3.47

The geometrical distribution of the conductivity values will be shown in conjunction with the other measurements (see Figures 3-6 — 3-9.

PACKER TESTS OVER 30-m SECTIONS

The packer tests over 30-m sections were performed in three core boreholes. Some sections of the boreholes were also excluded from these tests due to equipment problems. The sections tested are shown in Table 3-2.

Each test was performed as a 120-minute injection period at 200 kPa followed by a 120-minute fall-off period before the packer set was moved.

Data were evaluated under transient conditions for the fall-off period. The hydraulic conductivities were found to exhibit approximately log-normal distribution. An example is shown in Figure 3-3 and the results are summarized in Table 3-2.
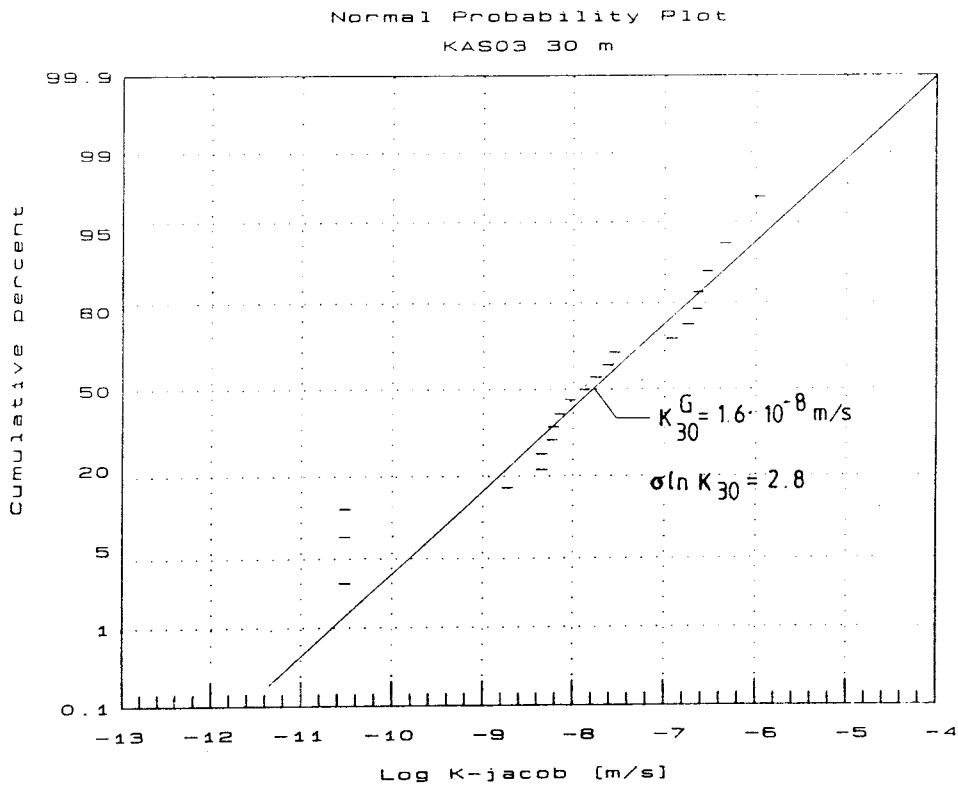

Figure 3-3. Cumulative plot of hydraulic conductivities for 30-m sections in KAS 03.

Table 3-2. Conductivity distribution for 30-m sections.

Borehole	Section (m)	Arithmetic mean K^A(m/s)	Geometric mean K^G(m/s)	Std. dev. S_{inK}
KAS 02	102-810	$2.9 \cdot 10^{-8}$	$6.3 \cdot 10^{-9}$	2.7
KAS 03	103-703	$7.1 \cdot 10^{-8}$	$7.9 \cdot 10^{-9}$	2.5
KLX 01	103-643	$2.2 \cdot 10^{-7}$	$5.6 \cdot 10^{-10}$	4.0

The geometrical distribution of the conductivity values will be shown in conjunction with the other measurements in Figures 3-6 — 3-9.

PUMPING TESTS AND SPINNER SURVEYS

After the end of drilling and testing operations the core boreholes were pumped in order to clean them up and to perform a hydraulic test on the entire borehole. This was made possible because of the telescope design of the boreholes.

This also made it possible to log the vertical water velocity in the boreholes by a spinner survey.

Data from the draw-down period of the pumping test were evaluated by a normal transient analysis and interference with other boreholes was checked. The hydraulic conductivity could then be determined approximately as the derivative of the spinner curve multiplied by the transmissivity of the borehole.

As an example the evaluation of data from KAS 03 is shown in Figure 3-4. The figure shows a conventional Jacob plot with an expressed straight line portion and a curve that approaches steady state at the end.
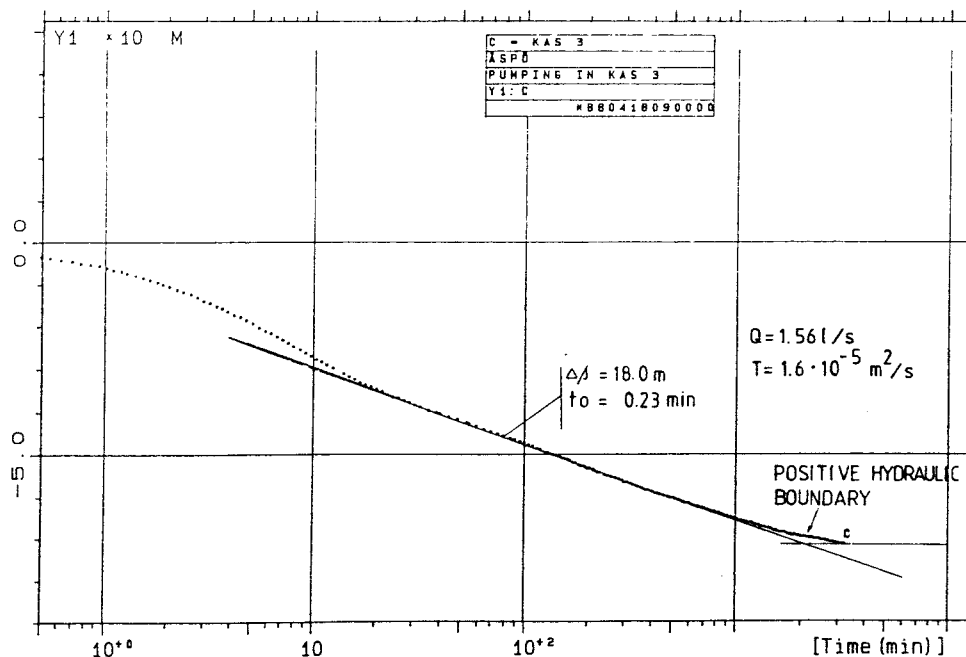

Figure 3-4. Drawdown graph of KAS 03 in semilog.
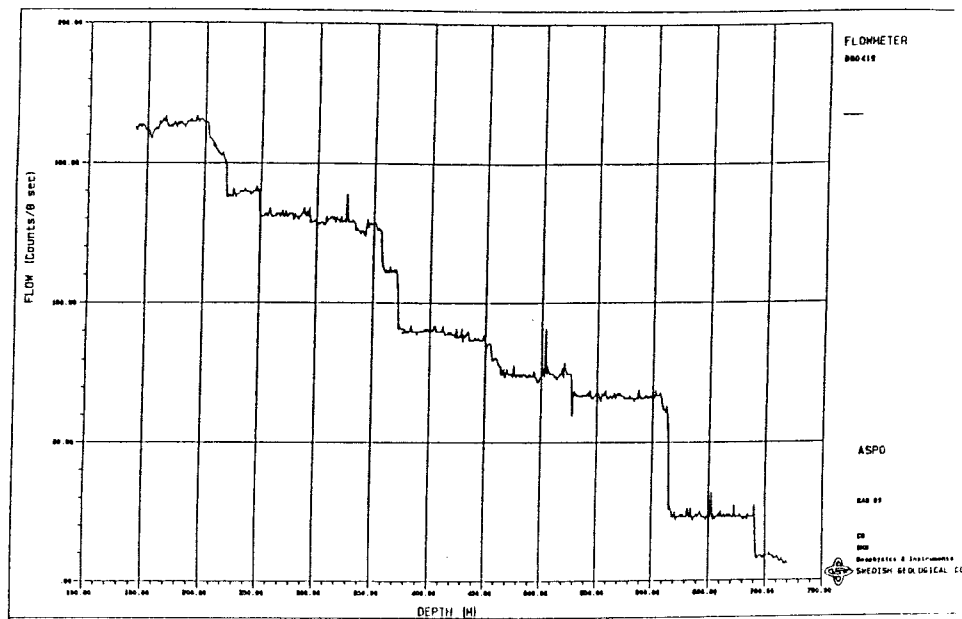
Figure 3-5. Spinner curve-flow meter survey in KAS 03.

The spinner curve for the same test is shown in Figure 3-5. As can be seen the inflow of water is restricted to very narrow zones, shown as steps in the graph.

The results of the core borehole pumping tests are summarized in Table 3-3.

Table 3-3. Results from pumping tests in core boreholes.

Borehole	Transmissivity T(m²/s)	Skin factor Sk(-)	Average conductivity Kₑ(m/s)
KAS 02	$1.5 \cdot 10^{-4}$	26	$1.7 \cdot 10^{-7}$
KAS 03	$1.6 \cdot 10^{-5}$	-5	$1.5 \cdot 10^{-8}$
KAS 04	$2.4 \cdot 4 \cdot 10^{-5}$	-4.5	$5.0 \cdot 10^{-8}$
KLX 01	$8.0 \cdot 10^{-5}$	-4	$1.2 \cdot 10^{-7}$

SUMMARY OF RESULTS

The hydraulic testing programme was designed so that tests were performed on different scales in the different boreholes. It is also evident that the tests also gave different results. The reason for this will be discussed in Section 3.1.3.

A simple way to present the results is to plot data from all tests performed in a borehole as a cumulative transmissivity versus depth, i.e. in the same manner as a spinner survey graph. Figures 3-6 — 3-9 show cumulative plots of all the test methods employed as a function of depth for the core boreholes.

Figure 3-6 shows that the main hydraulic conductor is situated at the bottom of the borehole, the fractures in that section made packer tests impossible there.
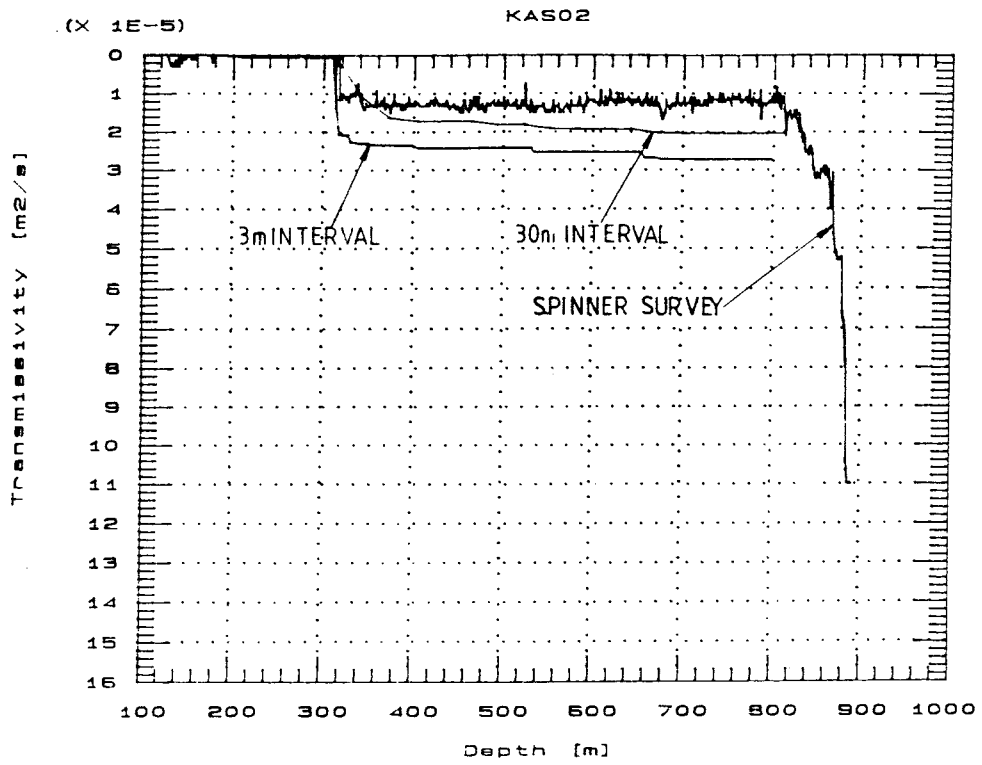
Figure 3-6. Cumulative plot of integrated hydraulic conductivity versus depth for KAS
02.
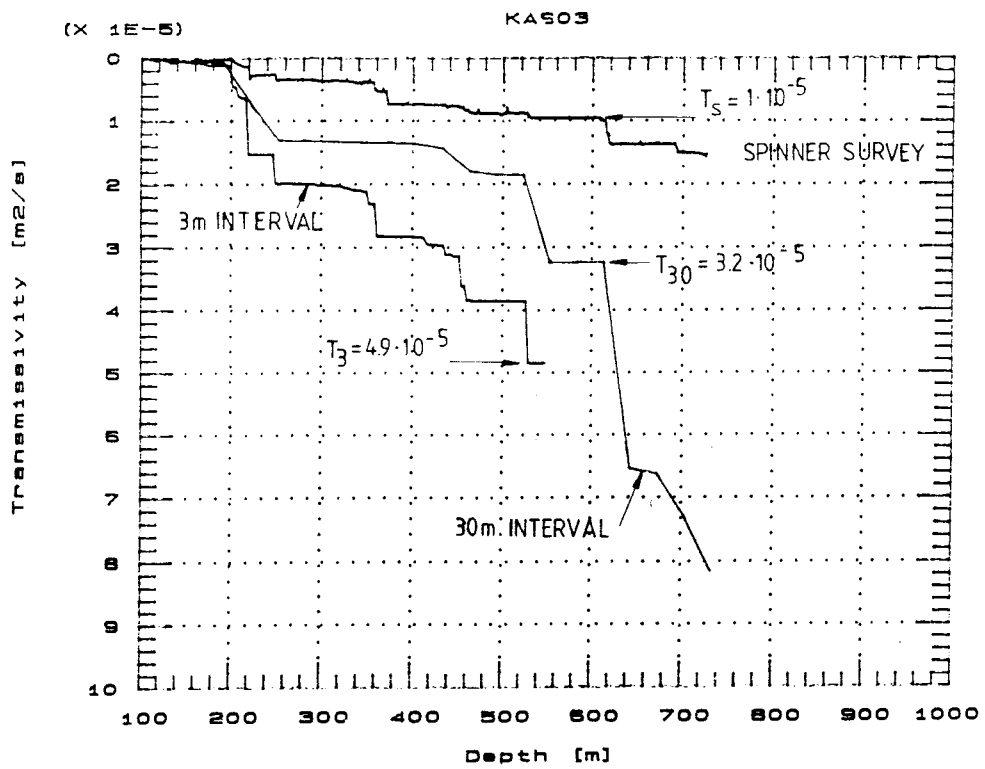
Figure 3-7. Cumulative plot of integrated hydraulic conductivity versus depth for
KAS 03.
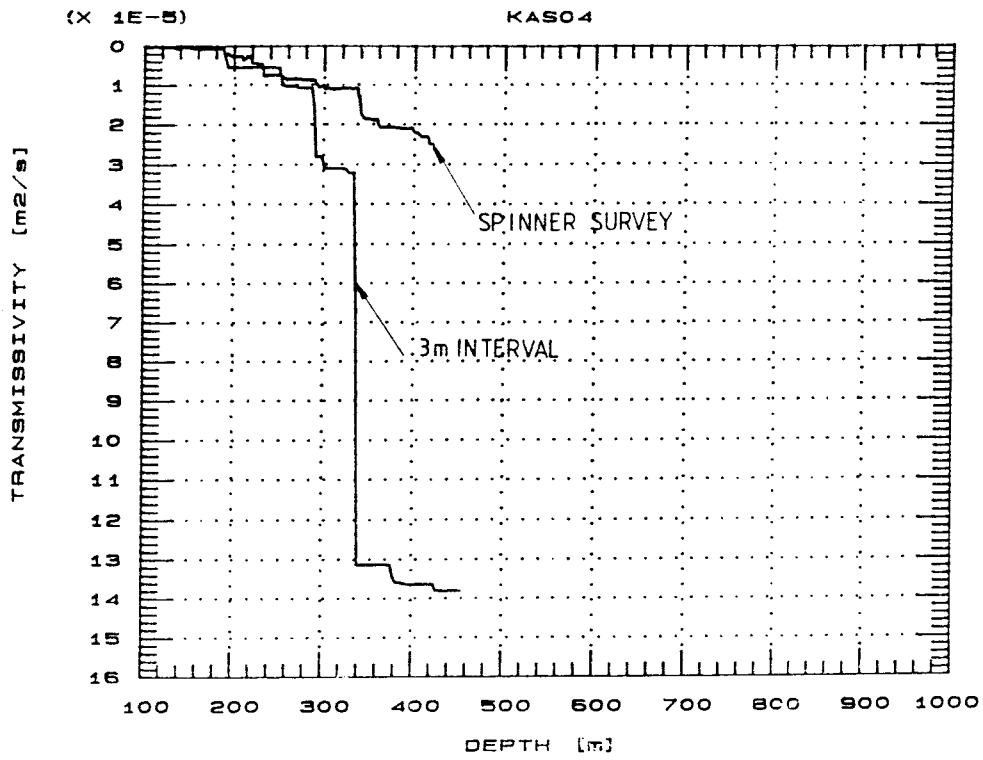
Figure 3-8. Cumulative plot of integrated hydraulic conductivity versus depth for KAS 04.
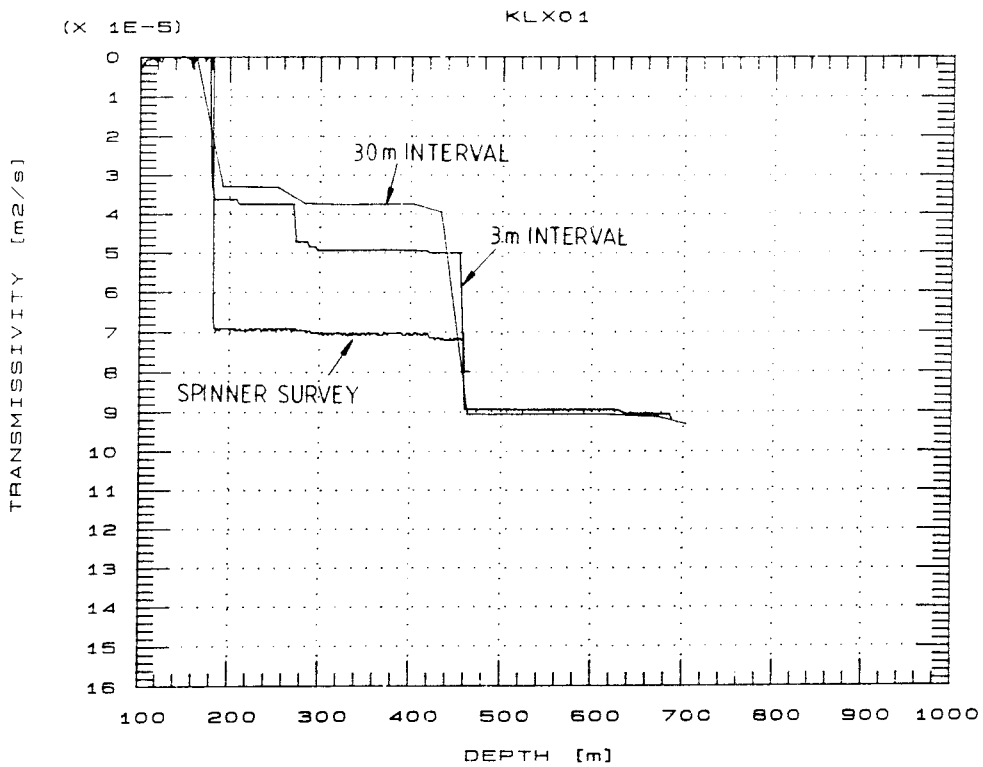
Figure 3-9. Cumulative plot of integrated hydraulic conductivity versus depth for KLX 01.

It is, however, clear that conductive sections show up in the same places for all the methods employed, which is common for all plots. It is also common that the spinner survey shows the smallest transmissivity, followed by the 30-m packer tests and the 3-m tests.

3.1.2 Transient Interference Tests

In the deep core boreholes, KAS 02-04, pumping tests were performed in selected sections. The test sections were selected on the basis of spinner surveys and packer tests in the boreholes. The field data are presented in borehole reports /Borrhålsrapporten: KAS 02, KAS 03; Hydrotester/ and the evaluation of test data is reported by /Rhen 1988/.

In all 9 pumping tests were performed during August and September 1988, of which 6 were done in KAS 03 and 3 in KAS 02 (see Figure 3-10).

The object of the tests was to determine the hydraulic properties of identified hydraulic conductors on Äspö, their extent and geometry.
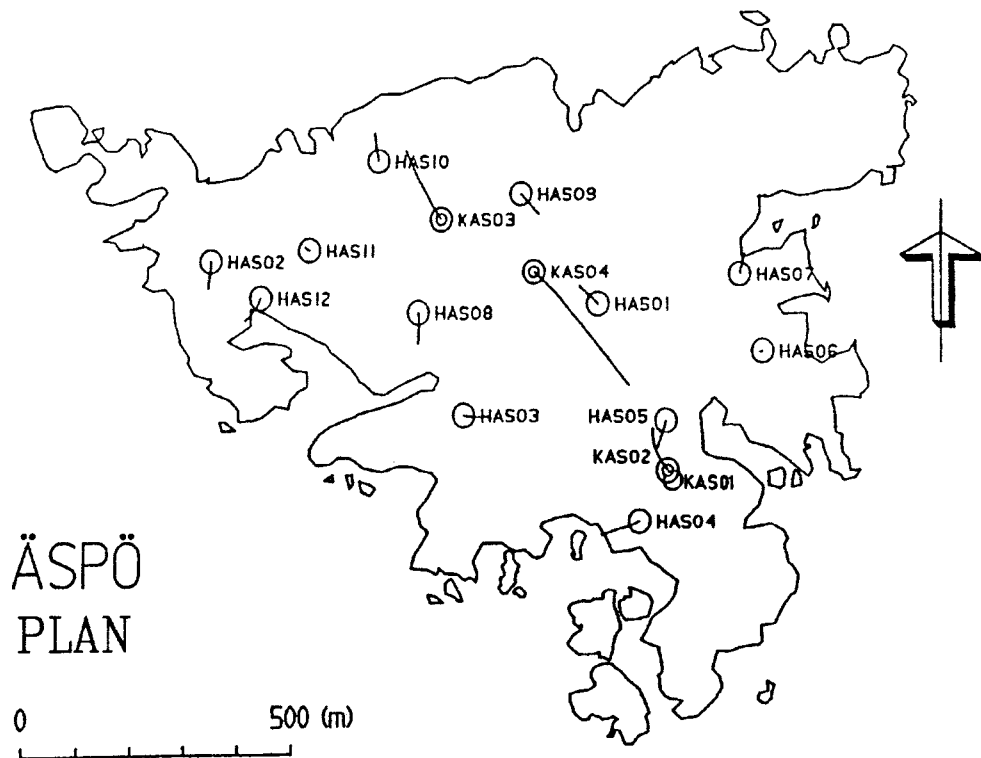
Figure 3-10. Borehole locations on Äspö.
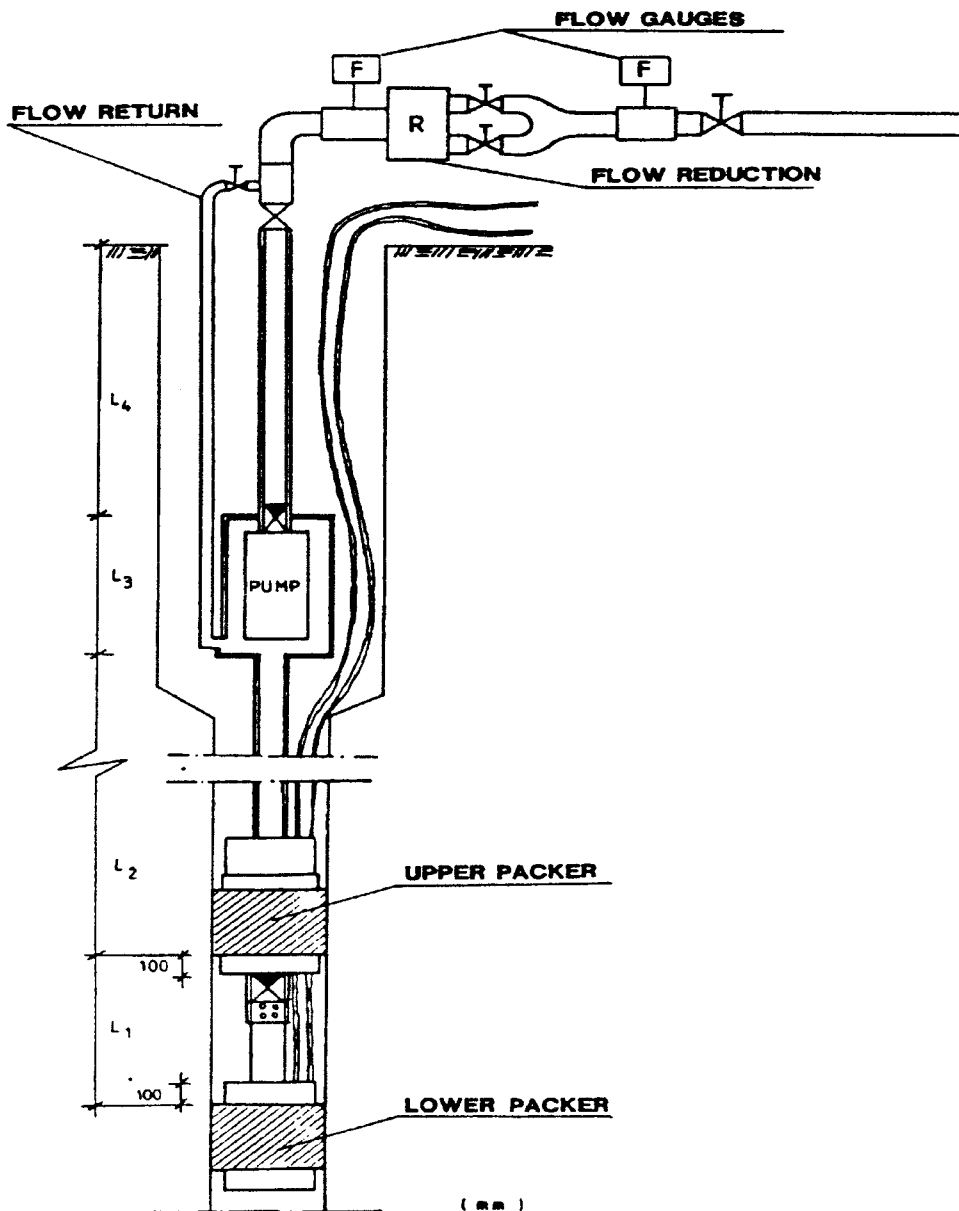
Figure 3-11. Test equipment for transient interference tests.

TEST PROCEDURE

All tests were made on sections within straddle packers (see Figure 3-11). The packers were connected by steel tubing to the pump, which was placed in the wide, upper part of the borehole. During tests the pressure in the borehole was measured between and below and above the packers. The rate of pumping was measured using double flow gauges.

In the surroundings, pressures were measured in all boreholes shown on Figure 3-10. In the core boreholes, KAS 02-04, multi-packer systems were used. In most of the percussion boreholes, HAS 01-12, a packer dividing the borehole into an upper and lower part was used. Pressure measurements were thus normally taken at two levels.

The test duration was 3 days for each section tested followed by a 3-day period before the next test was started.

93
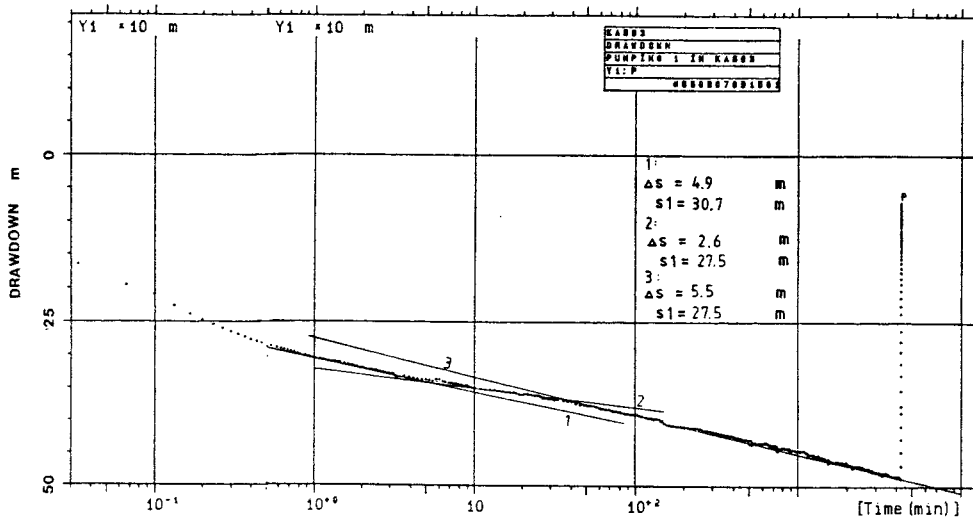
Figure 3-12. Draw-down between packers, KAS 03, 196 — 223 m.

EVALUATION

The evaluation of test data was made to clarify three matters:

o   The hydraulic properties of the conductor tested as seen from the well. The transmissivity and storage coefficient. The coupling of the well to the conductor.

o   The geometry and character of the conductor as seen from the well. The boundary conditions.

o   The hydraulic properties of the conductors and their geometry as seen from the interference data measured in the surrounding boreholes.

All pumping tests were evaluated under transient conditions using type curve and lin-log methods. As an example the evaluation of test No. 1 in borehole KAS 03, level 196-223 m, is summarized below. For a complete description see Rhen (1988).

In test No 1 section 196 — 223 m was pumped out at a rate of $Q = 1.75 \cdot 10^{-4}$ m^2/s (10.5 l/min). The total draw-down during the 72-h test was measured to be 48.5 m. The conductive section was identified by a spinner survey of the borehole and confirmed by packer tests (see Nilsson, 1988).

A lin-log plot of the draw-down between the packers is shown in Figure 3-12.

The curve is interpreted as being an initial linear fracture flow period, deduced from a log-log plot, followed by a dual porosity system, with two straight line portions, 1 and 3, showing the transmissivity of the structure, separated by a transition period. The hydraulic properties evaluated from the straight line portions are shown in Table 3-4.

94

Table 3-4. Hydraulic properties in KAS 03, 196 — 223 m determined for a draw-down period.

Straight line	Transmissivity T(10^{-5} · m^2/s)	Storativity S(10^{-5})	Skin factor Sk(-)	Wellbore storage C_D(10^{-4})
1	0.65	0.5	1	24
3	0.58	0.8	0	15

In the test no influence from boundaries can be inferred within approx. 300 m of the section tested. The conductive structure acts a plane in which radial flow to the well takes place.

The measurements in the surrounding boreholes were analyzed both as time-draw-down series and distance-draw-down plots. One such is shown in Figure 3-13.

From the distance draw-down plot it can be seen that several measured draw-downs lie close to the theoretical Theis curve. The hydraulic properties evaluated for different observation points are shown in Table 3-5.
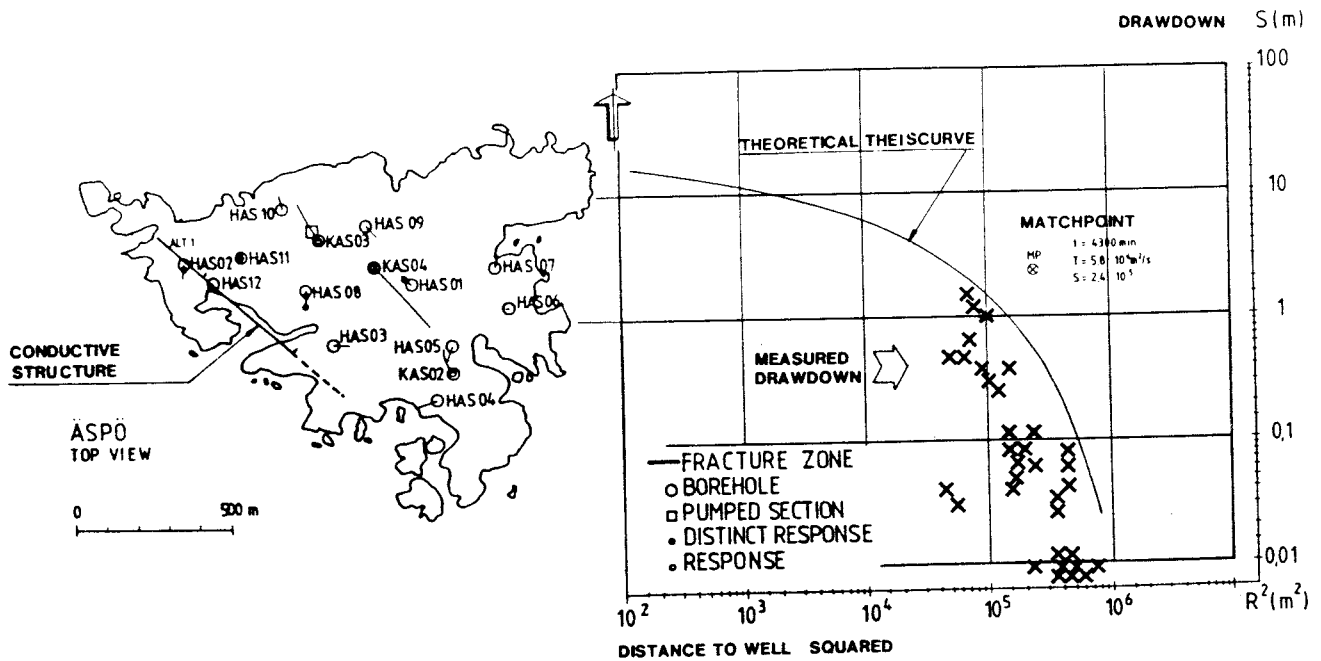
Figure 3-13. Distance draw-down plot for test in KAS 03, 196 — 223 m.

95

Table 3-5. Hydraulic properties evaluated for different observation points, KAS 03, 196 — 223 m, draw-down period.

Borehole	Level	Transmissivity $T(10^{-5}$ m²/s$)$	Storativity (10^{-5})
HAS 08	lower	2.6	1.6
HAS 08	upper	3.5	6.7
HAS 11	lower	2.3	4.3
Distance	Draw-down	0.58	2.4

Apart from the boreholes given above a hydraulic conductor was found in boreholes HAS 01, HAS 02, HAS 04 and KAS 01.

If the boreholes with good contact are assumed to penetrate the conductive structure the position of the structure can be deduced geometrically. In Figure 3-13, it's possible intersection with the ground surface is shown. It has a strike of 130° and a dip of approx. 30° towards the NE.

An evaluation of this type has been made for all 9 tests and a summary of the results is given below.

TEST RESULTS

A summary of the results is given in Table 3-6 below, together with some comments on them.

The test performed in borehole KAS 03 showed two groups of conductive structures (see Figure 3-14). One with a shallow strike 130° with a dip 30°, tests

Table 3-6. Summary of results from the transient interference test.

Test No.	Section	Transmissivity $T(10^{-5}$ m²/s$)$	Storativity $S(10^{-5})$	Boundary R_e(m)
KAS 03-1	196 — 223	0.7	0.8	> 300 m
-2	347 — 374	0.6	1.0	> 600 m
-3	453 — 480	1.0	2.0	> 400 m
-4	248 — 251	0.7	1.0	
-5	609 — 623	1.0	1.0	large
-6	690 — 1002	0.5	0.1	large
KAS 02-1	802 — 924	25	1.0	150
-2	308 — 344	1.8	1.0	
-3	117 — 126	0.004	1.0	

Test No.	Comment	Strike (°)	Dip (°)
03-1	Double porosity	130	30
-2	Linear from connected to radial	85	25
-3	Outwardly decreasing T	88	36
-4	Low T in contact with high T		
-5	Double porosity	70	60
-6	Double porosity	80	66
02-1	Radial to channel		
-2	Low T in contact with high T	162	90
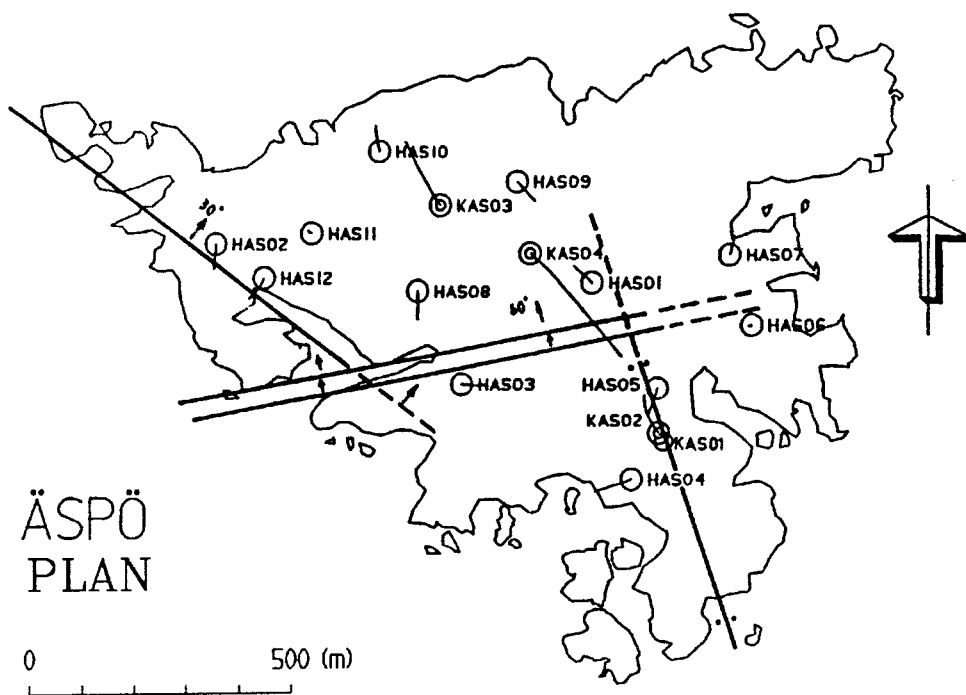
Figure 3-14. Conductive structures determined by interference tests.

1 and 4. They may, however, be the same zone, which in Test 4 is connected to the borehole by a distinct open fracture. The zone strikes parallel to the SW coast of Äspö and dips under the island. How far the zone goes towards the SE is not clear.

The second group consists of a series of interpreted zones striking 70 — 80°, dipping towards the north. These zones comply well with the E-W portion of the Mylonite Zone that forms the southern border of NW Äspö.

Tests in KAS 02 also show two distinct features. At depth the conductive structure complies well with the lower boundary of the diorite found in the core borehole, which also was indicated by the refraction seismic investigation.

The conductive structure at 308 — 344 m complies well with the upper boundary of the diorite, but interference data show a vertical conductive structure striking 162° (Figure 3-14).

3.1.3 Hydraulic Parameter Evaluation

The object of the hydrogeological parameter evaluation was to

— Prepare and present information satisfactory to establish a conceptual model and numerical models as to hydrogeological properties in the target area of the Hard Rock Laboratory.
— Prepare and present a description of the interrelated geological, geophysical and hydrogeological variables in the target area of the Hard Rock Laboratory.
— Evaluate how to optimize the hydrogeological investigations.
— Use the SKB database, GEOTAB, as an information source and to evaluate the methodology of data retrieval and adequate structure of data.

This project supports the hydrogeological co-evaluation focussing on the above four objectives. The study is reported by /Liedholm 1989/.

HYDRAULIC CONDUCTIVITY EVALUATIONS

The initial part of the evaluation involved intercorrelation of the hydraulic conductivity and depth, spatial distribution, rock types, alterations, fracture fillings, fracture frequencies, geophysical measurements and scale.

A general significant hydraulic conductivity-depth trend was not found for the four boreholes evaluated. For KAS 02 there exists a significant conductivity increase with depth by one order of magnitude per 460 m (see Figure 3-15). A conspicuous pattern is a relatively strong conductivity increase in KLX 01 at vertical depths greater than 350 m.

There exists a significant difference in conductivity between KAS 02 (low conductivity), and KAS 03 (high conductivity), and between KAS 02 (low conductivity) and adjacent KAS 04 (high conductivity). The trend representing differences between the boreholes becomes less pronounced at deeper levels. In KAS 02, at least three sections, 175—215 m, 300—(400) m and 630—730 m of borehole depth, are defined as enhanced conductivity sections. For KAS 03 and KAS 04 a more random pattern was found.

The differences between the rock types varies from borehole to borehole.

In KAS 02, aplite has a slightly higher conductivity level than other rocks. The monzodiorite in the lower parts is of relatively low conductivity compared with the aplite dykes. In KAS 03, only a weak, insignificant difference was noted, but significant differences were shown for KAS 04. For the total sample of KAS 02, KAS 03 and KAS 04 only the monzodiorite is significantly different (low conductivity) from the others. A large portion of the conductivities for monzodiorite in KAS 02 are found in the very narrow range of $3 \cdot 10^{-10}$ — $3 \cdot 10^{-11}$ m/s. A summary of the median hydraulic conductivities and their variances in different boreholes is shown in Figure 3-16.
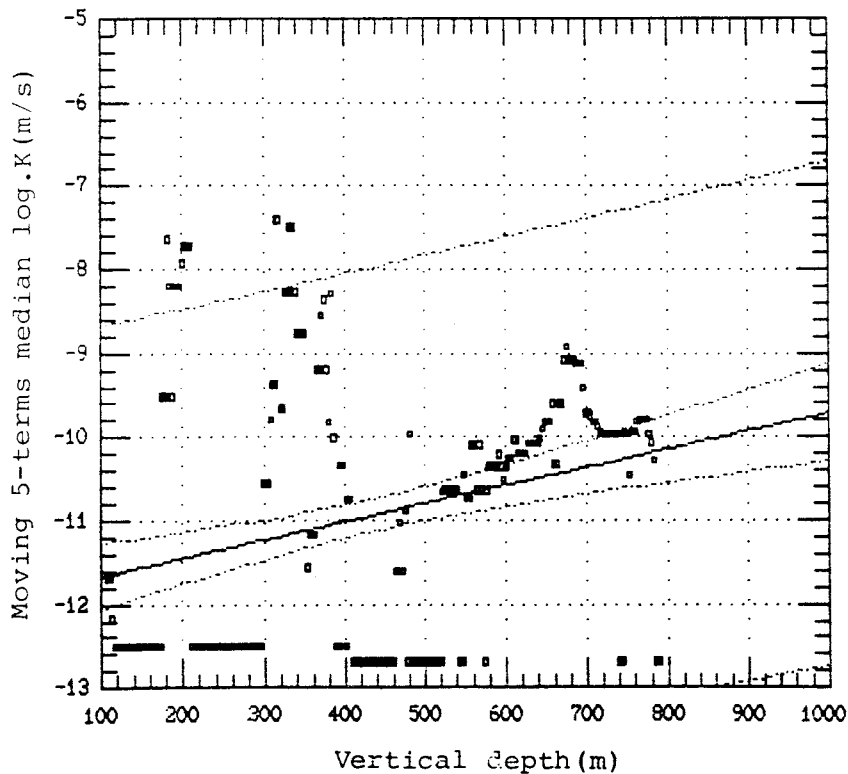

Figure 3-15. Regression analysis of depth-conductivity relation for 3-m packer tests in KAS 02 (evaluation limit included).
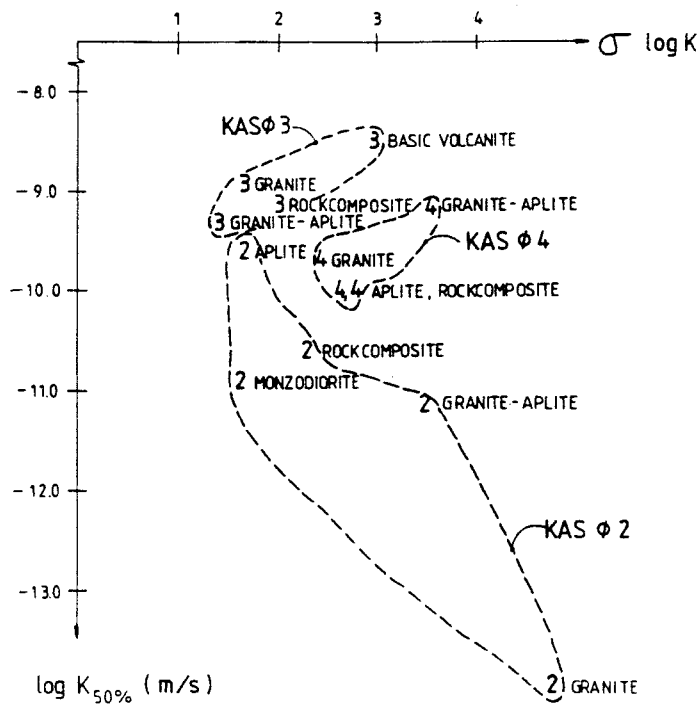
Figure 3-16. Hydraulic conductivities and their variances in different boreholes.

An analysis of the correlation between the fracture filling material has shown that the fracture filling mineral hematite correlates to some extent to the conductivity magnitude, an increased number of hematite fractures corresponds to increased conductivity.

There appears to be no significant difference in conductivity magnitude with regards to the oxidized or non-oxidized state of alterations in KAS 02. The impact of various fracture fillings on the conductivity magnitude is probably overruled by the impact from the total numbers of fractures from the same section. The fracture filling seems not to be a major hydrogeological variable.

In KAS 02, only about 7% of the variation in conductivity is explained by the fracture frequency. The conductivity first order trend increases significantly in KAS 02 with increasing fracture frequency, but the fracture frequency is not a major hydrogeological variable. But the individual character of some additional fractures is significant for the conductivity increase with higher fracture frequencies (see Figure 3-17).

By studying the correlation between hydraulic conductivity and the geophysical logs, the geophysical logs can be divided into three groups according to their relevance in correlation. Of all the 12 geophysical logs processed to provide a total of 60 different statistical geophysical variables, the median Normal Resistivity, the minimum Single-Point Resistance and the minimum Lateral Resistivity to some extent correspond to the conductivity magnitude, although the correlation differs in magnitude from borehole to borehole. The complexity of these relations and the lack of persistent, accurate correlations indicates that geophysical logs are not the proper instrument for hydraulic conductivity estimates. This is also valid for the exclusive borehole fluid properties, they can only be correlated to a marginal extent to the conductivity.

Predictions of the conductivity may thus be performed on the basis of selected geophysical logs in multiple linear or multiple non-linear models, but the accuracy of the models presented here is not better than +/- 1.5 orders of magnitude (see Figure 3-18).

Figure 3-17. Hydraulic conductivity of 3-m intervals correlated to number of fractures per section (evaluation limit included).
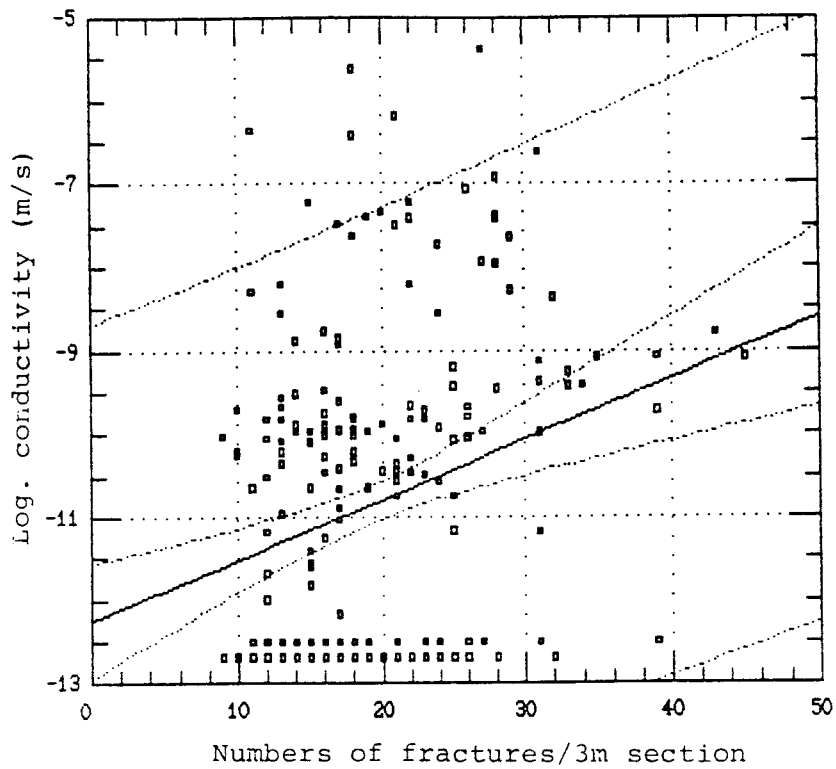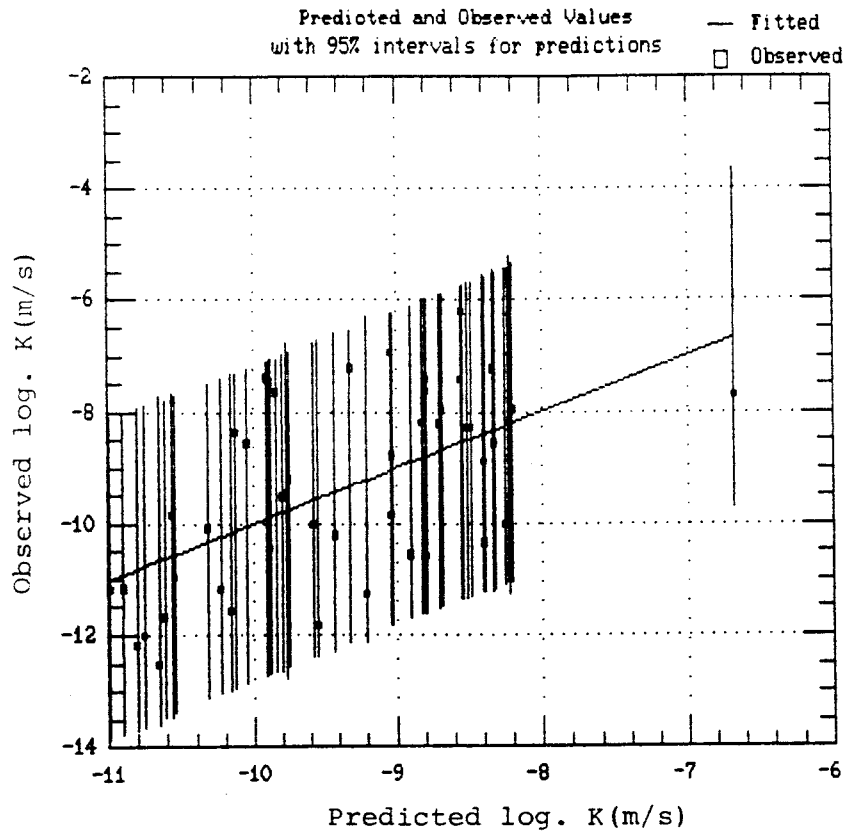

Figure 3-18. Cross plot of predicted and measured conductivities for KAS 02 values from a model based on self potential, single-point resistance and normal resistivity logs.

FRACTURE FREQUENCY ANALYSES

The second part comprised a study of fracture frequency and fracture distances followed by a borehole correlation study between KAS 02, KAS 03 and KAS 04.

Several different orders of ARIMA models were tested on the fracture frequency series in KAS 02. The current fracture frequency observation may be generated by a weighted average of the past, say, 5-m of observations, together with a random disturbance in the current section and including a moving average part of the process with a memory of only about 1 m. Fracture frequency predictions cannot be made accurately using advanced quantitatively explanatory time-series methods.

The fracture frequency increases significantly with depth in KAS 02. The fracture frequency varies from rock type to rock type. Only aplite possess a significantly higher fracture frequency than the other rock types in KAS 02.

By using information parts consisting of, in this case, several pieces of 3-m information, a visual correlation was formed between the Natural Gamma Radiation response in the lower parts of KAS 02 and KAS 03, identifying two aplite dykes of probably the same genesis.

SOME NOTES ON THE GEOTAB DATABASE

The last part describes some experiences and recommendations based on the scope and methodology of the project.

For technical users, there are no obvious advantages of a comprehensive understanding of the GEOTAB structure, if information can be obtained with the assistance of the information storage managers. It is, however, essential for technical users to understand the library (COUNT TAB) procedure in order to check the information available. The GEOTAB is at present best suited as a passive data base. Extensive structural organizing and statistical evaluation are preferably performed with the help of spread-sheet programs and statistical software outside the GEOTAB structure.

3.1.4 Regional Numerical Modelling

Ground water flow calculations on a regional scale around the future laboratory were performed /Gustafson, Liedholm and Lindbom, 1989/, on the basis of the conceptual model given in the previous report /Gustafson, Stanfors and Wikberg, 1988/.

TWO-DIMENSIONAL MODELLING

In order to achieve satisfactory understanding of the groundwater flow conditions around the site, several numerical modelling efforts on the geohydrological situation are planned. The present study, which comprises regional models, is aimed at describing the groundwater situation in a wide area round the planned laboratory and to assess the influence of it in order to define the boundary conditions for models covering smaller areas. However, it is difficult to find natural limits of an area to be modelled at this scale, i.e. the positions of the confinements of the model are extremely uncertain. Since the application of boundary conditions is essential for the modelling results, the results of the calculations
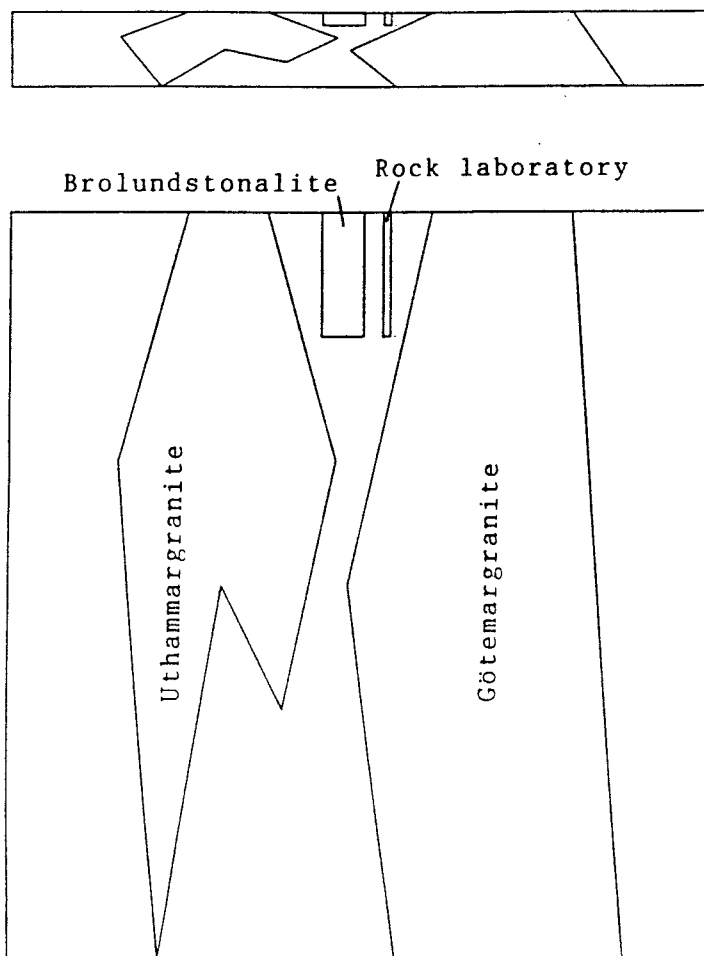
Figure 3-19. The geometry of the geological formation as modelled. The upper figure is to the same vertical and horizontal scale. The Småland granite is between other rock areas.

would suffer from inherent uncertainties, if incorrect positions for the boundaries are assumed.

It was therefore deemed feasible to perform this study in two steps. First, a two-dimensional-calculation was performed to investigate the impact of the different lithological units. The position of this vertical was based on gravimetry investigations and the boundaries of it were considered to be as rather well established (see Figure 3-19).

Four two-dimensional-cases were modelled with different material properties assigned; the laboratory was generically modelled in two of these cases. The purpose of the exercise in two dimensions was to elucidate whether or not there are hydrological means for a conceptual transfer of boundary conditions from the two-dimensional-calculation to a three-dimensional model covering the potential location of the laboratory and to estimate the influence radius from the shaft. By going to a smaller scale, a larger account of detailed information from the site investigations would be gained.

Figure 3-20 shows the potential and flow field for a basic case in which the hydraulic conductivity decreases with depth with a trend of one order of magnitude per 473 m. The hydraulic conductivities at the surface are shown in Table 3-7.
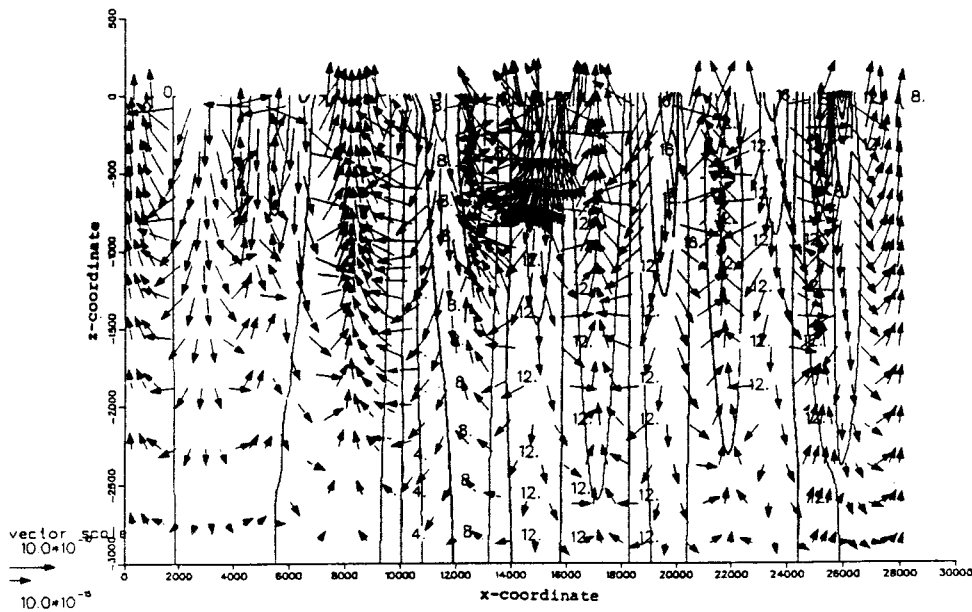
Figure 3-20. Flow field for basic case.
Note that the length of the flow vectors is to a logarithmic scale in accordance with
the legend at the bottom-left corner; the unit for flow is m/s.

Table 3-7. Properties from the two-dimensional domain.

Gravity modelling Geological dominance	Property areas	K_o (m/s)
Uthammar granite	Götemar-Uthammar	$1.12 \cdot 10^{-6}$
Brolund tonalite	Tonalite	$1.82 \cdot 10^{-7}$
Götemar granite	Götemar-Uthammar	$1.12 \cdot 10^{-6}$
Ambient rocks (Småland granite)	Granite to granodiorite	$3.01 \cdot 10^{-7}$

The relevant factor in determining the size of the three-dimensional model is the radius of influence. If the laboratory is introduced as an atmospheric pressure boundary as shown in Figure 3-19, the head difference between this model and the previous one will define the draw-down of the laboratory (see Figure 3-21).

As can be seen the radius of influence is in the order of 3—4 km.

103
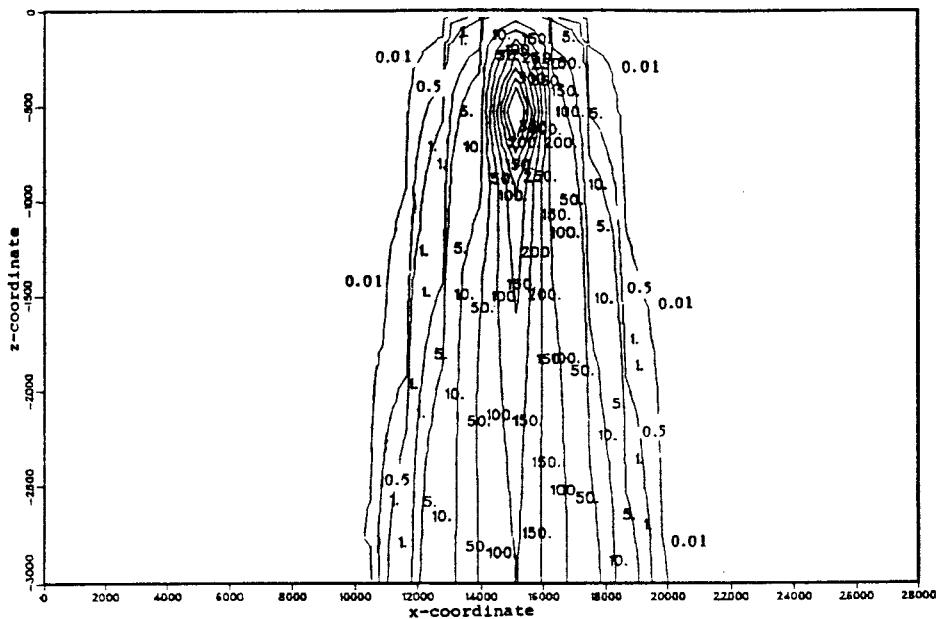
Figure 3-21. Calculated draw-down from the laboratory in two-dimensions.

THREE-DIMENSIONAL MODELLING

Two three-dimensional models were considered, both consisting of ten litohological units. The first one was referred to as the basic case, which was performed in order to analyse the regional flow system, and to investigate whether the vertical limits around Äspö are significant enough to be regarded as boundary conditions for future modelling exercises at a local scale around Äspö. The second run was with a generic model of the rock laboratory. This was done by assigning atmospheric pressure to the nodal points that are located near a "fictive" line of symmetry (to a depth of $z = -500$ m) of the shaft to be blasted. The purpose of this exercise was to study the regional effects of the presence of the laboratory.

With the extent of the model defined by the radius of influence of the laboratory calculated in two-dimensions, the same type of boundary conditions can be used, i.e. an upper constant head boundary defined by the topography and no lateral flow and bottom boundaries. The model chosen was a horizontal trapezoid measuring some 10x7 km in area with a depth of 3 km, divided into 8 layers.

The gravimetric model formed a basis for the assignment of the property areas for the two-dimensional model. In this case the profile was used to give the geometry of the pervious Götemar granite in the model area. This granite probably exists at depth in the whole model domain. The other property volumes are defined by the different investigation areas within the model domain. For areas outside the investigation areas data from Liedholm, (1987) were used. As in the two-dimensional models, the lithological units define the property volumes.

104
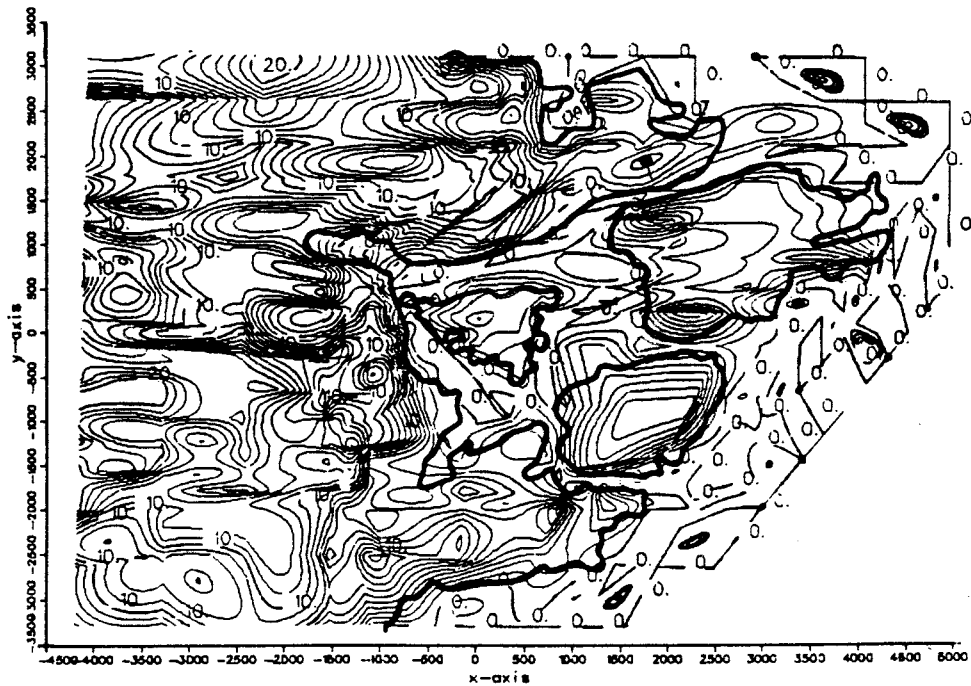
Figure 3-22. Top surface (i.e. the groundwater table) of the three-dimensional model. Values of pressure are expressed in metres (piezometric level) above sea level. The coastline is indicated by a thick solid line.

Figure 3-22 shows the groundwater table in the area. This is assumed to be governed by the topography and acts as a constant head boundary.

Figure 3-23 shows the calculated piezometric head 500 m below the surface, corresponding to the depth for the experiment area under natural conditions. As can be seen the lines of equal pressure potential are smoothed out, as could be expected.

In the two-dimensional modelling a crucial matter is the radius of influence from the laboratory. Figure 3-24 shows the drawn-down around the assumed laboratory at a depth equal to the proposed laboratory level.

DISCUSSION OF RESULTS

The general conclusions that can be drawn from the three-dimensional modelling are that the majority of the goals set up prior to the modelling have been fulfilled. The pressure distribution seems to be reasonably well described by the model, given that input data had its limits, and by comparisons with measured piezometric levels in three boreholes at the site. Even the regional pressure distribution seems to be appropriate, with an upper flow system governed by the local topography of the islands in the area and an underlying regional flow system originating from the topography of the mainland.

However, the calculated flow rates and the detailed directions of flow must be studied with care.

The calculated paths are also in agreement with what might be expected. However, they ought to be seen as illustrations of possible paths under the prevailing circumstances, rather than evidence of the resulting pressure distribution.
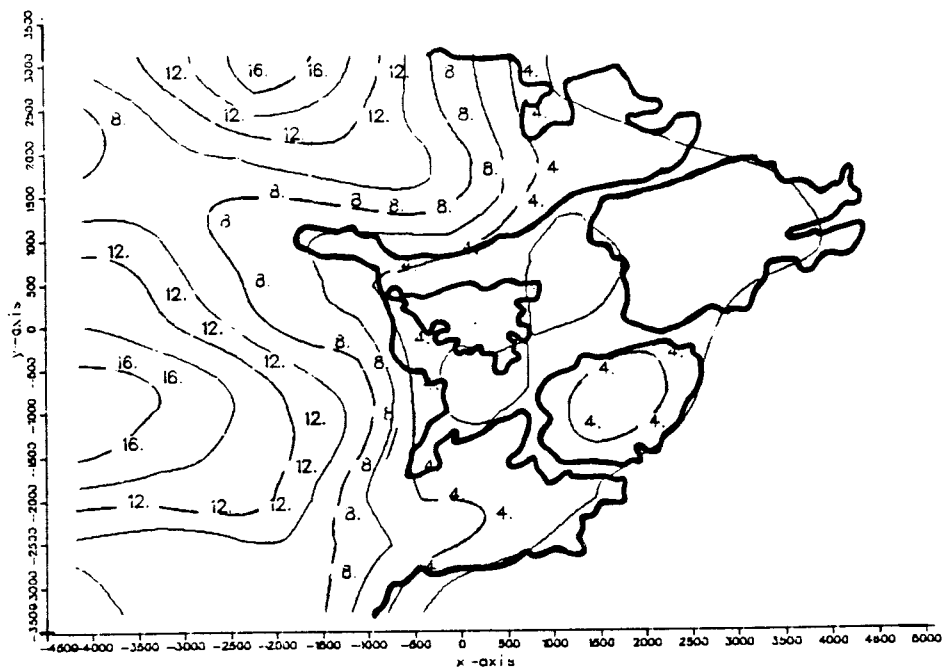
Figure 3-23. The distribution of pressure potentials at a level of 500 m below sea level.

Values of potentials are expressed in metres (piezometric level) above sea level. The coastline is indicated by a thick solid line.
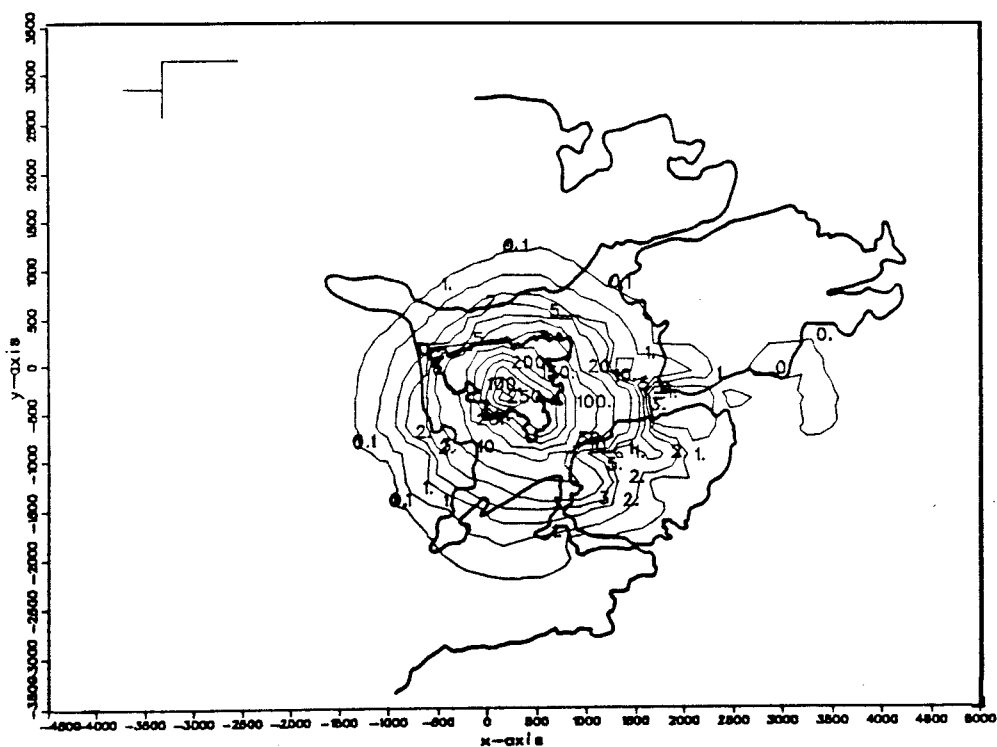
Figure 3-24. Distribution of differences in pressure potentials at a level of 500 m. Values of pressure potentials are expressed in metres (piezometric level). The coastline is indicated by a thick solid line.

Future modelling of the Hard Rock Laboratory will be done on a local scale relative to the one presented in this project. Future modelling will involve predictions of long-term pumping tests as well as the influence of the rock laboratory. The area of main concern is Äspö, where the field tests and the construction of the laboratory will take place.

Although it is known that salinity groundwater exists at depth, the influence of this on the pressure potential and flow conditions has not been considered in the model. The reason for this is that the codes used cannot cope effectively with the saline-front problem, but also that the saline-front problem in the area, with the low salinities of the Baltic involved, is being studied in a different project.

3.1.5 Numerical Models of the Saline Water Front

In order to understand the behaviour of a saline water front with small salinity contrast in a hydraulically inhomogeneous medium some numerical simulations were performed. The work is reported by /Svensson 1988/.

SPECIFICATION OF THE PROBLEM

The specific problem to be considered in this report, is shown diagrammatically in Figure 3-25. It is a coastal area where fresh groundwater meets the brackish seawater. Measurements also revealed the existence of more saline water (1%), which at sea resides more than 20 m below the sea bed. We thus need to consider
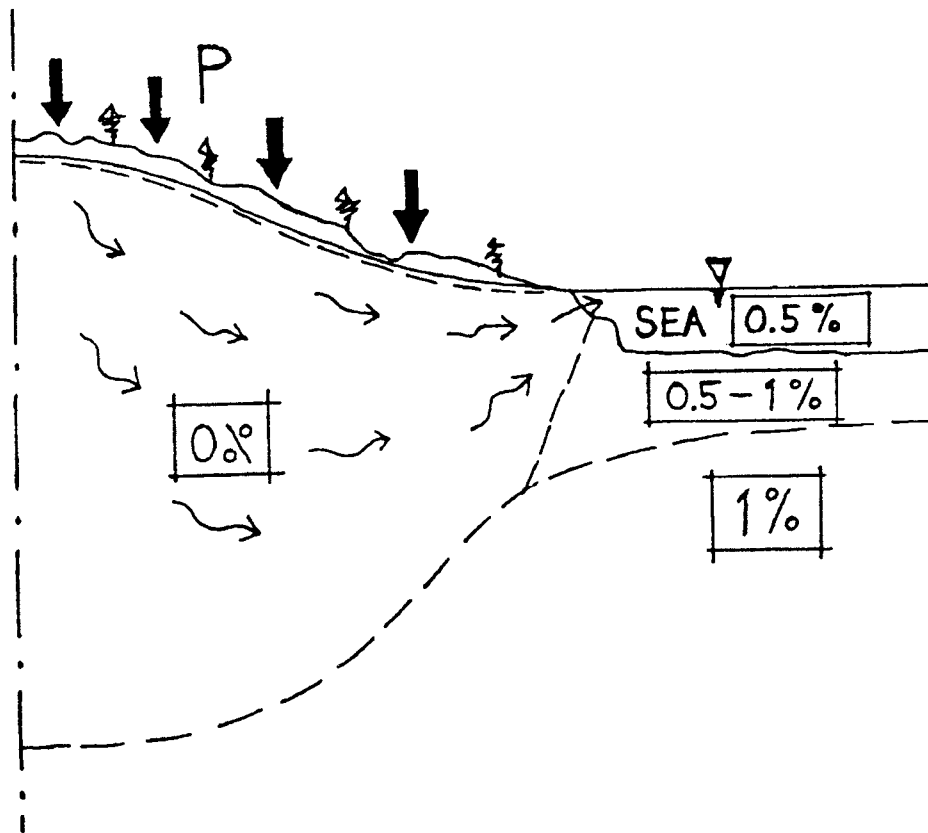
Figure 3-25. Salt water front under an island.

107

waters of three different salinities and hence different densities. Due to the density differences, it is expected that the 1% saline water will be found at a lower level under the land.

The purpose of the present report was to:

— Demonstrate that the numerical model used is compatible with other existing codes for density-stratified groundwater flows.
— Establish a realistic, although idealized, scenario that can be used as a reference case when carrying out sensitivity tests.
— Carry out sensitivity tests of parameters that specify the properties of the fractured porous medium, i.e. hydraulic conductivity, relations for the dispersion coefficient, etc, and, in particular, to investigate the effect of stochastically generated conductivities.

REFERENCE SIMULATIONS

In order to verify this application of the computer code used, PHOENICS /Spalding, 1981/, two reference problems were studied: Henry's problem /Voss and Souza, 1987/ and the Saline Dome problem /Herbert and Jackson, 1987/. In both cases the solution calculated using PHOENICS agreed well with the ones presented in literature.

THE REFERENCE CASE

The porosity, dispersion coefficient and hydraulic conductivity for the reference case are given in Figure 3-26 and the predicted salinity and flow field can be found in Figure 3-27. The salt water is found at a depth of 300 — 400 m at the left boundary, which represents the centre of the island.
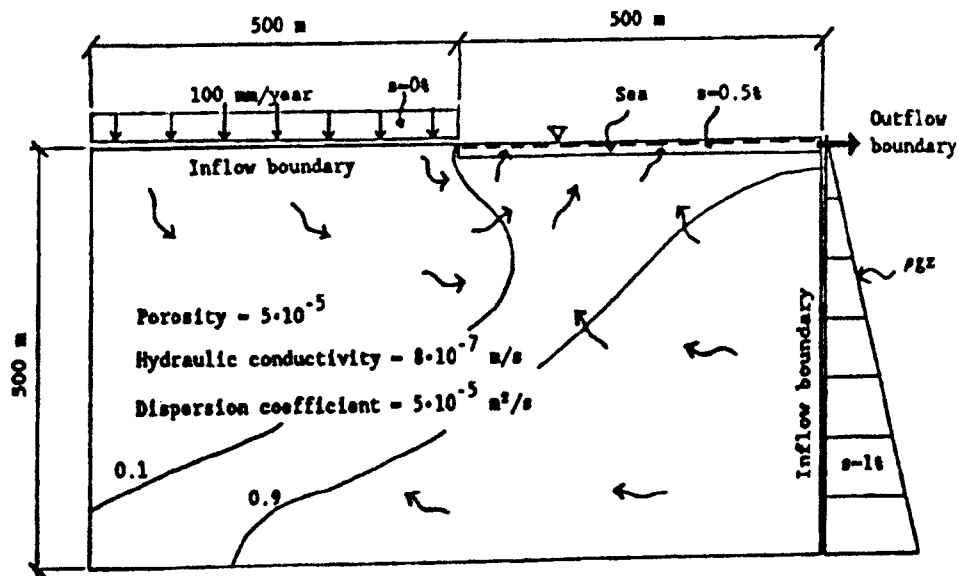
Figure 3-26. The reference case with assumed parameters.
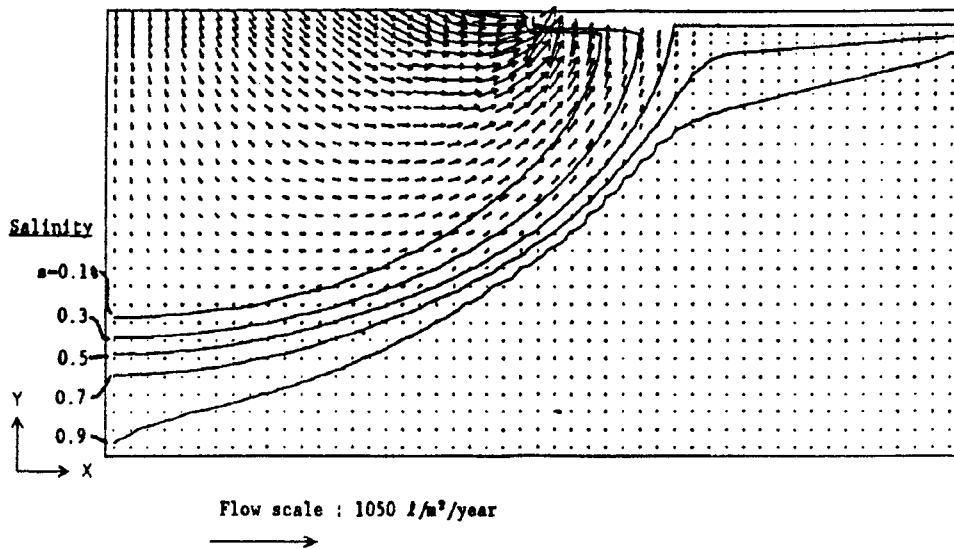
Figure 3-27. The homogeneous reference case.

Two more homogeneous cases were also tested, one with a dispersion coefficient proportional to the Darcy velocity, giving results very similar to the reference case, and one with a hydraulic conductivity decreasing with depth, showing that this forces the flow close to the surface, but also that the boundary between fresh and saline water is forced downwards.

STOCHASTICALLY GENERATED CONDUCTIVITIES

All results presented so far look very "smooth", which is a consequence of assuming constant or smoothly varying properties of the rock. The fractured rock can, however, only be attributed mean properties in a statistical sense. An attempt was therefore made to generate random hydraulic conductivities having a log-normal distribution. The mean conductivity used is the same as in the reference case. Results for three different standard deviations of lnK (1,2 and 4), but with the same set of random numbers, are shown in Figure 3-28. It is interesting to note that although the conductivities do not have any spatial correlations, streaks, as formed in the velocity field, this can to some degree be understood by first noting that due to the boundary conditions prescribed the average pattern must be the same as in the reference case, i.e. the precipitation must find its way out to the sea. If a new series of random numbers were used, another flow and salinity field would, of course, be obtained.

The results are exciting and show many features, such as higher salinities overlying lower ones, that has been recorded in the field investigations. The modelling technique used certainly deserves to be extended and further investigated. The possibilities of the method include the introduction of spatial correlations and testing of different statistical distributions.

In conclusion it can be stated that numerical models of the kind used in this study are useful tools for improving our understanding of the flow in a fractured medium.
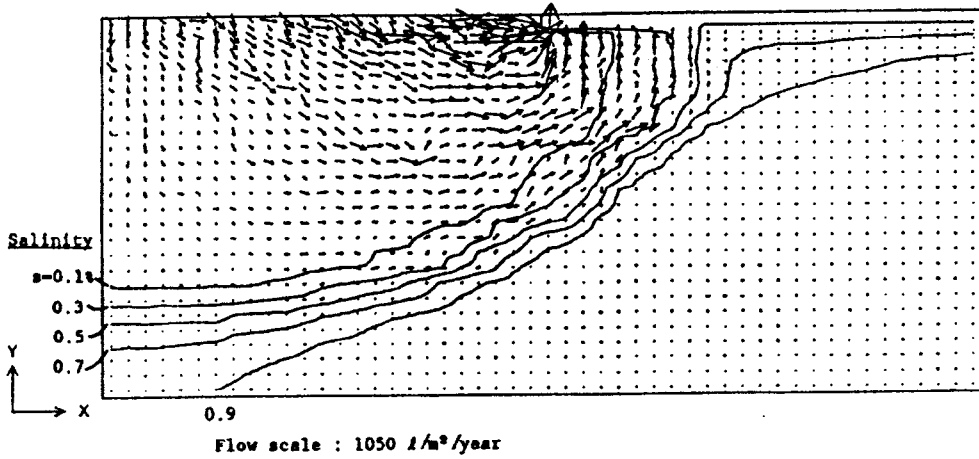
a) Standard deviation, lnK = 1
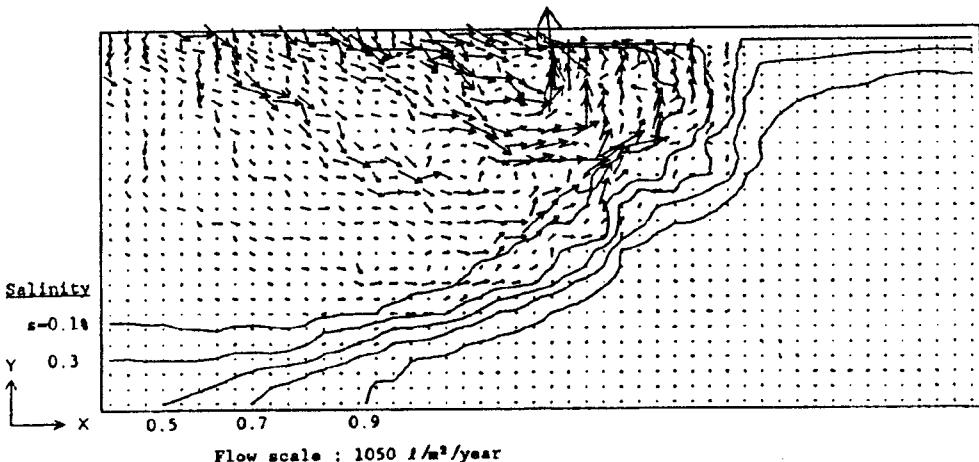
b) Standard deviation, lnK = 2
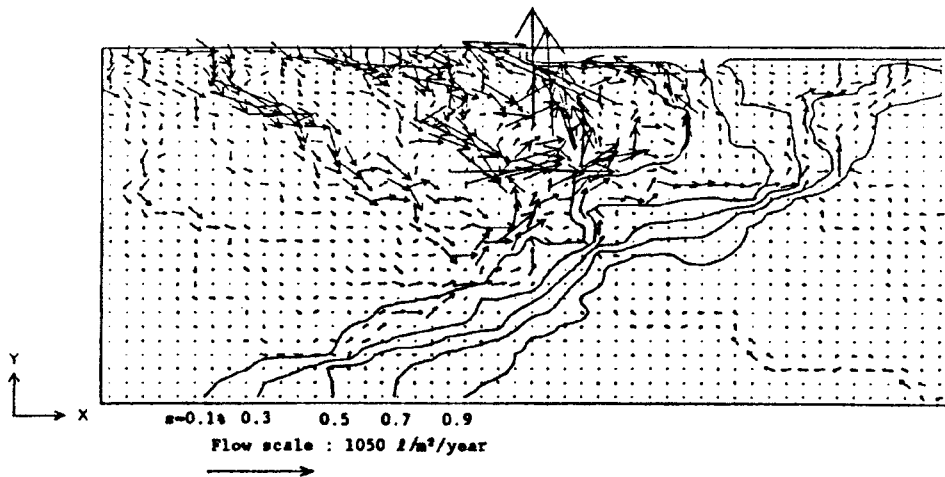
c) Standard deviation, lnK = 4

Figure 3-28. Simulations with stochastically generated hydraulic conductivities. Velocity and salinity fields.

110

3.2 CONCEPTUAL MODELS OF THE ÄSPÖ AREA

In the previous study conceptual models were proposed on different scales. This approach is also followed here. The scales can be illustrated with control volumes of different sizes. The largest control volume is the island of Äspö but smaller volumes can be seen as cubes of given size. The scales proposed in the conceptual models are thus:

Site scale	Island of Äspö
Block scale	50 m
Detailed scale	5 m

In this approach basically the same units are used and described as in the geological models. The conceptual models proposes the general, the important features rather than the details and the exceptions.

It should also be noted that values of hydraulic parameters etc. are estimates based on investigations and data from a limited number of boreholes in a large volume of rock. This means that they must be seen in a framework in which successive investigations lead to refinements in accuracy and spatial variation.

The conceptual models are thus based partly on **stated facts**, partly on *deduced analogies* and on some *professional judgement*. Thus, they may be regarded as the principal points of view at this stage of the investigations.

3.2.1 A Conceptual Geohydrological Model of Äspö

The model area covers the island of Äspö and the surrounding areas of the Baltic, Bornholmsfjärden, Norre fjärd and Granholmsfjärden. The depth of the model goes as far as there is information, i.e. from boreholes, down to 1000 m depth, and possibly down to 1200 m if information from the refraction seismic investigations is considered. The description of the geohydrological model of Äspö is supported by Figures 3-29 (plan), and 3-30 (profile).

SURFACE HYDROLOGY AND GROUNDWATER RECHARGE

The land surface of Äspö is slightly undulating, with a maximum height of a little more than 10 m above the sea. The valleys are filled with wet ground and the hills consist mainly of bare rock and some till. This means that there are no perennial streams in the area; the surface water is drained to the sea by the wet ground. In the wet ground there are some open surfaces of fresh water, at least in the spring and autumn.

The mean precipitation (P) is estimated at 675 mm/a, and the evapotranspiration (E) is calculated to be 490 mm/a, /Svensson 1987/. This leaves a surplus of P - E = 185 mm/a to be distributed as groundwater recharge and runoff.

The small runoff basins, however, imply that the terrain may be subdivided into a mosaic of in and outflow areas, thereby giving a small average annual recharge as long as the groundwater is not utilized or drained to an underground utility (see Figure 3-31).

The main recharge, takes place in conjunction with the melting of snow, thereby giving a maximum water level in the spring and a minimum in the late summer. The mean annual snow cover corresponds to approx. 125 mm/a.

Figure 3-29. Conceptual geohydrological model, plan.

112

0   100   200   300   400   500 (m)

NORTHERN
BLOCK

HAS10
HAS09
KAS03
HAS11
HAS02
HAS12
HAS08
KAS04
HAS01
HAS07
HAS06
HAS03
HAS05
KAS02
KAS01
HAS04

MYLONITE ZONE
MYLONITE ZONE

SOUTHERN
BLOCK

MAIN EW
FRACTURE ZONE

FW1 0.7
FW2 1.0
FW3 0.5

30°
60°
60°
75°
60°
55-70°
80°

2.5
FW4 1.8

$T = X \times 10^{-5} \ m^2/s$

ÄSPÖ
TOP VIEW
LEVEL 0 m
DATE 1989-03-05

COREDRILLED BOREHOLE (TOP)
PERCUSSION DRILLED BOREHOLE (TOP)
DRILLED BOREHOLE (GEOMETRY)
INTERSECTION BOREHOLE-CONDUCTIVE STRUCTURE

GREENSTONE
GRANITE, FINE-GRAINED
SMÅLAND GRANITE
DIORITE
MYLONITE
RQDZ GT 75
RQDZ 50-75
RQDZ LT 50
HIGHLY FRACTURED OR CRUSHED ZONE

MAJOR WATERBEARING ZONE
DISTINCT MAJOR WATERBEARING FRACTURE

CONDUCTIVE STRUCTURE
BLOCK BOUNDARY

Figure 3-30. Conceptual geohydrological model, section.

113
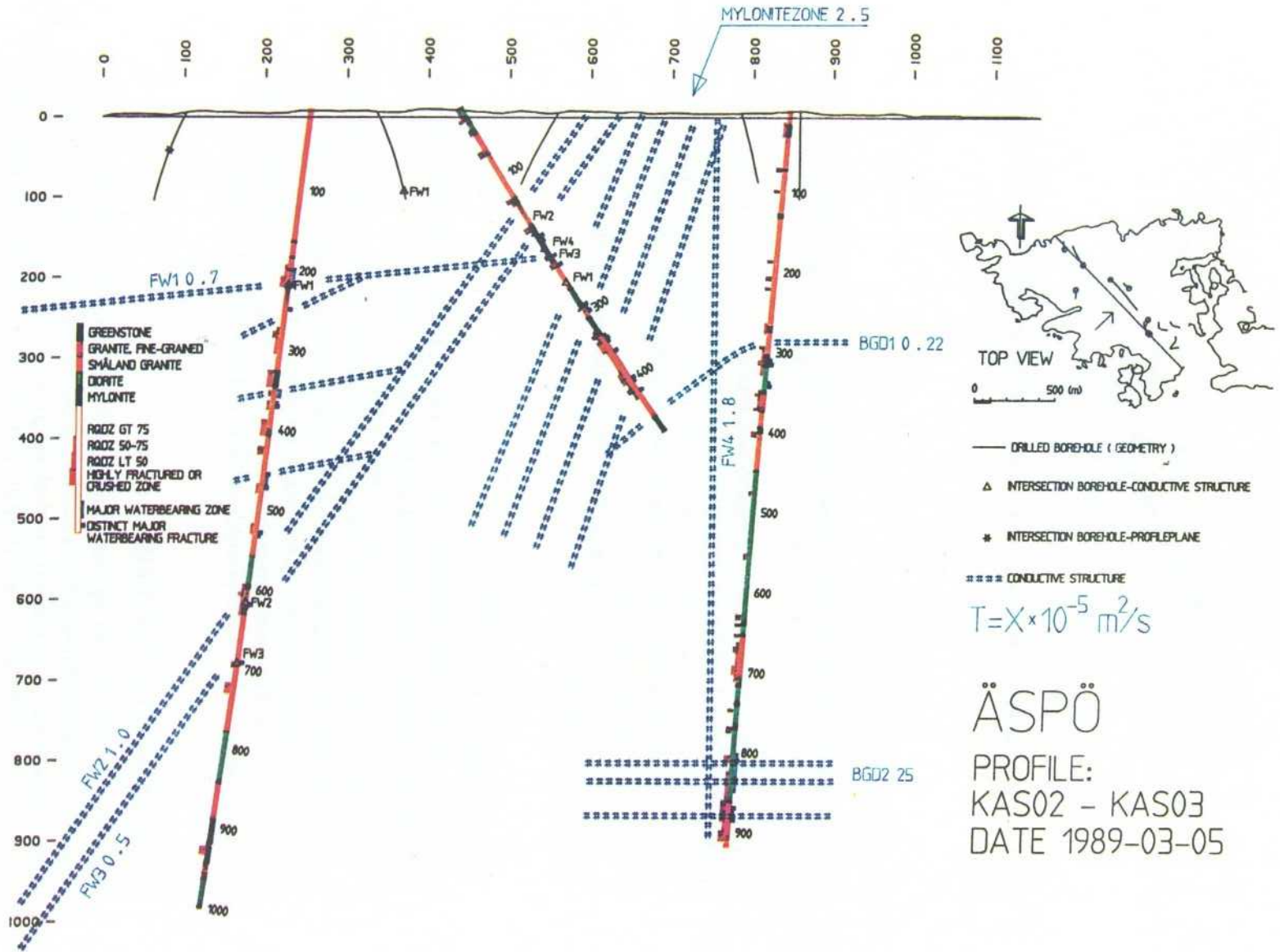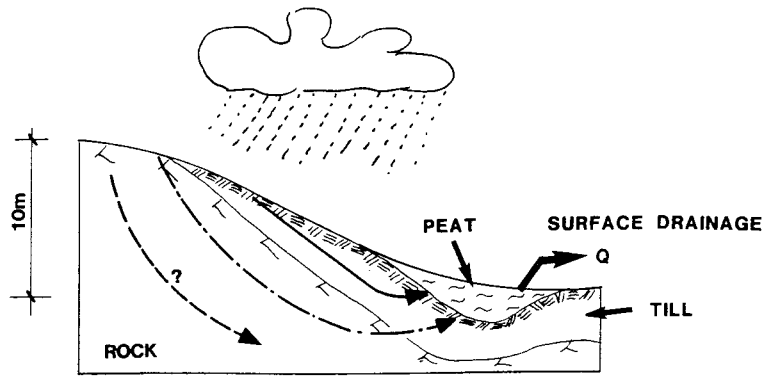
Figure 3-31. Flow pattern of surface water and shallow groundwater under natural conditions.

LITHOLOGICAL UNITS

There are basically three mass-formed lithological units of hydrogeological importance on Äspö, i.e. the Äspö diorite, the Småland granite and the fine-grained granite.

These rocks are described in the geological models and their hydrogeological properties will be described in the detailed-scale conceptual model.

As the section shows, Figure 3-30, the Småland granite is dominant in the upper part of the section and the lower part is dominated by Äspö diorite and bands of fine-grained granite.

The most pervious lithological unit is the fine-grained granite and the Äspö diorite is the tightest.

STRUCTURAL FEATURES

The combination of different rock units, dykes and fracture zones makes up a set of structural features with different geohydrological properties. The different features are described in detail in the block-scale models.

Some of them may be indicated in the geohydrological section. The main indicated groundwater conductors are either fracture zones or single open fractures. The fracture zones generally extend long distances and cut through all types of rock, even if the hydraulic properties vary with the rock type. The single open fractures occur in the brittle granites and are probably limited in extent.

MAIN HYDRAULIC FEATURES

The core boreholes, the hydraulic tests and the transient interference tests revealed a number of hydraulic conductors. Some of these are identified fracture zones, others are caused by lithological differences. The identification of them was done primarily using hydrological methods, supported by geological and geophysical data. The main hydraulic fractures are described and identified below. Their extents and positions are shown on Figures 3-29 and 3-30.

A Note on the Hydraulic Properties of Defined Structures

The main hydraulic features are given here in a deterministic framework, i.e. with a given transmissivity and a given position and direction. The transmissivity is given as an effective value determined by a pumping test for the whole structure. This means that the properties may vary considerably within the feature and there is reason to believe that the variability is of the same order as for other hydraulic parameters.

The hydraulic features given here are conclusive, in that their properties and geometrics have been determined by different methods. There is, however, no guarantee that a set of hydraulic structures is complete, because a determination of them requires that they be penetrated, observed and tested.

The magnatude of the storativity of the conductors for all tests is in the range of $0.8-2 \cdot 10^{-5}$, with the exception of one test, FW 3.

The Mylonite Zone

The Mylonite Zone is identified as one of the main structural features on Äspö. It has been identified by aerial and surface geophysics as a regional structure /Nisca and Triumph, 1989/. On Äspö it has a NE-SW strike and dips steeply towards the NW. It divides Äspö into two major blocks (cf. 2.2.1).

Its hydraulic importance is recognized in core borehole KAS 04, the lowermost 300 m of which penetrates a complex structure containing mylonites and fractured portions. The spinner survey identified 8 conductors. The pumping test on the entire borehole gave crosshole reactions along the zone in boreholes, HAS 01 and HAS 04, but also along other possible conductors that the borehole intersects, which will be identified later. The pumping test gave a transmissivity (T) of $2.4 \cdot 10^{-5}$ m²/s. This value can be referred to the Mylonite Zone.

FW 1

The principal magnetic interpretation map (Figure 2-20) indicates clearly a structure that strikes NW-SE in the NW part of the island. It has been identified as a major hydraulic structure by the transient interference tests. The transmissivity (T) was found to be $0.7 \cdot 10^{-5}$ m²/s.

The zone probably does not extend SE of the Mylonite Zone. Its strike is 130° and its dip is estimated to be 30°.

FW 2 and FW 3

From the principal magnetic interpretation map a main E-W fracture zone may be identified. Within this two parallel hydraulic conductors were identified by the interference tests. FW 1 has a strike of 80° and an estimated dip of 60° and a transmissivity (T) of $1.0 \cdot 10^{-5}$ m²/s. FW 2 also has a strike of 80° and an estimated dip of 70°. The transmissivity (T) was found to be $0.5 \cdot 10^{-5}$ m²/s.

FW 4

From geophysical data, geological mapping and hydraulic tests there is direct and indirect evidence of a subvertical hydraulic conductor striking 160° close to

KAS 02. The transmissivity was found to be $1.8 \cdot 10^{-5}$ m²/s. It is, however, unclear whether the structure extends north of the Mylonite Zone.

BGD 1

The boundary between the Småland granite and the Äspö diorite is complex and fractured and has a high hydraulic conductivity. The contact can be traced in the reflection seismic profile /Klitten and Plough 1989/ (cf. 2.1.2), where it can be assumed to be subhorizontal, slightly undulating and of limited extent. The transmissivity was found to be $0.2 \cdot 10^{-5}$ m²/s.

BGD 2

In the same manner the lower boundary of the Äspö diorite is fractured and forms a hydraulic conductor with about the same characteristics as the previous one. From the pumping test and the reflection seismics it was found to be limited in lateral extent. The transmissivity was found to be $25 \cdot 10^{-5}$ m²/s.

DEPTH DEPENDENCY OF HYDRAULIC CONDUCTIVITY

As stated by /Liedholm 1989/, no significant trends for the depth dependency of the hydraulic conductivity were found that cannot be explained by lithologic differences. This is contrary to the normal experience in Sweden and may need some explanation.

As can be seen from Figure 3-30 the upper portion of the Äspö section is dominated by Småland granite and lower by Äspö diorite, with sills of fine-grained granite. From the evaluation of the hydraulic rock types it is evident that the fine-grained granite is the most pervious rock in the area and it may be associated with the Götemar granite, which is the most pervious rock unit in the region.

If, as the gravimetric investigations suggest /Nylund 1987/, the Götemar granite exists at greater depth in the Äspö area its influence, as manifested by dykes and sills of fine-grained granite, is probably the cause of a lack of decreasing hydraulic conductivity trend.

HYDRAULIC CONDUCTIVITY AND SCALE

Hydraulic tests in the boreholes were performed on different scales; 3 m, 30 m and the entire borehole. An interesting comparison can be made if the distributions of the hydraulic conductivities for the different scales are compared. In this comparison only the portions of the boreholes for which there are complete sets of measurements of the different scales are used, i.e. for KAS 02 (102—801 m), KAS 03 (103—547 m) and KAS 04 (133—454 m).

From Section 3.1.1 it is clear that the tests on different scales does not give the same conductivity distributions. The average conductivity determined for the whole test section can be considered as some kind of effective value for the whole rock volume penetrated, including fracture zones and different lithological units. For each test scale an arithmetic and a geometric mean can then be calculated. The ratio of these means and the borehole averages are plotted against the test scale in Figure 3-32.

116
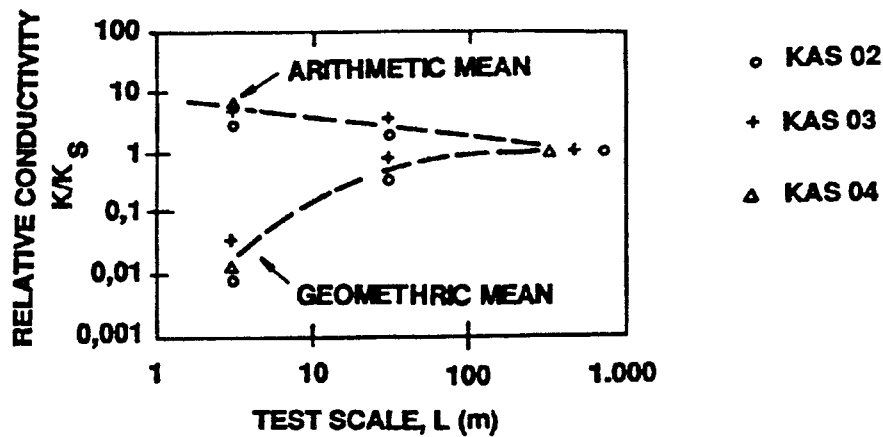
Figure 3-32. Relative hydraulic conductivities for different test scales.

It is evident that the characteristic means are influenced by the scales, but it is also evident that the values converge towards the borehole average. It should, however, be noted, that the arithmetic means are probably somewhat lower than the true values, since they are very much affected by the most conductive sections, which may be too low because of limitations imposed by the measuring equipment (see Figure 3.1.2). The geometric mean, which is close to the median, is far more accurate since it is dominated by the most commonly measured values.

The variance can also be analysed. In Figure 3-33 the standard deviations for the logarithmic distributions are plotted against the test scale. For comparison, the standard deviation for the three borehole averages seen as a population is also plotted.

From the figure it is clear that the variance decreases with scale, but the decrease is smaller than what can be expected if larger packer intervals are considered as samples of log-normally distributed shorter intervals.

It is clear that the variance also affects the effective conductivity as well as the means but the laws for these are not fully understood. The choice of effective
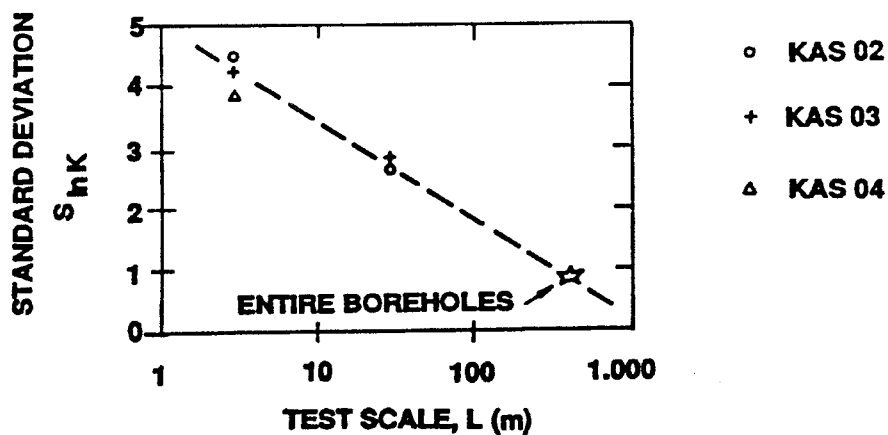
Figure 3-33. Standard deviations for logarithmic conductivity distributions on different scales.

117

conductivity for numerical models will therefore be crucial and depend on the scale.

HYDRAULIC PROPERTIES OF DIFFERENT AREAS

Äspö can be divided into two main blocks separated by the Mylonite Zone. From the analysis of conductivity data a clear difference between these areas can be found (see Figure 3.1-16). Thus, the SE part of the island is significantly less pervious than the NW part, with the Mylonite Zone in between. The reason for this may lie in the lithology or in a regional trend, which cannot be determined at this stage of the investigation. The difference must, however, be kept in mind when assessing parameters for numerical models.

3.2.2   Conceptual Geohydrological Models on Block Scale

In Section 2.2 conceptual geological models of different features are put forward on the 50-m block scale. In the hydraulic parameter evaluation (see Section 3.1.3), it has been possible to evaluate the hydraulic properties of these features directly and if not they can be deduced by different analogies. Since many of the interesting features are at least sub-planar the 3-m conductivity distributions have been used for the characterization. The note on hydraulic conductivity and scale is of course also valid for these conceptual models.

WATER-BEARING FRACTURE ZONE, Z-02

The conceptual geological model is shown in Figure 2-39e. In this case a fracture zone in Småland granite was observed.

This type of fracture zone, of which some are characterized as main hydraulic features in Section 3.2.1 is typically some 10 m wide and a large laterally. The most conductive ones have a transmissivity in the range of 10^{-5} m²/s. However, there is of course a gradual scale from the unfractured granite up to these very pervious zones.

/Liedholm 1989/ has shown, that there is a significant but weak correlation between fracture frequency and hydraulic conductivity for 3-m sections. This can be expressed as:

$$\log K_3 = -12.25 + 0.073 \, N_3, \quad R^2 = 7\% \qquad (3.1)$$

where K_3 is hydraulic conductivity and N_3 is the number of fractures per 3-m section.

Liedholm interprets this not as increased fracturing in itself increasing the hydraulic conductivity but rather that a larger number or fractures also increases the probability of one or more of them to being highly conductive.

The major fracture zones of this type govern to a large extent the groundwater movements through the rock and they must be identified and tested individually as major hydraulic features for the numerical modelling. The lower boundary to what can be considered as somewhat arbitrary.

It is known that the transmissivity along the zones varies, probably with a variance of the same magnitude as for the conductivity distributions obtained. However, no data are yet available to verify this.

SINGLE OPEN FRACTURE, L-03

Single open fractures are shown for the geological model in Figure 2-39c.

Some single open fractures were probably tested in the transient interference tests /Rhen, 1989/. Typical for them is that they are identified solely by hydraulic methods, i.e. spinner surveys and packer tests. They seem, however, to be of limited extent compared with the major fracture zones and seem in many cases to be linked to these hydraulically. They occur primarily in the brittle rock units Småland granite and fine-grained granite.

The transmissivity may be up to 10^{-5} m²/s. There is of cause also in this case a gradual scaling down to normal fractures. The transmissivity distribution within the conductors is not known.

GREENSTONE VEIN IN SMÅLAND GRANITE, Z-03

A greenstone vein in Småland granite is shown in the conceptual model in Figure 2-39f. The vein itself is often fractured and the fractures are often filled with clay and a clay zone sometimes exists within the greenstone vein.

From borehole KAS 03 a small sample of 7 tests is available for greenstone veins of this type. They show a median of $K_3 = 8.6 \cdot 10^{-7}$ m/s. The standard deviation, $lnK(S_3)$ is estimated to be 6.0. These figures should be used with caution since the sample is so small. They indicate, however, that the increased fracturing in the greenstone veins also gives rise to increased conductivity in spite of any clay filling.

DYKE OF FINE-GRAINED GRANITE, L-02

A dyke of fine-grained granite normally has a higher fracture frequency than the surrounding rock (see Figure 2-39b). It is difficult to obtain a conductivity distribution for the veins themselves but samples in which both the fine-grained granite and the adjacent rock are straddled by the packers were obtained in the test (see Figure 3.1-16) in granite-aplite.

A sample of 43 tests gave a median conductivity $(K_3{}^M)$ of $5.2 \cdot 10^{-10}$ m/s and a standard deviation, $lnK(S_3)$ of 4.2. These characteristics should be basically valid for the dykes of fine-grained granite.

ROCK COMPOSITE, L-01

In many cases dykes and veins of different compositions are associated with each other. The reason for this may by that the increased fracturing that may be caused by lithological differences also attracts later intrusions, i.e. of fine-grained granite (see Figure 2-39a).

A mixture of this kind is characterized as rock-composite in Figure 3-16. A sample of 61 tests gave a median conductivity $(K_3{}^M)$ of 10^{-10} m/s and a standard deviation, $lnK(S_3)$ of 4.9.

MYLONITE ZONE, Z-01

A small sample of 7 tests is available from the mylonites in the Mylonite Zone (see Figure 2-39d). The characteristics that must be used with caution because of the small sample are a median $(K_3{}^M)$ of $1.5 \cdot 10^{-8}$ m/s and an estimated standard

deviation, lnK(S₃) of 5.6. The hydraulic conductivity of the mylonite is significantly higher than that of the surrounding rocks.

3.2.3 Conceptual Geohydrological Models in Detail Scale

A detailed scale description of the three main rock types of Äspö is proposed in the conceptual geological model (Section 2.2). Geohydrological models of these comprise an assessment of the hydraulic properties of each type and a qualitative description of its geohydrological features.

SMÅLAND GRANITE, L-04

The Småland granite as defined in Figure 2-39g has a low-moderate hydraulic conductivity. The conductivity is weakly correlated to the fracture frequency.

Fracture zones of varying intensity and dykes and veins of fine-grained granites and greenstone occur within the granite. Increased conductivity is caused by all these features.

The hydraulic conductivity evaluations /Liedholm, 1989/ showed that there is a significant difference between the Northern and the Southern Block of Äspö. In the Northern Block the median hydraulic conductivity (K_3^M) for 3-m packer tests was found to be $1.0 \cdot 10^9$ m/s, and the standard deviation, lnK(S₃) was estimated to be 4.1. In the Southern Block the corresponding parameters were estimated to be $5 \cdot 10^{13}$ m/s and 8.6.

/Stanfors 1988/ noted that there is a difference in fracture frequency between the boreholes, but this cannot explain the large difference if the general correlation between fracture frequency and hydraulic conductivity is considered. Stanfors also notes that hematite and Fe-oxyhydroxide filled fractures, which are positively correlated to hydraulic conductivity, are abundant in KAS 03 but rare in KAS 02. This may, however, follow from conductivity rather than be the cause of it. Differences in rock stress may also be a cause, but so far no data are available on which to draw a conclusion. It must, however, be kept in mind that the effective hydraulic conductivity of a rock is a function of both the mean and standard deviations of the distribution. The difference in effective conductivity is not therefore as great as the difference between the medians would imply.

From inside a tunnel the granite appears dry to moderately wet. Inflows and drops of moisture occur as point flows along horizontal fractures and fracture intersections. More than 50% of the inflow to a tunnel is in the bottom area.

ÄSPÖ DIORITE, L-05

The Äspö diorite as defined in Figure 2-39h has a low hydraulic conductivity.

Within the diorite some dykes and sills of fine-grained granite occur. The granite is in itself more fractured and pervious but the fracture frequency of the diorite is frequently higher and its hydraulic conductivity is close to that of the granite.

The 3-m packer tests gave a median hydraulic conductivity of $2.5 \cdot 10^{11}$ m/s and a standard deviation, lnK(S₃) of 3.8. Thus, the diorite is less pervious and more homogeneous than most other rock types in the area.

From inside a tunnel the Äspö diorite appears dry. Some inflows and drops may occur at the boundary with other rocks.

FINE-GRAINED GRANITE, L-06

The fine-grained granite as defined by Figure 2-39i occurs as major dykes and sills in the Småland granite and the Äspö diorite. The fine-grained granite is generally the most pervious rock unit on Äspö.

The 3-m packer tests gave a median hydraulic conductivity of $2.3 \cdot 10^{-10}$ m/s and a standard deviation $\ln K(S_3)$ of 4.6. In considering these figures it should be noted that no data for the mass-formed fine-grained granite are available from the Northern Block of Äspö.

The fine-grained granite appears in a tunnel as areas with a somewhat greater fracture frequency and also greater water inflow. Specially the parts of the rocks close to other rock types are fractured and pervious.

3.3 VALIDATION OF THE PRELIMINARY CONCEPTUAL MODEL

The conceptual models of the Simpevarps peninsula in SKB Technical Report 88-16 were to three different scales.

Regional scale   (approx. 5 000 x 5 000 m)
Site scale   (approx. 500 x 500 m)
Detailed scale   (approx. 50 x 50 m)

The validity of these models in the light of the new results is discussed below.

The area covered by the geohydrological model may be roughly defined as the area between the Götemar and Uthammar granites.

Since the new data were almost exclusively are gathered on Äspö the validation is made in the light of this.

HYDRAULIC CONDUCTIVITY OF DIFFERENT ROCK UNITS

Information from KAS 02, KAS 03, KAS 04 and KLX 01 regarding the **conductivity-depth correlation** cannot validate the decrease in hydraulic-conductivity with depth /Rhén, 1987/. Depth-related trends of the hydraulic conductivities differ from borehole to borehole, and within the depth investigated no significance trend was found. /Liedholm, 1989/

When comparing predicted hydraulic conductivities with test data, the test scale and depth must be considered. Predicted values are based on data from percussion boreholes with a median length of 51 m. Values for the present investigation of the different rock units were obtained from 3-m packer tests. From Figure 3.2-4 it is evident that they must be adjusted to be comparable to the percussion borehole data. The basis for this adjustment is not fully understood, but if the empirical curve shown in Figure 3.2-4 is used an effective conductivity of approximately $K_3^M \cdot 30 = K_{50}^M = 3 \cdot 10^{-8}$ m/s for the Småland granite which is the only rock type that can be compared on the regional scale. On the regional scale the hydraulic conductivity (K_o) at the surface was found to be $3 \cdot 10^{-7}$ m/s.

The reason for the difference may either be systematic, i.e. the percussion boreholes, most of which are water wells, are sited in more pervious rock or that there is a more pervious portion of the rock at shallow depth, or that Äspö is an area with lower conductivity than that general in the region.

The relative difference in conductivities between the different rock types have been confirmed by low hydraulic conductivity in the diorite, intermediate in the Småland granite and the highest in the brittle fine-grained granite.

CONDUCTIVE STRUCTURES

The terrain analysis and geophysical investigation gave patterns that were interpreted as fracture zones. A first order pattern was zones striking N-S and E-W and a second order was NW-SE and NE-SW. In the regional well-data analysis a slightly tendency towards higher specific capacities was found along the NW-SE and NE-SW rather than the N-S and E-W system.

Conductive structures on Äspö were localized by means of the transient interference tests. Those that reach the surface within Äspö comply with lineaments and geophysical structures. The tests show, however, that both the NW-SE, NE-SW and N-S, E-W systems may form major hydraulic conductors.

PIEZOMETRIC LEVELS

The piezometric levels of shallow boreholes showed that the groundwater level at the surface is governed by the topography, as stated in the previous report.

MODEL GEOMETRY

The regional conceptual geohydrological model was characterized by the granite diapirs north and south of the larger area. No borehole has yet reached the Götemar-Uthammar granite in the area but the fine-grained granite that forms sills and dykes is likely to be associated to it. They have among other characteristics a significantly higher hydraulic conductivity than other rock units. They are the probable cause of the hydraulic conductivity not decreasing with depth.

The stated hydraulic conductivities are, as mentioned, probably higher than the actual ones, but the decreasing trend in the model gives conductivities at greater depth, approx. 500 m, reasonably dose to test data provided that they are adjusted to the same scale.

THE ISLAND OF ÄSPÖ

The island was divided into three geological units: The NW-part, the SE part and the border zone between, consisting of the Mylonite Zones and greenstone tenses. This division into three parts is still valid.

The division of Äspö into three geohydrological units can be identified in the conductivity study /Liedholm, 1987/. There exists a significant difference in conductivity means between KAS 02 (in area AS 3, SE Äspö) of low conductivity and KAS 03 (in area AS 1, NW Äspö) of high conductivity. The difference is also between KAS 02 and adjacent to KAS 04 (in area AS 2, the border zone).

4 CHEMISTRY

4.1 CHEMICAL STUDIES

In the preceding phase of the investigation surface waters and groundwater from shallow percussion holes were collected and analysed. The evaluation of these data was made by /Laaksoharju 1988/ and reviewed briefly by /Gustafson, Stanfors and Wikberg 1988/. The evaluation of groundwater chemical data in the present phase was made by /Laaksoharju and Nilsson 1989/.

From the three deep core boreholes, KAS 02, KAS 03 and KLX 01, groundwater was sampled in three different campaigns: during the drilling operation, in conjunction with the hydraulic pumping tests (see 3.1.2), and independently of other activities, with the equipment used for the complete characterization of the deep groundwater /Wikberg et.al., 1987/. Comparison of the results indicates that the water sampled during the drilling operation was not representative due to mixing with drilling water. Besides the elements sensitive to redox, and Eh, the samples from the pumping tests gave results which were as representative as those from the separate sampling campaign.

The chemical composition of the groundwater was compared by the saturation concentration of different minerals. This modelling exercise was performed using by the PHREEQE computer code and indicates that the water is oversaturated with respect to montmorillinite, hematite, uraninite and magnetite, in equilibrium with respect to quartz, goethite and calcite and, finally, undersaturated with respect to pyrite. The partial pressure of carbon dioxide is also below the saturation level.

A multivariant analyses called Chemometri was used to divide the groundwater samples into different classes. Based on the results of this classification the different waters are explained as a result of mixing with saline and non-saline water. The mixing portions are affected by the hydraulic head of the flow system. The hydraulic head and the flow regime can therefore be evaluated on the basis of knowledge of the chemical composition of the water. Two different types of predictive model are presented, both based on the assumption that the salinity of the water is a linear function of depth and that the only factor influencing a deviation from the linearity is the hydraulic head in the bedrock. The hydraulic head of the sampled section was calculated on this basis, as was the salinity of the water in the rock mass in which no boreholes are situated. These predictions will be checked in the next phase of the investigation when new holes will be drilled and the piezometric head of the sections monitored.

Table 4-1 shows the results of the water analysis for the main constituents. Table 4-2 contains the data on some specific parameters. In Figure 4-1 the dominating constituents, sodium, calcium and chlorine, are presented graphically. The concentration is given in mol/l for the ions. It should be noted that the next element, sulphate, is present in such a low concentration that it is not visible in the figure.

The accuracy of the chemical analyses were checked by ion balance calculations. The results of these calculations are statistically presented in Figure 4-2.

123

Table 4-1. The concentration of main constituents in the groundwater sampled from boreholes KAS 02, KAS 03 and KLX 01. All concentrations are given in mg/l except for pH. * indicates sections in which complete chemical characterization was made. Other depths were sampled in conjunction with hydraulic pumping tests. The data is from /Laaksoharju and Nilsson 1989/.

Borehole/ level (m)	Na mg/l	K mg/l	Ca mg/l	Mg mg/l	Fe^{2+} mg/l	HCO$_3$ mg/l	Cl mg/l	SO$_4$ mg/l	S-2 mg/l	SiO$_2$ mg/l	pH —
KAS 02/202*	1230	7.0	1000	68	.49	70	3800	110	.50	13	7.4
KAS 02/308	1720	8.8	1480	75	.62	32	5300	290	.16	4.3	7.6
KAS 02/314*	1700	9.0	1540	75	.78	26	5340	270	.01	2.0	8.2
KAS 02/463*	1800	8.2	1570	66	.50	25	5450	290	.13	3.3	8.3
KAS 02/530*	2100	8.1	1890	42	.22	10	6370	550	.18	4.1	8.3
KAS 02/802	2800	11.7	3690	39	.02		11000	522	.01	4.3	8.2
KAS 02/860*	2900	10.7	3800	35	.04	11	11000	520	.70	8.5	8.5
KAS 03/196	1200	6.3	480	60	—	60	2900	31	.05	4.6	7.7
KAS 03/248	1300	6.6	500	54	.28	53	3000	40	.17	4.4	7.8
KAS 03/347	1730	6.3	1400	45	.20	12	5180	340	.05	4.2	7.8
KAS 03/453	1710	6.2	1200	40	.19	27	4600	300	.11	4.1	7.8
KAS 03/609	2000	6.3	1740	39	.06	11	5880	470	.10	3.9	8.0
KAS 03/690	2130	6.6	2660	63	.05	11	8100	680	.10	3.9	8.0
KLX 01/272*	790	6.6	240	21	.20	91	1800	—	.60	5.5	7.9
KLX 01/456*	850	6.3	223	17	.04	77	1680	108	.63@	5.3	8.2
KLX 01/680*	1600	7.2	1410	21	.03	25	4890	380	2.60@	4.7	8.1

@ = Uncertain result.

Table 4-2. Characteristic parameters of the groundwater sampled from boreholes KAS 02, KAS 03 and KLX 01. W.flow is the pumping rate, D-W the amount of drilling water remaining in the sampled water, TOC the amount of organic material. * indicates sections in which complete chemical characterization was made. Other depths were sampled in conjunction with hydraulic pumping tests. The data is from /Laaksoharju and Nilsson 1989/.

| Borehole/ level (m)	W.flow ml/min	D-W %	Cond. mS/m	TOC mg/l	C-14 age/y	U-234/ U-238	O-18/ smow	Deut. smow	EH mV
KAS 02/308	5000	.7	1510	2.0	----	—	-12.7	-99.8	
KAS 02/314*	180	.6	1580	2.4	12960	3.06	-12.3	-100.6	-300
KAS 02/463*	160	.4	1630	3.0	13910	2.99	-12.8	-99.9	-300
KAS 02/530*	117	.3	1890	1.0	----	3.25	-12.3	-97.2	-300
KAS 02/802	15200	.2	2910	.5	----	—	-13.0	-96.8	
KAS 03/196	10000	2.7	910	1.0	21695	3.54	-14.6	-115.3	
KAS 03/248	4000	1.0	930	.5	20090	—	—	—	
KAS 03/347	18000	.8	1370	.5	----	3.00	-13.3	-104.9	
KAS 03/453	16000	2.1	1400	.5	----	—	—	—	
KAS 03/609	18800	2.2	1700	1.1	----	—	—	—	
KAS 03/690	13000	2.6	2260	.5	----	—	—	—	
KLX 01/272*	140	4.6	733	—	----	—	—	—	
KLX 01/456*	138	13.7	637	2.2	----	—	—	—	
KLX 01/680*	138	2.6	1714	1.2	----	—	—	—	
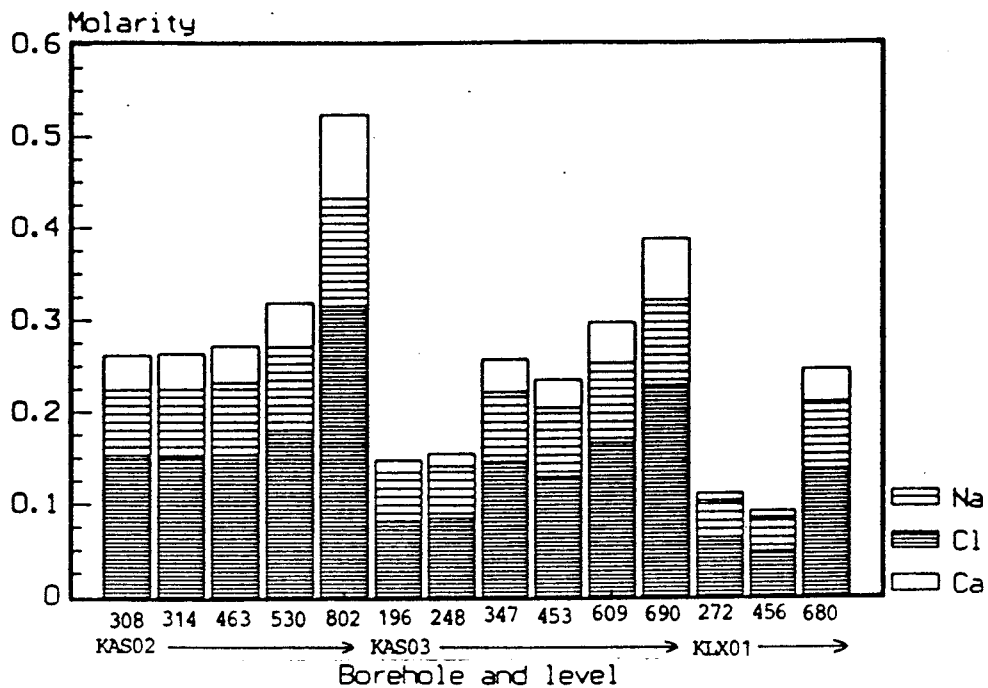
Figure 4-1. The composition of the groundwaters sampled at different depths in the deep boreholes (from Laaksoharju and Nilsson, 1989).
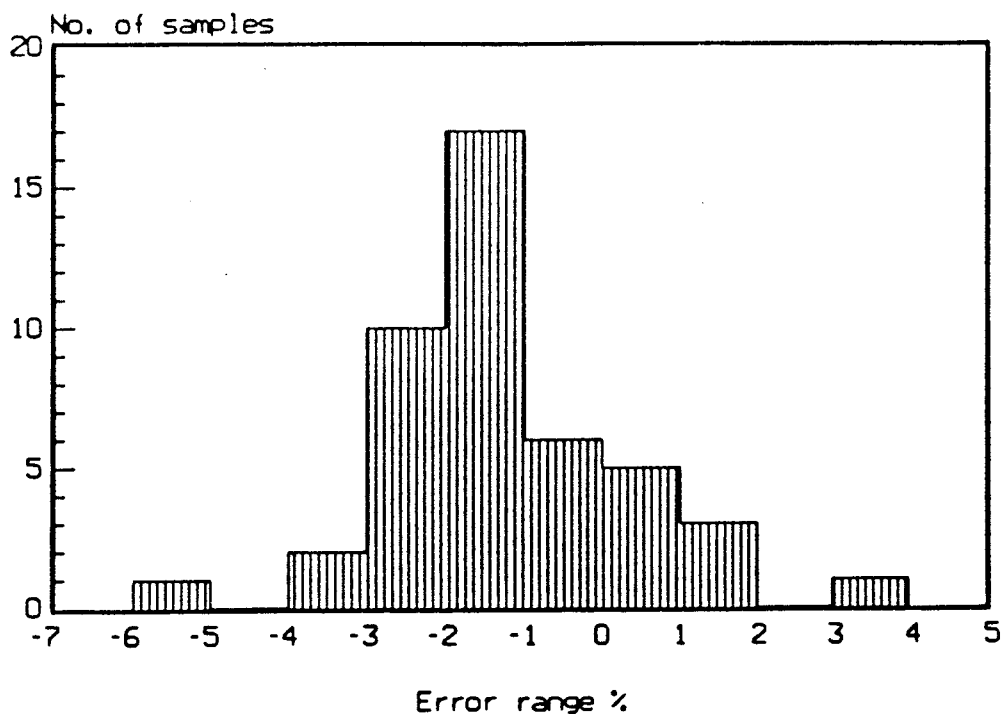

Figure 4-2. Statistical presentation of the ion balance calculations made on the analysed water samples. The error is defined as the difference between the sum of cations and anions divided by the sum of them (from Laaksoharju and Nilsson, 1989).

From the figure it is obvious that there is an excellent agreement between the sum of anions and cations. For groundwater analyses a variance of +/- 10% is acceptable whereas +/- 5% is considered excellent. Out of the 45 samples in Figure 4-2 only one falls within the error range -(5-6)%. Half of the samples lie in the range -(1-2)%.

A statistical evaluation of the fracture filling minerals was made by Tullborg /Wickman et al., 1988/. The percentage of fractures filled with calcite in the cores was analysed as a function of depth. The results suggest that calcite filling is common in all the boreholes regardless depth. This supports the results of the water analyses suggesting stagnant conditions. In a situation in which there is infiltration of surface water there is also a depletion of calcite in the uppermost part of the bedrock. Such a decrease cannot be seen in the cores from the boreholes deeper than some ten to twenty metres. This suggests that there is no intrusion of carbon-dioxide-rich surface water into the rock mass. The very low partial pressure of carbon dioxide in the sampled water is a consequence of this situation.

4.2 CONCEPTUAL MODELS OF THE ÄSPÖ AREA

In the previous study /Gustafson, Stanfors and Wikberg, 1988/ conceptual models were presented on different scales. This approach is also followed here. The different scales are defined as:

Site scale	500 m
Block scale	50 m
Detailed scale	5 m

In the previous two chapters these scales were adopted for the presentation of the geological and geohydrological conceptual models (cf. 2.2 and 3.2). The same scales will be used for the chemical models.

4.2.1 Site Scale

The two boreholes, KAS 02 and KAS 03 represent the Southern and Northern Blocks of Äspö. These two sites are fairly different from one another with respect to their geological and geohydrological conditions (cf. 2.2 and 3.2). A third subarea, with different conditions, is represented by a highly altered mylonitic zone which divides the island into the northern and southern parts (cf. 2.2). Borehole KAS 04 was drilled into the Mylonite Zone. No groundwater samples have been collected in that borehole so far.

Chloride is a conserving constituent in groundwater. Once dissolved it will stay in solution. The chloride concentration can therefore be used for tracing the origin and the residence time of the water. In the samples collected from KAS 02 and KAS 03 the chloride concentration varies from 3000 mg/l up to 11000 mg/l (see Table 4-1). The level in the surrounding Baltic Sea is 3000 mg/l. The salinity of the Baltic Sea around 7000 years ago was three times higher than the present level. At that stage the Sea was called the Litorina Sea.

As can be seen from Table 4-1 the chloride concentration increases with depth. The increase is, however, not linear. At depths below 300 m the chloride concentration is equal to that of the surrounding sea, 3000 mg/l. At depths from 300 to 500 m the concentration is slightly above 5000 mg/l. At greater depth the

126

increase seems to be almost linear. The constant concentration level is somewhat deeper in KAS 03 (350 — 600 m) than in KAS 02 (300 — 460 m).

The chloride in the water can result from sea water intrusion, modern and/or from the Litorina stage, dissolution of chloride containing minerals and/or other phenomenon that occurred prior to the last glaciation. It is also possible that the saline source in the northern part is different from that in the southern part. This is indicated by the Carbon-14 dating (see Table 4-2), which for greater depth and higher salinity in KAS 02 gives a lower apparent age than the shallower, less saline water in KAS 03.

The difference between the two most shallow levels in KAS 03 and the others is further indicated by the difference in sulphate concentration. The low concentration in KAS 03, 196 m and 248 m, indicates that the reducing conditions have resulted in an almost complete reduction of sulphate. It should be noted, however, that the sulphate/chloride ratio is much lower for all the sampled waters than for the sea water. This implies that the sulphate has been reduced to sulphide and precipitated as pyrite on the fracture walls. Consequently the redox potential is lower than under sulphate/sulphide equilibrium. This is supported by the stable Eh readings for KAS 02 (see Table 4-2).

Even though the chloride concentration is in some cases close to that of the Baltic Sea the sodium/calcium ratio is always very different. In the sea water this ratio is 30/1 whereas it is close to unity or even less in the groundwater. The difference may be due to ion exchange reactions in the rock minerals. The dissolution or weathering of calcium and chloride-rich minerals are also likely to contribute to this state. Since the tendency is that the chloride increase is followed by an increase in the calcium concentration. In step with the increase of chloride there is a decrease in the bicarbonate concentration. This indicates that there is a mixing of a carbonate water with a chloride water.

In both drillholes KAS 02 and KAS 03 the concentrations of dissolved iron decreases by depth. Such a trend has also been observed at other site investigations and is thought to be the result of the carbon dioxide weathering of minerals. At shallow depth the dissolved carbon dioxide weathers the iron-rich minerals such as biotite. Gradually the dissolved iron is precipitated as fracture minerals. In KAS 02 the highest iron concentration was found at a depth of 314 m. This is close to the lithological boundary between the acidic Småland granite and the basic diorite. The diorite, having the same chemical characteristics as the greenstones, is obviously the source of the higher iron concentration in KAS 02 compared with KAS 03. High iron concentrations in conjunction with greenstone lenses have been observed in earlier studies /Smellie et al. 1985/.

The northern and southern subareas of Äspö may be briefly described as follows:

Northern Äspö

According to the geohydrological models presented in 3.2 the northern part of Äspö is more conductive than the southern part. Chemically this is seen in the lower salinity of the water in KAS 03 than in KAS 02. The carbon-14 dating method gives apparent ages of 20,000 years in the uppermost sections indicating that the water circulation is extremely low (nonexistent).

Southern Äspö

Despite higher salinity in the upper sections of KAS 02 the carbon-14 dating gave an age of 13,000 years. The diorite has affected the chemistry with respect to the iron content. This is most easily seen in the boundary between the diorite and the Småland granite.

4.2.2 Block Scale
Water-Bearing Fracture Zones

These zones are, according to the geohydrological model in 3.2.2, the main hydraulic features in the area. They may extend a long way laterally but the transmissivities also vary largely within the zones themselves. Due to the large extent of the zones the groundwater in them is expected to have a composition placing it on the mixing line in the prediction made by /Laaksoharju and Nilsson 1989/. The salinity may be roughly calculated from

$$Cl = (1 \pm 1) + 10 \cdot D \qquad \text{with } Cl = \text{chloride (g/l)}, D = \text{depth/km}$$

Because of the continuous mixing no specific character defines the water within the fracture zones.

Single Open Fractures

According to the geohydrological models in 3.2.2 a single open fracture is characterized by a high transmissivity but limited extent. Therefore such a fracture is expected to transport low-salinity water from the surface or high-salinity from depths, depending on the direction of the connectivity.

4.2.3 Detailed Scale

In all the rock mass where the hydraulic conductivity is low as indicated in 3.2.2 and 3.2.3 the groundwater chemistry is defined by the chemical character of the rock-forming minerals. The dissolution rate largely determines the composition of the water. The basic rocks are supposed to give a more specific character to the groundwater than the acidic granite. The pH and the iron concentrations are expected to be higher in the basic rocks.

4.3 VALIDATION OF THE PRELIMINARY CONCEPTUAL MODEL

The preliminary conceptual models were presented on different scales in the previous evaluation /Gustafson, Stanfors and Wikberg, 1988/. Despite this the validation of the earlier predictions can be made regardless of the scales.

The data used in an earlier phase of the investigation was obtained from analyses of groundwater from shallow percussion drilled holes. In the shallow boreholes saline water was also found, the composition of which indicated both modern and relict sea water. This suggested that stagnant conditions prevailed in the bedrock underneath Äspö. These observations, combined with the geological and geohydrological conceptual models, indicated that conductive zones

would be expected to carry relict sea water whereas vertical, single fracture sets would be expected to carry fresh water.

The pumping tests in borehole KAS 03 gave continuously decreasing chloride concentrations. This is thought to be due to the presence of vertical, conducting fracture sets in the northern part of Äspö. Such features are not present in the southern part and consequently the salinity in the water remained constant throughout the pumping tests in KAS 02.

There is a significant difference between the iron concentrations in KAS 02 and KAS 03. This is thought to be due to the presence of the basic diorite in KAS 02 which contains more easily weathered minerals. Such an effect was expected in the boundary between the acidic Småland granites and greenstone lenses. The chemical character of the greenstone and the diorite may be considered to be the same.

5 THE LAXEMAR AREA

GEOLOGY

More or less homogeneous Småland granite constitutes the major part of the rock mass in the Laxemar area. Greenstone of gabbroic composition intruded by a great amount of granitic material occurs in the northern part of the area. Xenoliths of altered greenstone and dykes of fine-grained granite are common features in the porphyritic granite mass, which seems to be most homogeneous in the southern part of the area.

The Laxemar area is bordered to the N and to the SE by regional fracture zones trending ENE and NE respectively. Local fracture zones — geophysically indicated — intersect the area trending E—W, NE and NW.

Lineaments oriented NW—WNW are most expressed in the area and the general pattern of the fractures shows evident strikes round WNW, N and ENE. The general trend of the foliation in the area is normally between N70°E and E—W, with a more or less vertical dip.

Core borehole KLX 01 was sited in a major block of the part of the area. The aim of the borehole was to obtain basic information concerning bedrock composition and hydraulic properties at greater depth in a technically relatively undisturbed rock mass (Figure 5-1).

Småland granite of a composition between granite and granodiorite is by far the most dominating rock in the core. Fine-grained greenstones are most common at the levels 15—45 and 325—370 m. Diorite only occupies parts of the core at the levels 230—255 and 530—550 m. Fine-grained granite occurs as minor veins and dykes — the longest sections are about 10 m (425—470 m). Contrary to the cores from the Äspö boreholes, KLX 01 seems to be more coherent and not so affected by fracturing. The most frequent fracture-filling minerals, calcite and chlorite, are found throughout the core while minerals like hematite and epidote are concentrated to distinct zones.

GEOHYDROLOGY

The hydraulic tests in borehole KLX 01 consisted of test and clean-up pumping, combined with a spinner survey and packer tests with section lengths of 3 m and 30 m.

The pumping test gave a transmissivity (T_s) for the whole borehole of $8 \cdot 10^{-5}$ m^2/s. Cross-hole measurements in surrounding boreholes showed contact with only HLX 05, which is situated approximately 100 m towards the NE. The reaction in this borehole indicates an indirect connection. Other boreholes in the area, HLX 01 and HLX 07, indicated subvertical hydraulic conductors running in the direction NW-SE /Nilsson, 1988/. Since no other borehole reacted it is plausible that hydraulic conductors of the same type are penetrated by KLX 01.

The spinner survey revealed two distinct hydraulic conductors. Neither of them is associated with massive fracturing, which gives them the character of single open fractures. Their positions and transmissivities are given in Table 5-1.
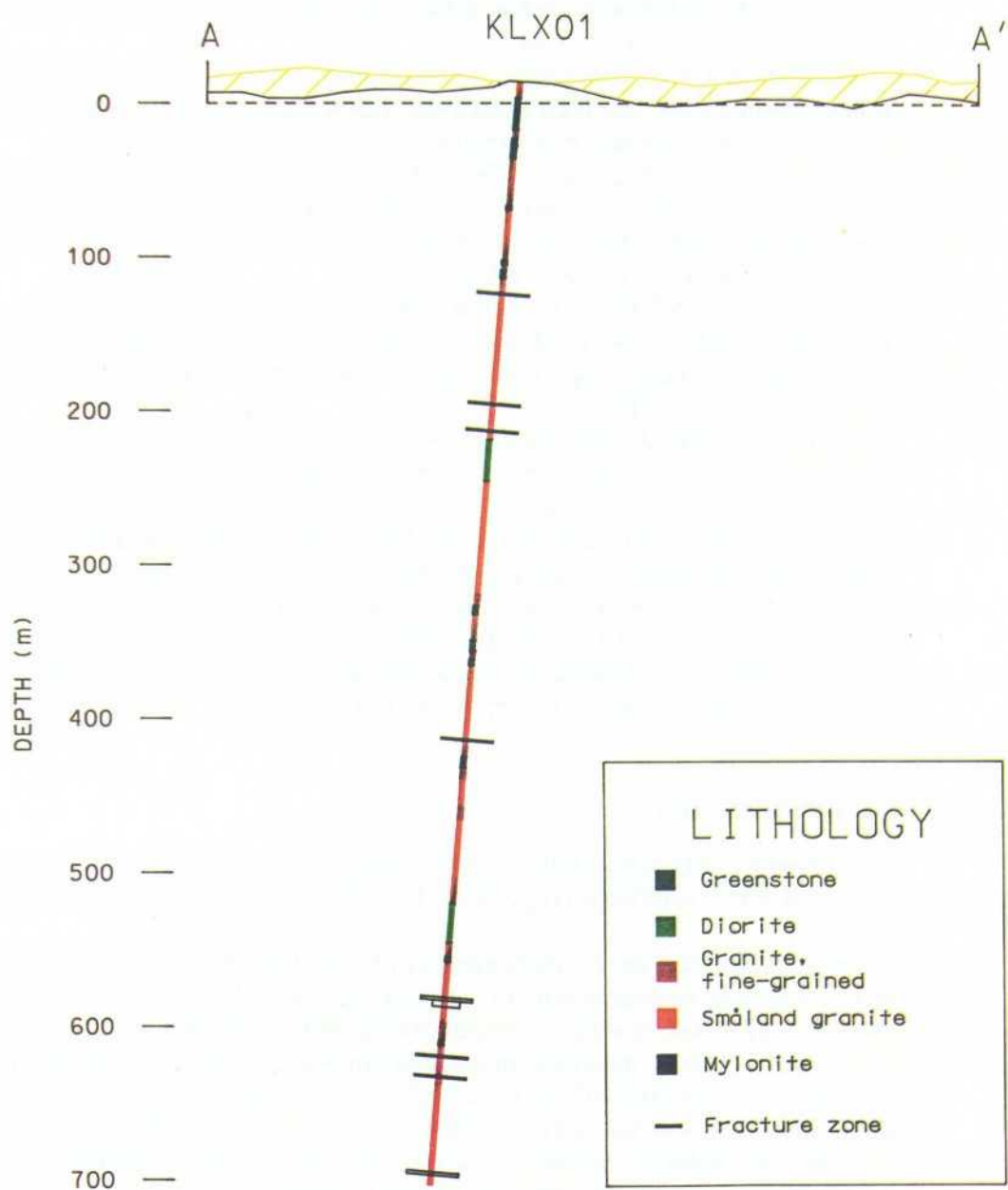
Figure 5-1. Cross section through the Laxemar area. Lithology and main fracture zones in core borehole KLX 01.

132

Table 5-1. Main hydraulic conductors in KLX 01.

Conductor	Conductive zone Z(m)	Flow peak Z(m)	Transmissivity T(m²/s)
KLX 01-A	182—185	183	$7.2 \cdot 10^{-5}$
KLX 01-B	460—461	460	$0.8 \cdot 10^{-5}$

Most of the borehole runs through Småland granite and the results may therefore be considered representative of the Laxemar area. The results are summarized in Table 5-2.

Table 5-2. Conductivity distributions for the packer tests in KLX 01.

Section length (m)	Section (m)	Arithmetic mean K^A(m/s)	Geometric mean K^G(m/s)	Std. dev. S_{inK}
3	106—688	$2.2 \cdot 10^{-8}$	$1.0 \cdot 10^{-10}$	3.47
30	103—643	$2.2 \cdot 10^{-7}$	$5.6 \cdot 10^{-10}$	4.0

Thus, compared with northern Äspö Laxemar consists of tighter rock but southern Äspö is even less pervious.

CHEMISTRY

From borehole KLX 01 water samples were taken at three different levels. The results are presented in Table 4-1 together with those from KAS 02 and KAS 03. From the table it is obvious that the water is of the same type in both Laxemar and Äspö. There are a few differences that should be mentioned.

The chloride concentration in the Laxemar borehole is much lower as a function of depth than in the Äspö boreholes. Such a situation is in good agreement with the results obtained in the percussion boreholes which at Laxemar exhibited much lower salinity than on Äspö. This simply means that the infiltration of surface water into the Laxemar bedrock is larger than it is on Äspö. The reason for this is obviously the fact that Äspö is an island, surrounded by the sea on all sides, whereas Laxemar belongs to the mainland.

The groundwater sampling at Laxemar was difficult to carry out because of several incidents resulting in technical failures. The borehole was therefore left open for long periods at a time when internal circulation in the borehole may have changed the chemistry of the groundwater in the sampled sections. For instance the high sulphide concentration in the lowermost section is uncertain, because it was unstable during the whole sampling period. The sampling in KLX 01 will therefore be repeated before the chemical character of the groundwater can be defined.

6 THE RELEVANCE OF THE METHODS OF INVESTIGATION

The investigations for the Hard Rock Laboratory involved a multitude of geological, geohydrological and geochemical methods. Of these some are old and well known but some, as far as we know, were used for the first time on a project of this kind.

The preinvestigations for the laboratory and the construction of the tunnel down to the experiment area can be seen as an important test before the final repository. The site-dependent factors must be understood and quantified. These factors either concern the geological framework formed by the lithology and the structural features or the processes within such a framework, as water transport, chemical environment and stability. In the following the relevance of the methods of investigation is evaluated with respect to these factors.

A relevant method of investigation is one that provides significant, comprehensive and conclusive information on the site-dependent factors at a reasonable effort. The matter of cost-effectiveness thus involved in our evaluation of relevance.

In the following the methods employed are evaluated within the above context. The evaluation is not made in a mechanical way, by setting points to different parameters etc, but rather as a reasoning around the experience gained during the investigations.

Finally, it should be stated that the experience is strictly only valid for the actual investigation area, with its specific geological environment, and that other experience may be gained in another area.

The aim of the second phase of the site investigation for the HRL was to characterize the geological and geohydrological conditions on a more detailed scale, on the island of Äspö and, to some extent, at a part of the Laxemar area as well. Now, based on our present experience, it may be of interest to try to estimate the relevance of the many different methods of investigation applied.

6.1 GEOLOGY

A three-dimensional model of a rock mass must be based on the characterization of the distribution of lithological units, fracture systems and fracture zones on a regional and local scale.

Recognition of small-scale structures, petrographic variations and fracture orientation within and near the site area on Äspö has been achieved through detailed surface mapping along cleaned trenches across the island. The results of these investigations, complemented with surface information, have been very useful in the geological characterization of rock volumes in the site area.

Aero-geophysical measurements which had been made earlier in the Simpevarp area constituted a good base for the analysis of the tectonic setting on a regional scale. In order to investigate the pattern of the fracture zones and the boundaries between different bedrock units on a more detailed scale, magnetic and resistivity measurements were made over the entire island of Äspö. The combination of detailed geoelectric and geomagnetic data provided very good information concerning the extent and orientation of fractures and fracture

zones. Data about the dip of the fracture zones and interpretation of open (water-bearing) zones are of great interest.

A good three-dimensional characterization of a rock mass needs data from subsurface investigation methods as a complement to surface information. Borehole evaluation and seismic reflection were the main methods used for this purpose. Very detailed petrographic and structural examination of the drill-cores, among other things, revealed a dioritic lithological unit at the level approx. 320—800 m in borehole KAS 02. This kind of rock had not been found during the surface mapping on Äspö. Indications of ductile structures in the cores gave directions how to correlate subsurface information to structures mapped on the ground. Mineralogical studies of fracture mineral fillings gave very valuable results especially about the distribution of calcite and Fe-oxyhydroxid with increasing depth in the boreholes.

Results from two reflection seismic profiles on Äspö identified two sections, 300—350 metres and 950—1150 metres probably reflecting a system of more less interconnected and irregular heterogeneities of fractured rock mass. These indications can be correlated to fracture zones observed in the boreholes. The seismic reflection method seems to be one of the most convenient methods for mapping major, low-dipping fracture zones at depth from about 300 m and downwards, even in the crystalline bedrock.

The objectives of the geophysical borehole surveys was to aid in the definition of the location and character of the lithological units and their contacts and to determine the distribution and character of fractures and fracture zones in the rock mass.

The sonic log and the logs of magnetic susceptibility and the natural gamma radiation intensity seem to be most relevant methods for lithological characterization. There is a specially significant correlation between high gamma radiation and the fine-grained granites in all the boreholes. The results from the caliper log and the electrical logs were of greatest interest in detecting fractures and fracture zones.

It seems, however, to be rather unnecessary to use three different electric logs which to a large extent give identical results. For future geophysical logging surveys we recommend the use of the single-point resistance log only. In addition we propose the use of the gamma-gamma and neutron logs.

To get the absolute orientation of structures like rock contacts, fractures and fracture zones single-hole radar measurements and TV-logging were performed. In the inclined borehole, KAS 04, the absolute orientation was also obtained using an iron-rod indentor during the drilling operation.

Single-hole radar reflections may give valuable information about the orientation of fracture zones — especially those intersecting the borehole at rather low angles. The fracture zone suggested by interpretation of radar reflections from boreholes KAS 02-03 and KLX 01, however, is not in accordance with seismic reflection results and hydraulic test data.

The use of the TV-logging method for absolute orientation of fractures in core boreholes was accompanied by many problems, especially concerning depth measurement. It is very difficult to find the same feature in the core as in the TV-log. On the other hand it is equally important that the depth measurement in TV-logging is correct. The reconstruction and relative orientation of the core, which be necessary to make an absolute orientation possible, is also very time consuming. On that account an attempt to use the Televiewer method for absolute orientation of structures in future boreholes will be made in current investigations.

6.2 GEOHYDROLOGY

The water movement in the bedrock is governed by the distribution in space of the hydraulic conductivity and the specific storage and also by boundaries and sources. If water transport of some pollution is also considered several other parameters have to be estimated. The objective of the hydraulic tests so far performed was to find main hydraulic structures in the bedrock and to estimate the hydraulic conductivity and specific storage of these hydraulic structures and the less conductive rock mass. Several tests have been performed and some brief comments are made below.

BOREHOLE CONFIGURATION

The core boreholes were all drilled following a telescope design. This has been an important advance compared with the traditional layout.

During drilling the telescope configuration made it possible to have an air-lift pump unit going on in order to minimize contamination of the bedrock by drilling water.

The telescope configuration also permitted spinner surveys to be done during the final test and clean-up pumping.

The telescope configuration permitted the carrying out of transient interference pumping tests on selected sections of boreholes.

Finally the telescope configuration also simplifies installation of packer systems and sensors.

HYDRAULIC TESTS

The tests performed were:

— Air-lift test
— Pumping test on the whole borehole
— Spinner test
— Injection test
— Interference test

Useful and inexpensive information can be obtained during percussion drilling if the drillers register carefully the drilling performance, levels and the amount of water leaking into or out of the borehole.

Air-lift tests has often been done during the drilling operation. This is also a cheap test to obtain a quick estimate of the hydraulic properties of the bedrock.

Pumping tests on the whole borehole gives a more accurate estimate of the effective hydraulic properties of the rock mass on a relatively large scale. If observation wells are used it may be possible to obtain indications of hydraulic anisotropy if the duration of pumping is long enough.

Spinner tests can be performed during the pumping tests and they give very important information of the location of main hydraulic conductors. Together with the pumping test it is possible to obtain a transmissivity distribution along the borehole.

The injection tests were performed with a double-packer system on 3- and 30-m sections. Transient analysis were performed when possible. With the injection tests it is possible to identify levels of main hydraulic conductors but not with the same precision as with spinner tests. The main purpose of the injection tests was,

however, to find the statistical distribution of the hydraulic conductivity on different test scales. Together with the pumping test these test are very useful for understanding the hydraulic behaviour of the rock mass.

Interference tests provided information on the hydraulic properties of some main hydraulic conductors and, in some cases, it has also been possible to determine the likely geometry of the conductors.

The tests provided, above all, significant information on water transport and, in some cases, a weak or strong indication of an important hydraulic structure. None of the tests gave individually comprehensive information but together they provided fairly comprehensive information on the hydraulic features of the target area.

GEOPHYSICAL LOGS

The geophysical logs are extremely dense in terms of the information they provide, with one measurement every 0.1 m, and they provide information of which only a small portion can yet be used.

With regards to the magnitude of the hydraulic conductivity, no comprehensive correlation with high accuracy has been found to any of the 12 logs or 60 different states of logs. Only when it is impossible to perform hydraulic tests, should some information be retrieved by using the above electrical logs.

The magnitude of the hydraulic conductivity can to some extent be determined from the (median) Normal Resistivity, the (minimum) Single-Point Resistance and the (minimum) Lateral Resistivity readings.

These geophysical logs provide information about the magnitude of the hydraulic conductivity just beyond or within the range of judgmental comprehension. They hardly provide selective information nor do they probably provide complete information about the hydraulic conductivity.

The hydraulic conductivity is to some extent dependent on the number of fractures. The numbers of fracture provide important information, but not complete or selective information about the magnitude of the hydraulic conductivity.

6.3   CHEMISTRY

The relevance of the chemical methods of investigation concern the sampling and the analyses of the groundwater. In order to be useful the groundwater samples must be representative of their surroundings and the analyses must be made in a way to ensure that the composition of the water does not change.

The groundwater is pumped out of a section sealed off with packers and the chemical analyses are made once a day. In this way the composition as a function of time is known. When the composition is constant the samples are thought to be representative. Due to the highly varying hydraulic conductivity of the sampling sections, 10^9 — 10^5 m/s, it is impossible to estimate in advance the time required to achieve a stable composition. The specific conditions in the borehole are also important for the time it takes to obtain representative water samples. On-site analyses are therefore necessary to optimize the time sampling should be carried on.

The cooling water used in drilling is always tagged by a tracer, a fluorecent dye called Uranine. In this way it is possible to identify the portions of drilling water in the groundwater samples. In most cases the highly conducting sections, $K=10^{-6}$ m/s, are severely contaminated by drilling water, due to the fact that

large amounts are lost in the bedrock during drilling. In the investigations on Äspö two different operations were performed to avoid this situation, namely:

— air-lift pumping during drilling
— sampling of the highly conducting sections in conjunction with the hydraulic pumping tests.

Air-lift pumping during drilling was possible due to the fact that the uppermost 100 m of the borehole had been enlarged from 56 to 150 mm. The pumping mostly removes as large a volume as the one used for the drilling, approximately 300 l/m.

Because of the very small amount of drilling water contamination representative groundwater samples were obtained after much shorter pumping periods than earlier. Consequently, the total duration at a section has been reduced from 3 or 4 to 2 or 3 weeks. With more experience it might be possible to reduce the pumping time to two weeks. It should be noted that air-lift pumping was not carried out during drilling of KLX 01. As can be seen in Table 5-2 the amount of drilling water is much larger in the samples collected in that borehole, compared with similar samples collected in KAS 02.

The sampling of sections with a hydraulic conductivity above 10^{-6} m/s is very time consuming because of the low capacity of the pump. The pumping tests on Äspö were performed with a pump of a capacity that was two orders of magnitude larger than that of the chemical sampling pump. The three day duration of the pump test was therefore sufficient to ensure representative water samples. However, this time was not sufficient to obtain stable readings on the Eh electrodes. Despite this drawback the combination of groundwater sampling and hydraulic pumping tests is very successful and should be employed whenever possible.

7 BOREHOLE SITING — SECOND BATCH

7.1 GEOLOGY

Results from core drilling, detailed lithological and structural mapping along well-exposed trenches, seismic reflection and magnetic and electric ground measurements during 1988 contributed to a better understanding of the lithological and structural setting of the island of Äspö.

Based on this knowledge the investigation of the next phase will be concentrated to an area on the southern part of Äspö (Figure 7-1).

The objective of the next borehole batch is characterization of the vertical and lateral distribution of lithological and structural units within this site area. Core mapping will be complemented by different geophysical borehole surveys.

7.1.1 Lithological Units

Information from surface mapping and one borehole (KAS 02) indicates that a medium-grained reddish-grey granite-granodiorite, with minor remnants of dark grey fine-grained greenstone, is the major component down to approx. 315 m in this rock mass, which is intruded by red fine-grained granite (aplite) in form of dykes and veins. In the following description this lithological unit is called "Granite".

From about 315 m to the bottom of the core, in borehole KAS 02, a dioritic rock is most common. This is especially interesting because the diorite, which seems to have a low permeability, has not been observed during the surface mapping within the Äspö area. This unit is called "Diorite".
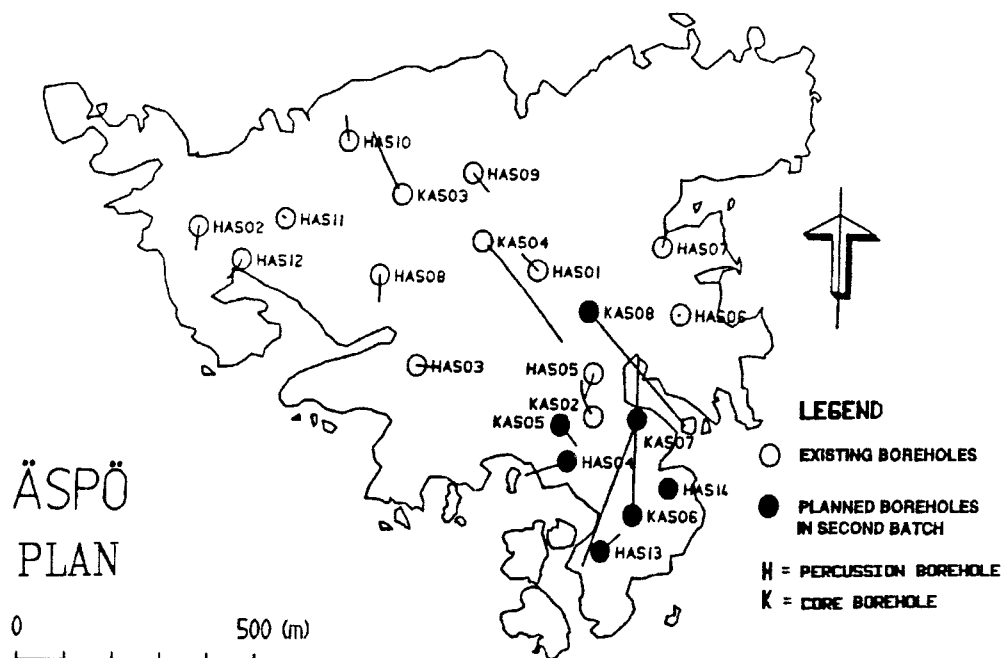

ÄSPÖ

PLAN

0 _____ 500 (m)

LEGEND

O EXISTING BOREHOLES

● PLANNED BOREHOLES IN SECOND BATCH

H = PERCUSSION BOREHOLE
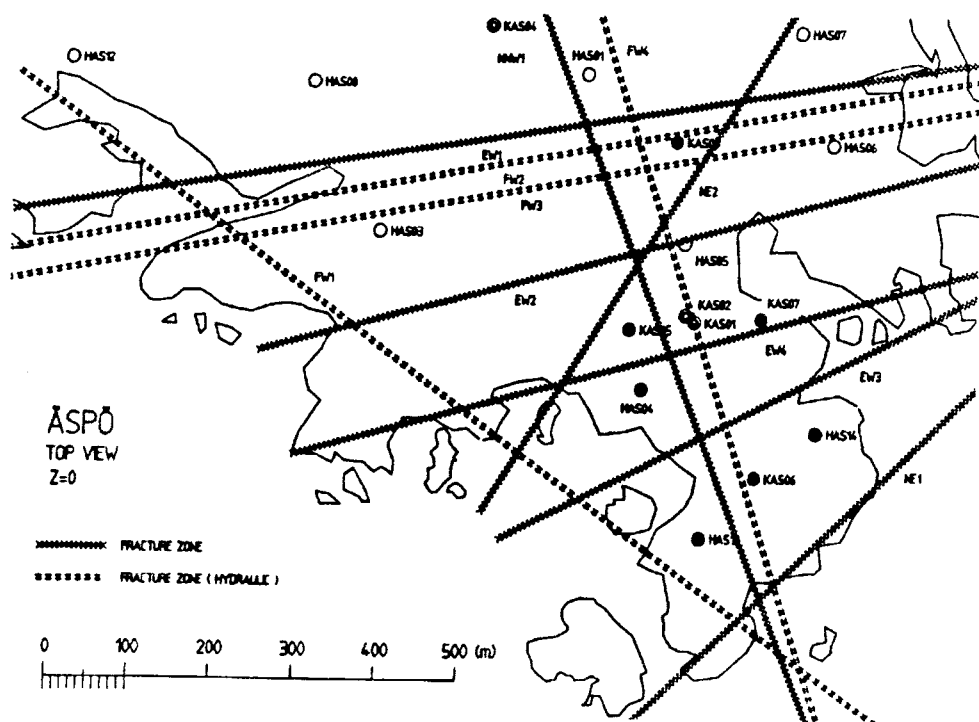
K = CORE BOREHOLE

Figure 7-1.

Figure 7-2.

7.1.2 Structural Units

Geophysical and structural analyses indicate the following main fracture zones shown in Figure 7-2. The site area is bordered to the north by the major fracture zone on Äspö — *"the Mylonite Zone"* — trending approx. NE (NE 2 in Figure 7-2).

The dip of the gently dipping fracture zone (NE 1), trending approx. 060, known at the surface in the southernmost part of Äspö, is not certain according to /Talbot 1988/ but many of the internal fractures dip 30 to the NNW.

Fracture zones EW 2 and EW 3 trend almost E-W. In outcrops they are 2—4 m wide — crushed and highly altered — with internal fractures dipping approx. 70 to the north (EW 2) and almost vertical (EW 3). Both of these zones are also geophysically indicated.

Fracture zone NNW 1 trends NNW and supposed to dip from 55°E to almost vertical. This zone is geophysically indicated and can be followed to the northern part of the island. The zone is also indicated as a probable hydraulic conductor as found by interference testing of borehole KAS 02.

Narrow, steeply dipping shear zones and fractures trending almost N-S as well as subhorizontal fracture zones at greater depth — indicated by seismic reflection — may also be considered when interpreting the borehole data.

7.2 GEOHYDROLOGY

The geohydrological information from southern Äspö was collected from pumping tests in percussion boreholes, packer tests in core boreholes and transient interference tests made on selected portions of the core boreholes. The hydraulic properties of different lithological and structural units have been estimated from information from geological and geophysical investigations. The

142

probable hydraulic properties of the rock mass and the structural units are given in the descriptions below. In these a small to moderate hydraulic conductivity can be interpreted as a median, $K_{50} = 10^{-10} - 10^{-8}$ m/s, and low hydraulic conductivity as a median, $K_{50} = 10^{-11} - 10^{-9}$ m/s. For a zone a high transmissivity can be interpreted as, $T = 10^{-7} - 10^{-5}$ m²/s, a moderate transmissivity as, $T = 10^{-8} - 10^{-6}$ m²/s, and a small transmissivity as $T = 10^{-9} - 10^{-7}$ m²/s.

7.3 CHEMISTRY

Water samples collected from the deep borehole, KAS 02, have been analyzed. The results, together with the information from the geological and geohydrological investigations, have been used to predict the chemical composition of the water in the highly conducting parts of the planned boreholes.

7.4 ROCK MASS DESCRIPTIONS

7.4.1 "Småland Granite"

Mostly faintly foliated rocks which can be classified as granite-granodiorite. Fracture frequency = 3-4 fr/m (crush-zones excluded). Dominant fracture fillings: Chlorite, calcite and epidote. Random minor remnants of fine-grained greenstone and some dykes of fine-grained reddish granite (aplite).

Random crushed or highly fractured zones (10—20 fr/m), 0,5—1 m wide, especially connected to the fine-grained granite. Some highly altered and fractured narrow zones in greenstone. Some, mostly steeply dipping shear-zones — epidotic/mylonitic and strongly foliated.

The hydraulic conductivity of the Småland Granite is small to moderate. Pervious structures exist either in connection with combined fine-grained granite-greenstone portions or as distinct fractures with high conductivity.

7.4.2 "Äspö Diorite"

Rocks which can be classified as monzodiorite-diorite, sometimes with winding foliation intersected by a few dykes of fine-grained granite. Fracture frequency = 1—2 fr/m (crush-zones excluded).

Random crushed or/and highly altered zones 0,5—1 m wide. Dominant fracture fillings: Chlorite and calcite.

The hydraulic conductivity is low. Some pervious portions are associated with the dykes of fine-grained granites.

7.4.3 "G-D Boundary"

The contact section may be complex: medium-grained granite — greenstone — fine-grained granite — diorite with increased fracturing and alteration.

The G-D Boundary has probably a high transmissivity, and is one of the major geohydrological units of the target area.

The G-D Boundary probably contains a sodium, calcium and chlorine-bearing water with a salinity of approximately 4000 — 6000 mg Cl/l.

7.4.4 "Zone EW 1"

Increased fracturing in medium-grained — fine-grained granite in a section 10—30 m wide.

Parallel and close to EW 1 two hydraulically indicated zones have been located, FW 2 and FW 3. One of them may be identical with EW 1, and together they may act as a composite zone with high transmissivity (see Figure 7-2).

7.4.5 "Zone EW 2"

Intensely foliated zone in rock of hybridic composition — fine-grained granite and greenstone — 20—50 m wide. More open highly fractured sections in fine-grained granite changing with steeply dipping remnants of greenstone — which are assumed to be more tight.

The transmissivity of the zone is probably moderate.

7.4.6 "Zone EW 3"

Intense fracturing and partly altered in a 5—10 m wide section mostly in granite and perhaps also in greenstone.

The transmissivity of the zone is probably moderate.

7.4.7 "Zone EW 4"

Intense fracturing and part altered in medium-grained granite, greenstone and fine-grained granite.

The transmissivity of the zone is probably moderate.

7.4.8 "Zone NNW 1"

Intense fracturing in fine-grained granite or/and single open fractures in medium-grained granite.

A hydraulically identified zone, FW4, has been found parallel and close to NNW 1. This zone may be identical to NNW 2 and its transmissivity is probably high.

7.4.9 "Zone NE 1"

Increased fracturing in medium-grained-fine-grained granite in a section 10 — 30 m.

The transmissivity of the zone is probably small.

7.4.10 "Zone NE 2"

May be the border to the SE of the big "Mylonite Zone". Complex zone, 10—50 m wide, changing from intensely fractured and partly altered sections to highly foliated, sometimes mylonitic, and more tight sections.

The transmissivity of the zone is probably moderate.

7.4.11 "Zone FW 1"

Except for these zones a NW trending structure dipping 30 — 50 E has been localized by the transient interference tests i borehole KAS 03. The zone does not hit the surface within the target area and it is uncertain whether it extends as far as SE Äspö. The zone contains calcium, sodium, chlorine and sulphate-bearing water with a salinity of 6000 — 8000 mg Cl/l.

7.5 PROPOSED BOREHOLES

Four additional core boreholes (KAS 05-08) and two percussion boreholes, HAS 13-14, will be drilled in the site area (Figure 7-1).

One percussion borehole (HAS 13, approx. 150 m) is planned to check fracture zone NNW 1 and the gently dipping zone, NE 1.

The percussion borehole (HAS 14, approx. 150 m) is planned to be vertical and penetrate fracture zone NE 1.

The percussion borehole (HAS 04) will be drilled deeper, to approx. 200 m, to check whether FW1 reaches SE Äspö.

The main aim of borehole KAS 05, (approx. 600 m long, dipping 85° SE) located in a possible vertical shaft site is to determine the lateral extent of the diorite and to correlate data from borehole KAS 02.

Borehole KAS 06, (approx. 600 m, dipping 60 NNE) will mainly be used to locate and characterize fracture zones EW 3 and NE 1 and the lateral extent of the diorite.

Another borehole — KAS 07 — is planned to be approx. 600 m long, with a dip of 60 degrees to the SW. This hole will also permit interpretation of the lithological contact between the granite and diorite. Fracture zones EW 3, NNW 1 and NE 1 may be penetrated and characterized.

The main aim of borehole KAS 08 (600 m long, dipping 60° SE) is to check fracture zones NE 2, EW 2 and possibly NE 1. This hole will also provide information on the lateral extent of the diorite.

145

8 DISCUSSION OF THE RESULTS WITH RESPECT TO THE SITING OF THE HARD ROCK LABORATORY

The geological, geohydrological and chemical predictive models (see Chapters 2, 3 and 4) are presented in such detail that it is possible to define the main features of the rock mass in the different rock blocks investigated. It is therefore possible to define the conditions that are likely to be found in the laboratory. As the investigation has been focused on Äspö this discussion will deal only with Äspö and especially a proposed site on the southern part of the island.

The conditions that it is desirable to determine in an underground laboratory are of course of a geological, hydrological and chemical character. However, there are also a few fundamental aspects which should be addressed separately. The most important of these is to have a large enough rock block to place the laboratory in. Äspö is divided into a northern and a southern subarea by a 300 m wide mylonitic zone. The zone dips to the north, making the area available in the southern part larger at depth. This is the primary reason for locating the laboratory on the southern part of the island. In addition, there are a number of favourable circumstances which make this selection even more obvious.

According to information from core boreholes KAS 02 and KAS 03 the lithological distribution is very similar in the two granitic blocks on Äspö down to a depth of about 300 m. At approximately the 300—600 m level in the southern-block (KAS 02) a more basic rock type dominates — the Äspö diorite.

Evaluation of data from core examination indicates favourable properties of the diorite, such as rather low fracture frequency and a high degree of homogeneity, compared with the corresponding level in the northern block (KAS 03).

The southern part of Äspö is less pervious than the northern part, especially in the 300—600 m depth where the dioritic rock type predominates. This difference is also detectable from the comparison between fractures containing hematite and those containing iron oxy-hydroxide. Such fractures are statistically correlated to high conductivities. In borehole KAS 03, the northern part, such fractures are present whereas they are absent in KAS 02, the southern part.

The fact that the Mylonite zone is also certainly dipping northwards points towards the possibility of finding a suitable site for the HRL in the southern block at a depth of about 500 m below the "subhorizontal zone" indicated by seismic reflection measurements and core logging. In these circumstances the spiral tunnel down to the laboratory will preliminary be affected or cut by a set of two or three narrow ENE-trending fracture zones probably dipping subvertically to the north, at least one N-S trending almost vertical fracture zone and one NE trending zone probably dipping steeply to the NW.

With respect to the geohydrological conditions a localization of the Hard Rock Laboratory to southern Äspö is favourable both with respect to the local conditions and the possibility of reaching certain features within a reasonable distance by access tunnels.

The following geohydrological features can be identified:

— To the NW the regional Mylonite zone crossing the island can be found. This zone consists of a complex pattern of conductive and tight parts. It has a NE-SW strike and dips steeply towards the NW.

— Below the block, at greater depth, the fine-grained granites can be reached by boreholes. They are considerably more conductive than the actual block itself and may be an influence from the Götemar-Uthammar Granites.

— Around Äspö, on all sides, areas covered by sea can be accessed.

— At some distance, at Laxemar, an area with homogeneous Småland granite can be reached.

— The existence of a saline water front complicates the numerical modelling of the groundwater behaviour, but on the other hand the saline water front below the island gives, if properly used, permits the use of a natural tracer in the saline inflow of groundwater to the laboratory.

We have used the present data in two ways, to describe the area investigated and to predict the conditions at depth, especially for the southern part of Äspö. The prediction is made assuming that no unexpected features are encountered at depth.

There is, however, always a possibility of encountering unexpected conditions. The question is therefore not if, but rather which type of unpredicted features we will encounter. This is what will determine the basis for the future detailed site investigations.

REFERENCES

Borrhålsrapport "Borehole Report". (In Swedish).
(All borehole data is collected in separate reports, one for each hole.)

Ericsson L 1988:
Fracture mapping study on Äspö island. Findings of directional data.
SKB, PR 25-88-10

Gustafson G, Stanfors R, Wikberg P 1988:
Swedish Hard Rock Laboratory first evaluation of preinvestigations 1986—87
and target area characterization.
SKB Technical Report 88-16

Gustafson G, Liedholm M, Lindbom B 1988:
Groundwater Flow Calculations on a Regional Scale at the Swedish Hard Rock
Laboratory.
SKB, PR 25-88-17

Herbert A W & Jackson C P 1987:
Coupled groundwater flow and solute transport with fluid density strongly de-
pendent upon concentration.
Submitted to Water Resour Res, Vol 23, No 10

IUGS SUBCOMISSION ON THE SYSTEMATICS OF IGNEOUS ROCKS

– 1973: Classification and Nomenclature of Plutonic Rocks. Recommendations.
— N. Jb. Miner. Mh 1973, H4, 149—164.

– 1980: Classification and Nomenclature of Volcanic Rocks, Lamprophyres, Car-
bonatites and Melilitic Rocks.
— Geol. Rundschau 69, 194—207

Jarl L-G and Johansson Å 1988:
U-Pb zircon ages of granitoids from the Småland-Värmland granite-porphyry
belt, southern and central Sweden.
Geologiska Föreningens i Stockholm Förhandlingar.

Kornfält K-A, Wikman H 1988:
The rocks of the Äspö island. Description to the detailed maps of solid rocks in-
cluding maps of 3 uncovered trenches.
SKB, PR 25-88-12

Laaksoharju M 1988:
Shallow groundwater chemistry at Laxemar, Äspö and Ävrö.
SKB, PR 25-88-04

Laaksoharju M, Nilsson A-C 1989:
Models of groundwater composition and of hydraulic conditions based on chemometrical and chemical analyses of deep groundwater at Äspö and Laxemar.
SKB, PR 25-89-04

Liedholm M 1987:
Regional Well Data Analysis.
SKB, PR 25-87-07

Liedholm M 1989:
Combined evaluation of geological, hydrogeological and geophysical information.
SKB, PR 25-89-03

Nilsson L 1988:
Hydraulic tests at Äspö 1988.
SKB, PR 25-88-14

Nisca D 1988:
Geophysical laboratory measurements on core samples from KLX01, Laxemar and KAS 02, Äspö.
SKB, PR 25-88-06

Nisca D, Triumf C-A 1989:
Detailed geomagnetic and geoelectric mapping of Äspö.
SKB, PR 25-89-01

Nisca D, Triumf C-A 1989:
Detailed geomagnetic and geoelectric mapping of Äspö.
SKB, PR 25-89-01

Niva B, Gabriel G 1988:
Borehole radar measurements at Äspö, Boreholes KAS 03 and KAS 04.
SKB, PR 25-88-03

Nordenskjöld C E 1944:
Morfologiska studier inom övergångsområdet mellan Kalmarslätten och Tjust.
Medd Lunds Geogr Inst Ark VIII

Nylund B 1987:
Regional gravity survey of the Simpevarp area.
SKB, PR 25-87-20

Olsson P, Stille H 1989:
Preliminary Rock Mechanic Report.
SKB, PR 25-89-07

150

Plough C, Klitten K 1989:
Shallow reflection seismic profiles from Äspö, Sweden.
SKB, PR 25-89-02

Rhen I 1987:
Compilation of geohydrological data.
SKB, PR 25-87-10

Rhen I 1988:
Transient interference tests on Äspö 1988.
SKB, PR 25-88-13

Sehlstedt S, Triumph C-A 1988:
Interpretation of geophysical logging data from KAS 02—KAS 04 and
HAS 08—HAS 12 at Äspö and KLX 01 at Laxemar.
SKB, PR 25-88-15.

Smellie S, Larsson N-Å, Wikberg P and Carlsson L 1985:
Hydrochemical investigations in crystalline bedrock in relation to existing
hydraulic conditions.
SKB, Technical Report 85-11.

Spalding D B 1981:
A general-purpose computer program for multi-dimensional one- and two-
phase flow.
Math and Comp in Simulation, XIII, pp 267—276

Stanfors R 1988:
Geological Borehole Description KAS 02, KAS 03, KAS 04, KLX 01.
SKB, PR 25-88-18

Stråhle A 1988:
Plot pictures of drillcore data from KAS 02, KAS 03, KAS 04 and KLX 01.
SKB, Internal Report

Stråhle A 1989:
Drillcore investigation in the Simpevarp area. Boreholes KAS 02, KAS 03,
KAS 04 and KLX 01.
SKB, PR 25-88-07

Svedmark E 1904:
Beskrifning till kartbladet Oskarshamn. - SGU Ac 5.

Svensson T 1987:
Hydrological conditions in the Simpevarp area.
SKB, PR 25-87-09

Svensson U 1988:
Numerical simulations of seawater intrusion in fractured porous media.
SKB, PR 25-88-07

Talbot C, Riad L, Munier R 1988:
The geological structures and tectonic history of Äspö SE Sweden.
SKB, PR 25-88-05

Voss C I & Souza W R 1987:
Variable density flow and solute transport simulation of regional aquifers containing a narrow freshwater-saltwater transition zone.
Water Resour Res, Vol 23, No 10, pp 1851—1866

Wikberg P, Axelsen K, Fredlund F 1987:
Deep groundwater chemistry.
SKB Technical Report 87-07, Stockholm

Wikman H, Kornfält K-A, Riad L, Munier R, Tullborg E-L 1988:
Detailed investigation of drillcores KAS 02, KAS 03 and KAS 04 on Äspö island and KLX 01 at Laxemar.
SKB, PR 25-88-11

Wikström A 1989:
General geological-tectonic study of the Simpevarp area with special attention to the Äspö island.
SKB, PR 25-89-06

List of SKB reports

Annual Reports

1977-78
TR 121
KBS Technical Reports 1 – 120.
Summaries. Stockholm, May 1979.

1979
TR 79–28
The KBS Annual Report 1979.
KBS Technical Reports 79-01 – 79-27.
Summaries. Stockholm, March 1980.

1980
TR 80–26
The KBS Annual Report 1980.
KBS Technical Reports 80-01 – 80-25.
Summaries. Stockholm, March 1981.

1981
TR 81–17
The KBS Annual Report 1981.
KBS Technical Reports 81-01 – 81-16.
Summaries. Stockholm, April 1982.

1982
TR 82–28
The KBS Annual Report 1982.
KBS Technical Reports 82-01 – 82-27.
Summaries. Stockholm, July 1983.

1983
TR 83–77
The KBS Annual Report 1983.
KBS Technical Reports 83-01 – 83-76
Summaries. Stockholm, June 1984.

1984
TR 85–01
Annual Research and Development Report 1984
Including Summaries of Technical Reports Issued during 1984. (Technical Reports 84-01–84-19)
Stockholm June 1985.

1985
TR 85-20
Annual Research and Development Report 1985
Including Summaries of Technical Reports Issued during 1985. (Technical Reports 85-01-85-19)
Stockholm May 1986.

1986
TR 86-31
SKB Annual Report 1986
Including Summaries of Technical Reports Issued during 1986
Stockholm, May 1987

1987
TR 87-33
SKB Annual Report 1987
Including Summaries of Technical Reports Issued during 1987
Stockholm, May 1988

1988
TR 88-32
SKB Annual Report 1988
Including Summaries of Technical Reports Issued during 1988
Stockholm, May 1989

Technical Reports

1989
TR 89-01
Near-distance seismological monitoring of the Lansjärv neotectonic fault region Part II: 1988
Rutger Wahlström, Sven-Olof Linder,
Conny Holmqvist, Hans-Edy Mårtensson
Seismological Department, Uppsala University,
Uppsala
January 1989

TR 89-02
Description of background data in SKB database GEOTAB
Ebbe Eriksson, Stefan Sehlstedt
SGAB, Luleå
February 1989

TR 89-03
Characterization of the morphology, basement rock and tectonics in Sweden
Kennert Röshoff
August 1988

TR 89-04
SKB WP-Cave Project
Radionuclide release from the near-field in a WP-Cave repository
Maria Lindgren, Kristina Skagius
Kemakta Consultants Co, Stockholm
April 1989

TR 89-05
SKB WP-Cave Project
Transport of escaping radionuclides from the WP-Cave repository to the biosphere
Luis Moreno, Sue Arve, Ivars Neretnieks
Royal Institute of Technology, Stockholm
April 1989

TR 89-06
SKB WP-Cave Project
Individual radiation doses from nuclides
contained in a WP-Cave repository for
spent fuel
Sture Nordlinder, Ulla Bergström
Studsvik Nuclear, Studsvik
April 1989

TR 89-07
SKB WP-Cave Project
Some Notes on Technical Issues

Part 1: Temperature distribution in WP-Cave: when
shafts are filled with sand/water mixtures
Stefan Björklund, Lennart Josefson
Division of Solid Mechanics, Chalmers Uni-
versity of Technology, Gothenburg, Sweden
Part 2: Gas and water transport from WP-Cave
repository Luis Moreno, Ivars Neretnieks
Department of Chemical Engineering, Royal
Institute of Technology, Stockholm, Sweden
Part 3: Transport of escaping nuclides from the
WP-Cave repository to the biosphere.
Influence of the hydraulic cage
Luis Moreno, Ivars Neretnieks
Department of Chemical Engineering, Royal
Institute of Technology, Stockholm, Sweden
August 1989

TR 89-08
SKB WP-Cave Project
Thermally incuded convective motion in
groundwater in the near field of the
WP-Cave after filling and closure
Polydynamics Limited, Zürich
April 1989

TR 89-09
An evaluation of tracer tests performed
at Studsvik
Luis Moreno[1], Ivars Neretnieks[1], Ove Landström[2]
[1] The Royal Institute of Technology, Department of
Chemical Engineering, Stockholm
[2] Studsvik Nuclear, Nyköping
March 1989

TR 89-10
Copper produced from powder by HIP to
encapsulate nuclear fuel elements
Lars B Ekbom, Sven Bogegård
Swedish National Defence Research Establishment
Materials department, Stockholm
February 1989

TR 89-11
Prediction of hydraulic conductivity and
conductive fracture frequency by multi-
variate analysis of data from the Klipperås
study site
Jan-Erik Andersson[1], Lennart Lindqvist[2]
[1] Swedish Geological Co, Uppsala
[2] EMX-system AB, Luleå
February 1988

TR 89-12
Hydraulic interference tests and tracer tests
within the Brändan area, Finnsjön study site
The Fracture Zone Project – Phase 3
Jan-Erik Andersson, Lennart Ekman, Erik Gustafsson,
Rune Nordqvist, Sven Tirén
Swedish Geological Co, Division of Engineering
Geology
June 1988

TR 89-13
Spent fuel
Dissolution and oxidation
An evaluation of literature data
Bernd Grambow
Hanh-Meitner-Institut, Berlin
March 1989

TR 89-14
The SKB spent fuel corrosion program
Status report 1988
Lars O Werme[1], Roy S Forsyth[2]
[1] SKB, Stockholm
[2] Studsvik AB, Nyköping
May 1989

TR 89-15
Comparison between radar data and
geophysical, geological and hydrological
borehole parameters by multivariate
analysis of data
Serje Carlsten, Lennart Lindqvist, Olle Olsson
Swedish Geological Company, Uppsala
March 1989